Optimal Placement of Battery Energy Storage System for Voltage Profile Improvement and Power Loss Reduction

Prepared by:

Nkululeko Justice Skunana

SKNNKU001

Department of Electrical Engineering

University of Cape Town

Prepare for Supervisor: Prof K. A Folly

and Co Supervisor: Mrs K.O Awodele

Department of Electrical Engineering

University of Cape Town

Date 15/01/2025

Submitted to the Engineering and Built Environment Department of Electrical Engineering in partial fulfilment of the requirements for the degree of Master of Science specialising in Nuclear Power.

Keywords— Battery Energy Storage Systems, Photovoltaic Systems, Particle Swarm Optimization (PSO), Genetic (GA) Algorithm, Voltage Profile Deviation, Power losses.

i. Plagiarism Declaration

- I know the meaning of plagiarism and declare that all the work in this document, save for the properly acknowledged, is my own.
- I have cited and referenced all sources according to IEEE guidelines. A complete list of references is included in this final year project report.
- I have not allowed and will not allow anyone to copy my work with the intention of passing it off as their own work.
- This thesis/dissertation has been submitted to the Turnitin module, and I confirm that my supervisor has seen my report, and any concerns revealed by such have been resolved with my supervisor.

Name: Nkululeko Justice Skunana

Signature: Signed by candidate Date: 19 / 01 / 2025

ii. Acknowledgements

First and foremost, I would like to express my gratitude to Almighty God for His boundless kindness, unmerited favour, and the blessings bestowed upon me before, during, and after completing this program. May we always give praise to His name.

Secondly to my ancestors, I deeply appreciate the legacy of my ancestors, whose enduring spirit and perseverance inspire me as I finalize my minor dissertation towards completion of my master's journey. Their sacrifices and wisdom have been a guiding light throughout my academic pursuit.

iii. Abstract

This dissertation investigates the optimal placement of Battery Energy Storage Systems (BESS) in a modified 16-bus Witzenberg radial distribution network incorporating renewable energy sources, particularly photovoltaic (PV) systems. As the distribution networks increasingly integrate intermittent renewable energy sources, the strategic deployment of BESS becomes crucial for maintaining system stability and efficiency. This dissertation aims to investigate the most effective location for BESS placement to minimize total system costs associated with active power losses and voltage profile deviations.

The methodology employs a dual-software approach, utilizing MATLAB for optimization algorithms and DigSilent PowerFactory for load flow analyses. Initial assessments establish a baseline scenario without BESS, followed by the application of Particle Swarm Optimization (PSO) and Genetic Algorithm (GA) to identify optimal BESS locations. The study conducts comprehensive simulations with BESS at various buses, including algorithm to identify optimal location and other strategic positions within the network.

Performance evaluation incorporates a percentage voltage deviation index (PVDI) to quantify improvements in voltage deviations. The research also compares the effectiveness of PSO and GA in minimizing the objective function, providing insights into their applicability for BESS placement optimization.

Results demonstrate significant improvements in voltage profiles and reductions in active power losses through strategic BESS placement. Two key results include:

- BESS placement at the optimal location (bus 13) led to a substantial reduction in active power losses from 8 MW to 3.3 MW, representing a significant 58.75% decrease.
- The overall percentage voltage deviation index (PVDI) was reduced from 11.98% to 5.24% with optimal BESS placement, indicating a 56.26% improvement in voltage stability across the network.

These results highlight the potential of BESS in enhancing the performance of distribution networks with high renewable energy penetration. The dissertation results demonstrates that strategic BESS placement can simultaneously address both research aims: reducing active power losses and improving voltage deviations profile.

iv. Dedication

I humbly dedicate this dissertation to my cherished family and friends, whose unwavering support and encouragement have been the bedrock of my journey. To my beloved children, Qhayiya, Enzo, Entle, Kwanele, Hlonipha, and Khanya – your belief in my abilities and your understanding of the sacrifices we have made together have provided me with the strength to persevere. This work is a testament to your patience and love.

To my late mother, whose memory continues to inspire me every day, and my late aunt, my greatest advocate and guardian angel – I am deeply grateful for your enduring influence and guidance from above. I also extend my heartfelt gratitude to my co supervisors, Prof. K. A. Folly, and Mrs. K. O. Awodele, for their invaluable guidance, wisdom, and patience throughout this academic endeavour. Your dedication to my success has been instrumental in shaping the direction and quality of this research.

To my friends and colleagues especially Mr Emmanuel Okafor, thank you for your continuous support, insightful discussions, and for believing in me during this challenging journey. Your encouragement and camaraderie have been a source of motivation and resilience. This dissertation is dedicated to all of you, with the hope that it serves as a testament to our collective efforts and a foundation for future successes.

V. Table of Contents

vi. List of Figures

vii. List of Tables

viii. List of Abbreviations

BESS	Battery Energy Storage System
BMS	Battery Management System
EMS	Energy Management System
PCS	Power Conditioning/Conversion System
PWM	Pulse width modulation
HV	High Voltage
MV	Medium Voltage
LV	Low Voltage
MV	Medium Voltage
POC	Point of Connection
PCC	Point of Common Coupling
PV	Photovoltaic
DOD	Depth of Discharge
SOC	State Of Charge
SOH	state of heath
IPP	Independent Power Producer
MW	Mega Watt
kWh	Kilowatt–Hour
Mvar	Mega Volt-Amps Reactive
RES	Renewable Energy Source
DG	Distributed Generation
PHS	Pumped Hydro Storage
GHG	Green-House Gas
p.u	Per Unit
BB	Bus Bar
OPF	Optimal power flow
MTS	Main Transmission Substation
BESF	Battery Energy Storage Facility
IPS	Interconnected power system (IPS)

Chapter 1: Introduction

1.1 Background of the study

The urgent need to address climate change and move toward cleaner, more sustainable power generation methods is leading a huge revolution in the global energy sector. While fossil fuel-based power generation has long been the backbone of global energy production, particularly in South Africa [1], [2], its environmental impact and sustainability challenges have necessitated a shift towards renewable energy sources (RES) and advanced energy management technologies [3].

The energy industry now places a high priority on the integration of renewable energy sources (RES), primarily solar and wind power, into the existing distribution network. These renewable energy technologies, along with their associated integration systems, offer numerous benefits, including environmental sustainability, enhanced energy security, economic growth, and improved public health [4]. However, the intermittent nature of RES presents significant challenges for distribution system stability and power quality, particularly in distribution networks that were traditionally designed for unidirectional power flow (from generation to loads) especially weak radial distribution networks [5], [6].

As distribution networks evolve to accommodate a higher penetration of RES, new challenges emerge in maintaining distribution system stability and power quality. These issues are compounded in South Africa by an aging generation fleet, lack of investment in new baseload generation plants, and high energy demand [2]. Since renewable energy sources like solar and wind are inherently intermittent and cannot provide consistent power output throughout the day, energy storage solutions are essential to balance supply and demand. This has led to increasing interest in investigating the possible advantages of Battery Energy Storage Systems (BESS) to improve distribution networks and address this stability and power quality challenges.

Recent advances in battery technology, combined with significant cost reductions and improved performance, have made BESS a viable way to deal with these issues and challenges [7]. BESS can store excess power generated from RES and discharge it during periods of high demand or when there's low generation, thereby improving system stability and enabling higher RES penetration [8], [9]. The strategic deployment of BESS in sub-transmission and distribution networks has become a crucial topic within the renewable energy sector, offering potential solutions for enhanced voltage profile regulation, reduction of active power losses, peak shaving, and increased network capacity, etc, [7].

In South Africa, recent advancements in the electrical industry, reflected in the Integrated Resource Plan (IRP), showcase a strong push for increased penetration of

renewable energy sources (RES) [2]. The national electricity supplier, Eskom, has recognized the potential of BESS and has planned significant investments in BESS projects totalling over 1440 Mega-Watt hours (MWh) in its first two phases [10]. These projects aim to support ancillary services such as voltage support, peak shaving, and increased network capacity, etc.

1.2 Introduction of the study

This dissertation aims to determine the optimal ideal location for BESS to enhance voltage profiles improvement and reduce power losses in distribution networks integrated with RES, particularly photovoltaic (PV) systems.

The dissertation focuses on the Witzenberg distribution network, located within the Cape Winelands District in the Western Cape Province. The Witzenberg distribution network, is a 16-bus modified radial distribution network, which is used as a case study to investigate the impact of BESS placement on network performance to improve voltage deviation profiles and reduction in active power losses.

The integration of BESS in distribution networks presents both opportunities and challenges. While BESS can potentially improve voltage deviation profiles and reduce active power losses, improper BESS placement location can lead to unintended consequences, such as increased active power losses or voltage profile violations. Therefore, it is crucial to develop and apply optimization techniques that can determine the most effective locations for BESS deployment [11], [12].

This dissertation employs metaheuristic optimization algorithms, specifically Particle Swarm Optimization (PSO) and Genetic Algorithm (GA) to identify the optimal location of BESS placement within the Witzenberg distribution network. The dissertation aims to demonstrate how strategically placed BESS can significantly improve voltage profiles and reduce active power losses, thereby enhancing overall network performance and reliability.

The optimization process is conducted using MATLAB, while load flow studies are performed using DigSilent PowerFactory. The objective function for BESS placement is formulated based on the total system costs due to active power losses and voltage profile deviations. This approach allows for a comprehensive evaluation of the techno-economic benefits of BESS integration in distribution networks coupled with PV system.

1.3 The Aim and Objectives of the study

1.3.1 The aim of the study

The primary aim of this minor dissertation is to enhance voltage profile improvement and to reduce active power losses within the modified Witzenberg 16 bus distribution network through the optimal location of BESS placement.

1.3.2 Objectives

The specific objectives of this dissertation are to:

1. Investigate the impact of integrating BESS in distribution networks coupled with PV systems, focusing on voltage profile regulation and power loss reduction.
2. Develop an optimization framework using PSO and GA techniques to determine optimal BESS placement locations in the 16-bus Witzenberg distribution network with PV integration.
3. Evaluate the effectiveness of optimal BESS placement by:
    a. Analysing voltage regulation and power loss characteristics.
    b. Comparing network performance across different BESS placement scenarios.
    c. Quantifying improvements using the Voltage Deviation Index (VDI).
4. Formulate evidence-based recommendations for BESS deployment strategies in distribution networks with RES penetration based on the simulation results.

1.4 Methodology for Optimal BESS Placement in Distribution Networks

BESS Placement Optimization methodology process:

1. Initial Network Analysis
    - Conduct load flow analysis using DigSilent PowerFactory
    - Evaluate baseline voltage profiles and active power losses without BESS.
2. Optimization Setup
    - Implement PSO and GA algorithms in MATLAB.
    - Define objective function: minimize total system costs.
    - Set constraints for BESS placement.
3. BESS Placement Optimization
    - Run PSO and GA to determine optimal BESS locations.
    - Use predefined BESS reference sizing.
4. Comprehensive Simulations

- Perform simulations with BESS at various locations:

    - Optimal locations identified by PSO and GA
    - Other strategic network points
5. Performance Evaluation
    - Analyse voltage profile improvements
    - Assess reduction in active power losses.
    - Calculate Voltage Deviation Index (VDI)
6. Comparative Analysis
    - Compare PSO and GA performance in finding optimal BESS placement.
    - Evaluate effectiveness in minimizing the objective function.
7. Results Interpretation
    - Assess overall impact of BESS on network performance.
    - Determine most effective BESS placement strategy.
8. Documentation and Reporting
    - Compile findings and insights
    - Prepare comprehensive report (Chapter 4 of the dissertation).

1.5 Research Questions

The research questions of this minor dissertation are:

- How can optimal BESS placement be determined to effectively improve voltage profiles and reduce power losses in the Witzenberg distribution network?
- How can optimization techniques be applied to determine the most effective BESS placement locations in the distribution network?
- How does BESS placement at optimal locations affect network performance in terms of voltage regulation and power loss reduction?
- How does different BESS placement locations scenarios compare in terms of their effectiveness in addressing voltage profiles improvement and reduction of active power loss problems?

1.6 Scope and Limitations of this dissertation

1.6.1 Scope of the dissertation

The scope of this dissertation encompasses the steady-state analysis of optimal BESS placement in the 16-bus modified Witzenberg distribution network using DigSilent PowerFactory and MATLAB. While the study investigates voltage regulation and power loss reduction through optimal BESS placement, it excludes BESS sizing optimization, dynamic simulations, and economic feasibility analysis.

1.6.2 Limitations of the dissertation

While this dissertation provides valuable insights into the optimal location of BESS placement in distribution networks with PV system, it is important to acknowledge several limitations:

- The dissertation is limited to the modified Witzenberg area 16 – bus network, which may not be fully representative of other areas with different network configurations and environmental conditions.
- The research primarily uses static load flow analysis, which does not capture the dynamic behaviour of the network under rapidly changing conditions. Transient events, such as sudden changes in renewable generation or load, are not fully accounted for in this static model.
- Single Objective Optimization is used to minimize power loss and improve voltage profile in power systems through optimal placement of BESS. The optimization focuses primarily on enhancing voltage profile improvement and reduction of power losses. Other potential objectives, such as frequency regulation, investment costs, or environmental impact, are not included in the optimization process.
- While technical aspects are explored, regulatory constraints and detailed economic analysis of BESS implementation are beyond the scope of this dissertation.
- The findings are specific to the Witzenberg distribution network and may not be directly applicable to other distribution networks with different characteristics.

The research focuses on steady-state analysis and does not include dynamic simulations or economic feasibility studies of BESS implementation. These limitations should be taken into consideration when interpreting the results and conclusions of the study.

1.7 Dissertation Report Structure

The report is structured as follows.

Chapter 1: Introduction

This chapter provides an overview of the minor dissertation by introducing its background, aims, objectives, scope of work and limitations. It describes the methodology used, outlines the research's contribution to existing knowledge, and addresses the scope and limitations of the work. Furthermore, it details the structure of the dissertation.

Chapter 2: Literature Review

This chapter reviews existing literature on BESS, RES, and their integration into distribution networks. It covers the optimal placement of BESS by using optimization techniques such as PSO and GA in MATLAB environment. Furthermore, it discusses technical aspects related to voltage profile enhancement and power loss reduction. Key studies and theoretical frameworks are also reviewed to establish a foundation for the dissertation.

Chapter 3: Mathematical Modelling and Problem Formulation

This chapter provides a comprehensive overview of the mathematical modelling and problem formulation for the selected modified Witzenberg distribution network.

Chapter 4: Simulation Results and Discussions

This chapter presents and analyses simulation results in detail, showing the impact of BESS on distribution networks, comparing scenarios with and without BESS implementation. The discussion interprets findings in relation to objectives, examines implications for the selected network, and compares different scenarios using visual aids.

Chapter 5: Conclusions and Recommendations for Future Work

Presents conclusions based on the dissertation findings and the results obtained in chapter 4. The final chapter summarizes the findings and their significance. It summarizes the content of the dissertation findings, presents resulting observations. Furthermore, recommendations are made for potential future research work.

Chapter 2 : Literature Review

This chapter provides a comprehensive literature review of distribution networks, examining their evolution from traditional one-way power flow systems (centralized) to modern networks that accommodate two-way power flow (decentralized). The review covers Distributed Generation (DG) technology and Renewable Energy Sources (RES) such as solar and wind generation, along with Energy Storage Systems (ESS) Technologies. This chapter investigates various factors that characterize energy storage systems, including power output, energy density, cycle life, discharge duration, and efficiency.

Specific focus is given to BESS technology and its applications in sub-transmission and distribution system operations. Furthermore, the advantages and disadvantages of different commercially mature battery technologies are examined. The chapter concludes with a summary of key findings and highlights observations from the reviewed literature, setting the stage for the dissertation's subsequent analysis and discussions.

2.1 Overview of the Power System

Traditional power systems follow a hierarchical structure with three main sections: generation, transmission (including sub-transmission), and distribution to end users. In this conventional model, power flows in one direction - from large, centralized power plants, through the transmission network, and finally through distribution networks to reach consumers. Figure 2.1 (a) illustrates this traditional centralized power system topology and contrasts it with modern decentralized systems where power can flow in multiple directions due to the integration of distributed generation sources [13], [14].

In South Africa, most coal-fired power plants are concentrated in the northern regions near coal mines. This means electrical power must be transmitted over long distances to reach load centers across the country. To minimize power losses during this long-distance transmission, power is transported at high voltage levels through the transmission grid before being stepped down for distribution to end users.

The integration of Renewable Energy Sources (RESs) has introduced smaller generation power plants in the distribution networks, changing the traditional power flow patterns in the system.

The distribution network represents the final stage in delivering power to individual customers. While traditional power systems rely on large, centralized plants, modern networks also accommodate smaller generating units connected directly to sub-transmission or distribution networks near load centers. Figure 2.1(a) shows a typical vertically integrated power system with centralized generation. As power demand

grows, the generation, transmission, and distribution networks must be expanded to maintain voltage and frequency within acceptable operating limits [13].

South Africa's electricity generation heavily relies on fossil fuels, particularly coal, leading to significant greenhouse gas emissions and environmental impacts. This dependence creates uncertainty about the future sustainability of the power system. To meet the Paris Agreement goals and limit global warming, greenhouse gas (GHG) emissions are expected to peak by 2025 and decrease by 43% by 2030 [15].

Furthermore, complying with South African Grid codes requires proper coordination of the traditional vertically aligned network infrastructure. Therefore, effective power system planning becomes crucial, considering previous growth, investment in generation, transmission, and distribution.

However, the power system planning environment is facing challenges which necessitates regular evaluation to address uncertainties and changes. The power system's structure is shifting away from centralized generation and transitioning towards decentralized clean generation [16], as represented in Figure 2.1(b).

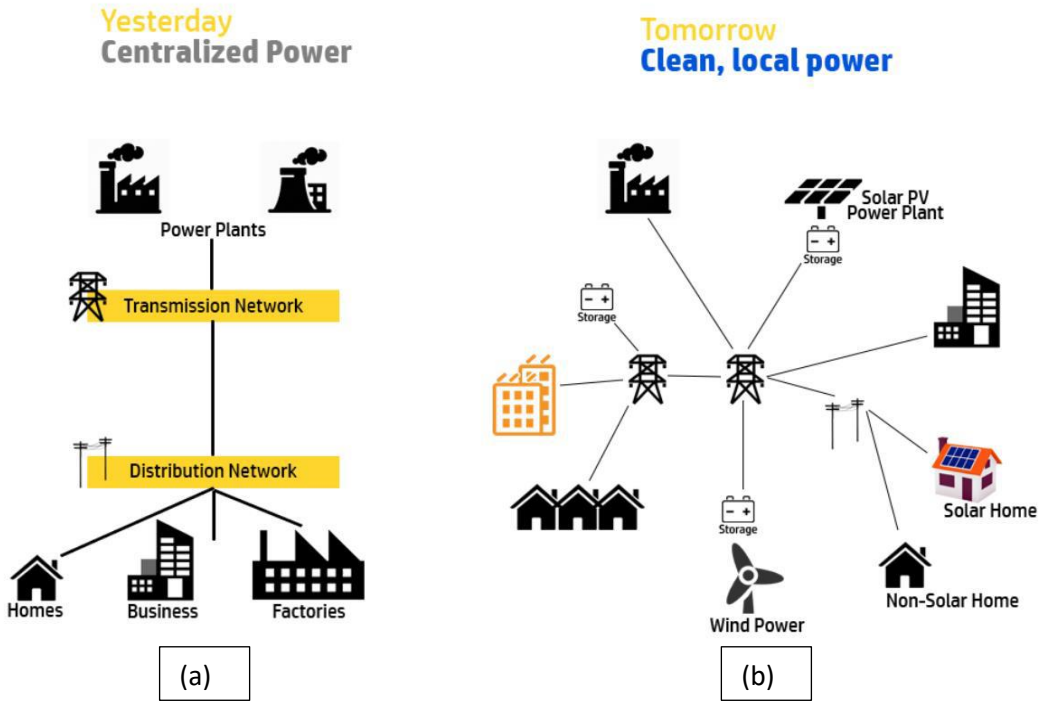

Figure 2.1: Demonstrating the difference between (a) centralized power generating plants and (b) clean decentralized power generating plant.

This transition from centralized power systems to decentralized renewable energy sources (RESs) represents a fundamental change in power system architecture [14],[16]. Figure 2.1(b) illustrates the integration of RESs into the traditional distribution network topology. Due to limited infrastructure investment in Eskom's distribution network, alternative solutions are being considered to improve network performance. The integration of RES alongside BESS presents a potential alternative to traditional network strengthening projects.

2.1.1 Limitations of the traditional vertical integrated centralized Power System

The traditional vertically integrated centralized grid faces several inherent limitations, including vulnerability to single points of failure, transmission losses, limited scalability, resistance to innovation, lack of flexibility and resilience, environmental impact, and limited customer engagement. These challenges stem from its centralized nature, relying on large power plants and extensive transmission infrastructure.

To address these challenges, there is a growing need to transition towards decentralized, resilient, and sustainable distribution networks. This involves integrating RESs such as PV and wind system, and energy storage systems (ESS) like BESS, Microgrids, and advanced power system distribution network management technologies.

While decentralized power generation can introduce complexities such as multi-directional power flow, voltage profile fluctuations, integration of BESS with RES can assist in ensuring voltage profile enhancement, power loss reduction, and reliability power supply.

2.1.2 Distributed Generation (DG) Technology

DGs is a growing trend in power systems where electricity is generated at multiple areas within the distribution network including near load centers. DG encompasses various technologies and methods that generate electricity on a smaller scale compared to conventional power plants (DG sources technology options for decentralised generations are given in appendix B). It offers advantages such as flexibility, reduced transmission losses, and the utilization of sustainable energy sources. RESs in the form of solar and wind, hydroelectric, biomass, etc, play a significant role in DG by generating electricity closer to the point of consumption. The International Council on Large Electric Systems (CIGRE) defines DG as small generation units located near customer sites, with a capacity of 30 MW or less [17], [18].

DGs can be categorized into dispatchable and non-dispatchable energy sources. Non-dispatchable sources include some forms of RES technologies such as wind and solar generators. Dispatchable sources encompass sources such as ESS, etc, [19]. The adoption of DGs contributes to a more sustainable and resilient energy infrastructure by leveraging RESs and improving operational efficiency.

DGs are connected near to the loads, which can reduce the need for new transmission and distribution networks, thus lowering infrastructure costs. DGs have the potential to play a significant role in the future of energy provision. For DGs to play an even more significant role there is a requirement that they must be reliable, properly sized, and located in the right locations [4], [20].

However, integration of DG has significantly impacted power flow and voltage regulation in distribution networks. In South Africa, all grid connected DGs and RESs, including wind and solar installations, must comply with the South African Grid Code requirements [21]. Despite this regulatory compliance, the intermittent nature of renewable sources still presents challenges for distribution network voltage regulation and power quality.

A key consideration in power system operation is that reactive power must be produced close to its point of consumption, as it cannot be efficiently transferred over long distances due to energy losses and voltage drops [13]. Whiles real power can be delivered over large distances through interconnected grid. The sudden loss of sub transmission lines requires the immediate use of local reactive power to compensate for increased losses in moving the same amount of power over fewer sub transmission lines. Without adequate local reactive power support, voltage levels will drop [22].

Therefore, this makes voltage, rather than frequency, the key indicator of stress in distribution networks, as frequency is a global parameter that can remain normal even during local voltage issues.

2.2 Renewable Energy Sources (RES) in Distribution Networks

Renewable Energy Sources (RES) are classified as non-dispatchable energy sources due to their output being uncontrollable and difficult to schedule for meeting power demand. Unlike conventional dispatchable sources such as natural gas, coal-fired, or nuclear power plants, RES like wind and solar energy are heavily influenced by weather conditions, making their output variable and less predictable [4], [6], [23].

This inherent variability presents significant challenges for integration into existing distribution networks, requiring careful management and advanced control systems.

The integration of RES into distribution networks, particularly radial networks, offers substantial benefits for both the environment and energy security. RES produce minimal greenhouse gas emissions compared to fossil fuels, significantly reducing the carbon footprint and contributing to climate change mitigation. Furthermore, RES can enhance energy access in remote or underserved areas, facilitating rural electrification and providing reliable power where traditional infrastructure is lacking. This decentralized approach not only supports environmental sustainability but also boosts local economies through job creation in installation and maintenance [6], [23], [24].

Despite these advantages, RES face several significant technical constraints and operational challenges. A primary limitation is their lower capacity factor, with an average Energy Availability Factor (EAF) of approximately 35% compared to conventional sources [4]. RES typically operate at full capacity for fewer hours per year - about 2000 hours - compared to coal, gas-fired, and nuclear power plants that can run up to an average of 7500 hours annually of their installed power capacity [2], [4]. Additionally, RES installations require more physical space to generate the same amount of electricity as traditional thermal power plants.

The integration of RES into distribution networks presents specific operational challenges that must be carefully managed. These include voltage profile variations, transient effects during source switching, increased short-circuit currents, and varying losses based on production and consumption patterns. Network congestion and effects on supply quality and reliability may also occur, necessitating coordinated network protection measures [5], [6], [24]. Moreover, when the installed capacity of RES connected to the distribution network exceeds local load demand, reverse power flow can occur, potentially causing network congestion and affecting power supply quality and reliability [6], [23], [25].

While advancements in Energy Storage Systems (ESS) and smart grid technologies help manage these challenges [6], [26] successful RES integration requires careful planning and implementation. The higher initial development costs of RES facilities compared to fossil fuel power plants must be balanced against their long-term environmental and economic benefits. Furthermore, coordinated protection measures are essential to manage reverse power flow and ensure the stability and security of the distribution network are maintained. Through proper planning and the implementation of appropriate control strategies, these challenges can be effectively addressed, allowing the full potential of RES to be realized in modern distribution networks.

2.2.1. The integration of Wind Power system

Wind energy, a long-standing player in the RESs, has historically been employed for tasks like water pumping on farms. This evolution revolves around the utilization of wind turbines and generators. There are two types of wind turbines namely horizontal-axis and vertical-axis wind turbines. Alongside the three types of wind generators namely direct current (DC), alternating current (AC) synchronous, and AC asynchronous types [26], [27].

The cornerstone of modern wind energy systems lies in the predominance of variable-speed generators within wind turbines, a departure from fixed-speed counterparts. The variability in turbine speed aligns with the fluctuating nature of wind speeds, mitigating stress on the drive train. AC asynchronous generators, notably induction generators, have emerged as the preferred choice for contemporary wind turbines, offering flexibility in speed, [26]. Furthermore, the integration of double-fed induction generators (DFIGs) underscores a pivotal advancement, showcasing bidirectional AC power transmission capabilities, thus playing a central role in electricity generation from wind turbines.

In contrast, constant-speed squirrel cage induction generators (SCIGs) face efficiency challenges due to heavy gearboxes and their propensity to absorb reactive power, leading to a preference for DFIG integration. This shift towards DFIGs is propelled by their superior efficiency and grid compatibility. Furthermore, wind energy conversion encompasses various losses, including aerodynamic, electrical generator, and

converter losses, necessitating a holistic approach towards optimization in wind power systems [27].

2.2.2 The integration of Photovoltaic (PV) systems

A photovoltaic (PV) system, also known as a PV farm, is a technology that converts sunlight energy into electrical power. It consists of solar panels made up of photovoltaic cells that capture the sun's energy and convert it into electrical energy through the photovoltaic effect, where certain materials generate an electric current when exposed to light. A typical PV system includes solar panels, an inverter for converting direct current (DC) to alternating current (AC) power, and often a battery bank for storing excess energy.

RES technology, such as PV systems, presents both integration challenges and benefits for enhancing distribution network stability. In recent years, the deployment of PV systems has significantly increased, with installations doubling as global technology trends shift towards RES generation. PV systems, composed of photovoltaic cells arranged in arrays, convert sunlight into electrical power through the photovoltaic effect. These systems typically include solar panels, inverters that convert DC to AC, and sometimes battery banks for energy storage.

Although the efficiency of PV systems is below 40% and they depend on sunlight availability—which introduces variability and system losses—they play a crucial role in stabilizing the voltage profile of the distribution network [28]. To accurately model the behaviour of PV systems and their impact on voltage profiles, researchers use various mathematical approaches, including the Lambert W-Function model [29], [30] Figure 2.2 is the diagram of the Lambert W-Function model.

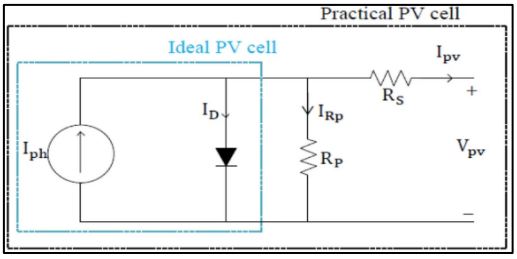

Figure 2.2: Model for the ideal PV cell and for the containing series and parallel resistances equivalent circuit.

Equivalent Circuit Models: Equivalent circuit models represent a PV cell or module using a combination of resistors, capacitors, and current sources. These models aim to simulate the electrical behaviour of the PV device based on a set of parameters. Examples of equivalent circuit figure 2.2 model include the single diode-resistor model and the practical PV cell model [31]. Models for stand-alone PV system, including PV cells, play a crucial role in understanding and predicting their performance. These software tools allow researchers and engineers to analyse PV system behaviour using built-in components and custom model implementations.

For example, MATLAB/Simulink offers specialized power system blocks for implementing both single-diode and two-diode models, while PVsyst includes detailed module characterization using the single-diode model. These models assist in determining the maximum power point, estimating energy production, and evaluating system performance under different operating conditions. By utilizing these models, researchers, engineers, and system designers can enhance the efficiency and reliability of stand-alone PV system.

2.2.2.1 Stand-alone Photovoltaic Model device

The performance of a solar photovoltaic cell or array is highly dependent on various factors such as the location and level of solar irradiation, and ambient temperature. A typical photovoltaic cell is composed of a matrix of cells interconnected in series and parallel, with the behaviour of each individual cell greatly affecting the performance of the entire array. To model the photovoltaic cell, a circuit equivalent can be used, which includes a light-generated source I_{ph}, a diode to represent the intrinsic p-n junction characteristics, and parallel and series resistances R_p and R_s, respectively.

Figure 2.3 represents the model diagram of the ideal PV cell and practical PV cell [31]. The single diode model is a popular choice due to its balance between accuracy and simplicity. More complex models, such as the double exponential and three-diode models, have also been proposed to account for additional effects not considered by the single diode model. For explaining the PV device operation, figure 2.3 should be ideal.

The single-diode model is a widely used in simplified representation of a PV cell. It assumes that the cell can be represented by a single diode connected in parallel with a current source. This model considers the key parameters of a PV cell, such as the diode saturation current, diode ideality factor, series resistance, and shunt resistance. It allows for the estimation of the current-voltage (I-V) characteristics and the maximum power point (MPP) of the PV cell.

The two-diode model is an enhanced version of the single-diode model, introducing an additional diode to account for the recombination losses within the PV cell. This model provides a more accurate representation of the complex behaviour of a PV cell by considering the voltage-dependent recombination processes. It can better capture the effects of temperature and irradiance variations on the cell's performance.

According to [28] the Lambert W-function model is an advanced mathematical model used to analyse the performance of PV cells. It incorporates more detailed and complex calculations compared to the single- or two-diode models. This model accounts for various factors such as series resistance, shunt resistance, and non-linear behaviour of the diode. The Lambert W-function model provides a highly accurate representation of the I-V characteristics and allows for precise prediction of the cell's performance under different conditions [28].

Modelling PV systems is essential for understanding their impact on network performance. Key components in PV modelling include the PV generator, DC cabling, and the inverter [29], [31].The behaviour of PV systems is often represented by equivalent circuit models and mathematical equations that describe their current-voltage characteristics [31]. PV systems offer significant environmental benefits, such as reduced reliance on fossil fuels and lower greenhouse gas emissions. Technological advancements and decreasing installation costs have made PV systems more affordable and accessible [4] .

However, their efficiency can be influenced by factors such as weather conditions, shading, and panel orientation. Proper planning and installation are crucial for optimal performance. With a typical operational lifespan of 20 to 30 years [2], PV systems contribute significantly to a greener energy future by providing a low-carbon alternative to conventional energy sources and supporting climate change mitigation efforts [32], [33].

2.2.2.2 Understanding the Functioning of a Photovoltaic Cell

A photovoltaic cell is a type of semiconductor that has a P-N junction that is exposed to light. These cells are made from different types of semiconductors using various manufacturing processes. Currently, the most popular types of photovoltaic cells, such as monocrystalline and polycrystalline silicon cells, are only available on a commercial scale. Silicon photovoltaic cells are typically composed of either a thin silicon film or a thin layer of bulk silicon that is connected to terminals. To create a P-N junction, one side of the silicon layer is doped. Once the P-N junction is formed, a thin metallic grid is placed on the surface of the semiconductor that faces the sun [32], [34]. The physical structure of a PV cell is shown in Figure 2.3.

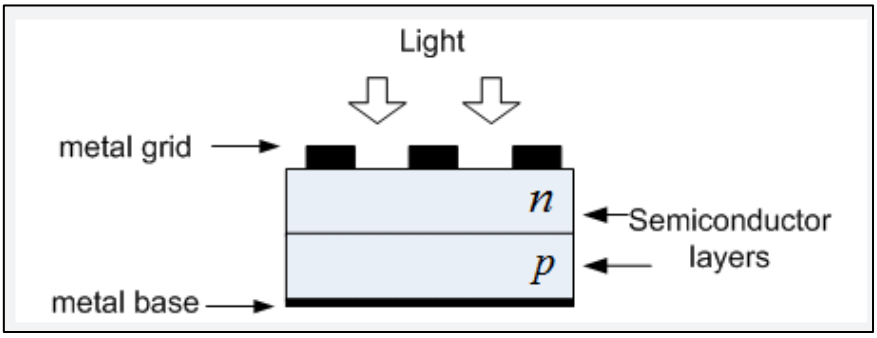

Figure 2.3:Physical structure of a photovoltaic cell.

When light strikes a photovoltaic cell, it generates charge carriers capable of producing an electric current under short-circuit conditions. These charge carriers are created when solar photons possess sufficient energy to break the covalent bonds between electrons and the semiconductor, liberating the electrons. This process is dependent on both the semiconductor material and the wavelength of the incident light. In essence, a PV device functions by absorbing solar radiation, generating, and

transporting free carriers at the P-N junction, and collecting the resulting electric charges at its terminals.

The production rate of electric charge carriers is influenced by the semiconductor's absorption capacity and the intensity of incident light. The absorption capacity is primarily determined by the semiconductor's band gap, surface geometry and treatment, temperature, and other factors. Solar radiation comprises photons with a spectrum of energies. Photons with energy below the PV cell's band gap threshold will not generate current. Conversely, photons with energy exceeding the band gap threshold will produce electricity [34].

While other semiconductor materials may have better conversion efficiency than silicon, they come at a higher cost, making their fabrication process economically unfeasible on a large scale. As a result, silicon remains the only commercially viable material for PV cell production.

2.2.3 Impact and integration of Renewable Energy Sources in Distribution Networks

The widespread adoption of RES systems has significantly transformed distribution networks, but it also introduces notable challenges. RES systems provide fluctuating power to the grid, leading to difficulties in balancing supply and demand, and causing voltage and frequency variations that can destabilize the network [35]. Such fluctuations can result in power system instability, potentially damaging sensitive equipment, causing power outages, and destabilizing the entire distribution network. Integrating RES systems into the distribution network, particularly at the Point of Coupling (POC), presents additional technical issues, including voltage and frequency regulation, protection coordination, and harmonic distortion [36], [37]. A comprehensive understanding of these impacts is crucial for maintaining a reliable and stable power supply [4].

In the early stages of RES system integration, only a few systems were connected to the distribution network, allowing for disconnection during faults and reconnection after the fault was resolved. However, with the increased penetration of RESs, this approach is no longer viable. Modern RESs (such as wind and photovoltaic system) contribute substantial power to the distribution network and disconnecting them during high generation can cause significant voltage and frequency variations, leading to production losses. To address these challenges, ESS such as batteries, pumped hydro, and compressed air storage are increasingly used in conjunction with PV systems [36].

ESS can store excess energy generated during periods of low demand and release it when demand is high, enhancing the reliability and predictability of RES and supporting a more stable integration into the distribution network [36], [37]. This approach not only improves the efficiency of RES integration but also contributes to reducing greenhouse gas emissions and combating climate change. The next section will provide an overview of ESS technologies.

2.3 Overview of Energy Storage System (ESS) Technologies

ESS involves the conversion of electrical energy into a form, that can be stored and then converted back into electricity for later use [38]. ESS technologies encompass a diverse range of storage mediums, including batteries, pumped storage hydro schemes, compressed air energy storage, flywheels, and thermal storage. Each technology offers unique characteristics in terms of energy storage capacity, efficiency, scalability, and cost-effectiveness. In this overview, we will explore the different types of ESS technologies, their working principles, and their applications, ranging from grid-scale to residential and commercial systems.

One prominent ESS technology is BESS. BESS utilizes rechargeable batteries to store and discharge electrical energy. It is widely studied due to its flexibility, fast response time, and scalability. BESS research focuses on optimizing performance, extending battery lifespan, improving efficiency, and developing advanced control strategies. These studies contribute to enhancing the capabilities and effectiveness of BESS in various applications such as voltage profile enhancement and support, ranging from grid-scale installations to residential and commercial systems. As the energy landscape continues to evolve, the advancement of ESS technologies, including BESS, holds great potential to transform the energy sector, promote RES integration, and enable a more sustainable and resilient energy future [3], [39], [40], [41].

2.3.1 Classification of Energy Storage System (ESS)Technologies

ESS technologies encompass a diverse range of storage mediums that can be classified based on two main criteria: function and form [3], [38], [40], [42]. Understanding these classifications is crucial for selecting the most appropriate storage solution for specific applications. The growing need for energy storage has driven continuous efforts to develop new storage system solutions that are more effective and cater to specific requirements.

When considering the form of energy storage, various technologies have emerged to meet different needs. These include Battery Energy Storage Systems (BESS), pumped storage hydro schemes, compressed air energy storage, flywheels, and thermal storage. Each of these technologies offers unique characteristics in terms of energy storage capacity, system efficiency, scalability potential, cost-effectiveness, response time, and operational lifetime [40], [42].

Among these technologies, BESS has gained prominence due to its flexibility, fast response time, and scalability [42], [43]. Current research in BESS focuses on optimizing performance, extending battery lifespan, improving efficiency, and developing advanced control strategies. These studies contribute to enhancing the capabilities and effectiveness of BESS in various applications, ranging from grid-scale installations to residential and commercial systems.

The selection of an appropriate energy storage technology requires careful analysis of fundamental characteristics and established benchmarks. This evaluation process ensures informed decision-making and optimal application of ESS technologies for various use cases. For a detailed comparison of secondary battery technologies, including their specific characteristics, strengths, weaknesses, and applications, readers can refer to Appendix A.

As the energy landscape continues to evolve, advancements in ESS technologies play a crucial role in transforming the energy sector. These developments promote renewable energy source (RES) integration and enable a more sustainable and resilient energy future [3], [39], [40]. The ongoing research and development in this field continue to expand the possibilities for energy storage applications across different scales and contexts.

2.3.2 Comparison and Characteristic of Energy Storage System (ESS)

Electricity cannot be directly and cheaply stored, but it can be stored in other forms and converted back to power when needed. According to [42], there are many ways of storing energy and each with their strength and weaknesses. Therefore, it is crucial to critically analyze the fundamental characteristics of ESSs to create benchmarks for selecting the best technology. ESSs play a crucial role in managing power supply, improving energy infrastructure resilience, and generating cost savings for utilities and consumers.

With a wide range of technological solutions available, it is important to assess the key features of each ESS types to establish benchmarks for selecting the most suitable technology. By conducting a critical analysis of their fundamental characteristics, informed decision-making can be achieved, ensuring optimal utilization of ESSs across different applications. ESS technologies can be classified into different types based on their structural mechanisms such as: mechanical, electrochemical, chemical, electrical, and thermal storage [44]. As shown below in Figure 2.4 ESS technologies are grouped based on several classifications, including characteristics or application.

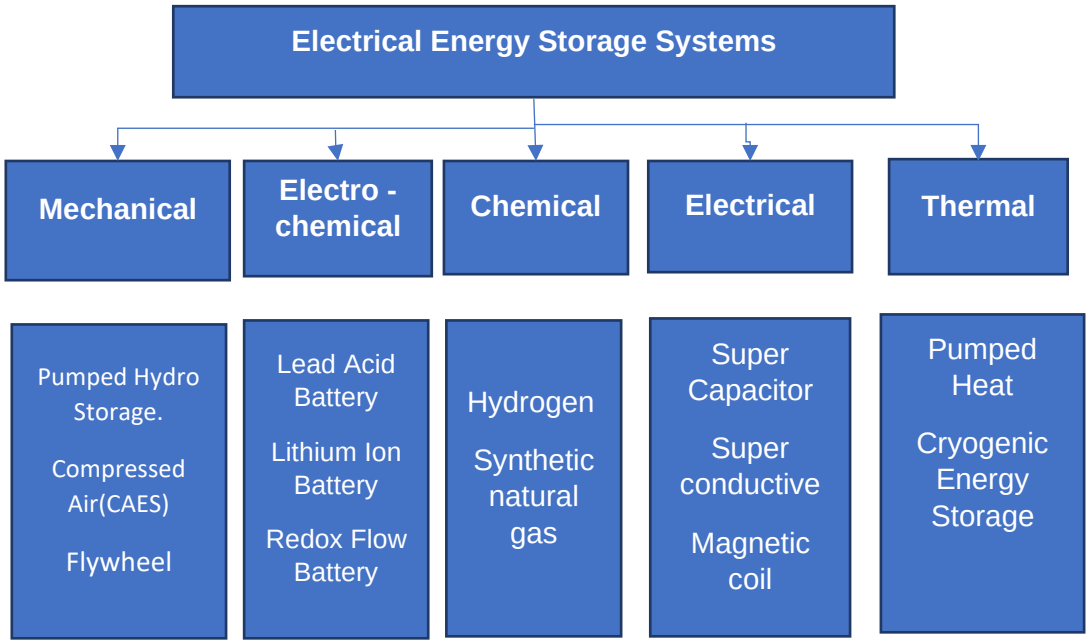

Figure 2.4:Common ESS technologies.

2.3.3 Review of Battery Energy Storage Systems (BESS) Technologies

BESS play an increased vital role in enabling the high integration of RESs and improving voltage and frequency variations leading to distribution network stability. The EES systems utilize various types of batteries, such as lithium-ion, sodium-sulphur, lead acid, and redox flow batteries, for grid applications [7]. Each type of battery offers unique characteristics in terms of energy density, efficiency, lifetime, and costs [9]. In this section, we will explore the key features of these secondary battery types and their suitability for energy storage applications, refer to appendix A for the key characteristics table of secondary battery types.

Among the commonly employed battery technologies used in EES are lead acid batteries, lithium-ion batteries, and sodium sulphur batteries. Each of these battery types has its advantages and disadvantages regarding energy storage capacity, efficiency, lifespan, and visual considerations. Understanding the characteristics of each battery type is essential in selecting the most suitable option for specific energy storage requirements. The table in appendix A outlines the key characteristics of each secondary battery type [3], [7]. This includes the battery type, characteristics, strength, weakness, and applications.

2.3.3.1 Battery Technology Comparison

According to [3], lithium-ion batteries have emerged as the preferred technology for BESS in distribution networks. Their flexibility, efficiency, and numerous advantages make them the technology of choice. Lithium-ion batteries offer high energy density, allowing for the storage of a significant amount of energy in a compact size. They also exhibit fast charging and discharging capabilities, enabling quick response times to meet fluctuating energy demands. Furthermore, lithium-ion batteries have a longer lifespan compared to other battery technologies and require minimal maintenance.

The advantage of lithium-ion batteries is evident in their higher power and energy density, ensuring greater storage capacity and efficient energy utilization. In addition, they boast high efficiency levels, allowing for maximum energy conversion during charging and discharging processes. Furthermore, lithium-ion batteries have low daily self-discharge rates, minimizing energy loss when the batteries are not in use.

Considering these factors, the industry has tremendously embraced lithium-ion batteries for their superior performance and reliability [7]. The costs for lithium batteries have been dropping drastically over the years. Their widespread adoption is reflected in their use as the preferred choice for BESS technology in various applications within the power distribution network grids [45], [46].

2.3.3.2 Battery Energy Storage System Components

The BESS consists of several key components:

2.3.3.2.1 Power Conversion System (PCS)

The Power Conversion System, also known as a converter or inverter, is a crucial component in ESS like PV and wind generators. Its main function is to convert power between AC and DC during charging and discharging of the storage. During discharging, it converts DC power from the storage cells to AC power for the grid, and during charging, it converts AC power from the grid to DC power for the storage cells. The size of the converter determines the power output of BESS and is measured in watts (W, kW, MW). The converter has a longer lifespan compared to the storage cells.

The PCS is essential in the BESS as it efficiently converts electrical energy between AC and DC forms. It consists of power electronic components like inverters and converters, enabling bidirectional power flow between the battery and the electrical grid [47]. During charging, the PCS converts AC power from the grid into DC power for storage, and during discharge, it converts DC power from the battery back into AC power for the grid or local demand [48].

The PCS plays a critical role in ensuring the stability, reliability, and power quality of BESS. PCS regulates voltage and frequency, manages overall power system performance, and incorporates advanced control systems to optimize charging and

discharging processes, maximizing energy transfer efficiency, and extending battery lifespan [7]. Additionally, the PCS includes protection mechanisms such as overcurrent and overvoltage protection to safeguard the battery and connected electrical equipment [3], [7].

2.3.3.2.2 Battery Management System (BMS)

The BMS plays a critical role in controlling and monitoring the performance of batteries in various applications. One of its primary functions is ensuring safety by continuously checking for overcurrent, over/under voltage, and over/under temperature conditions [7]. When the battery operates outside the safe range, the BMS takes appropriate actions such as opening a switch to disconnect the battery or sending warnings to replace the battery. It also activates fans or heaters to regulate the ambient temperature and prevent thermal issues [7], [49].

In addition to safety measures, the BMS monitors the performance of the battery. It calculates the state of charge (SOC), which is a dynamic measure of the amount of dispatchable energy available in the battery. The SOC provides crucial information about the battery's current energy level. The BMS also evaluates the state of health (SOH), which reflects the general condition and expected capacity of the battery based on its historical operation and environmental factors. This information is valuable for determining the overall health and remaining lifespan of the battery [7], [46], [49], [50].

The BMS further tracks the number of charge-discharge cycles the battery undergoes, which is essential for estimating its aging and performance degradation. This cycle count data helps in assessing the battery's usage patterns and predicting its future performance. Furthermore, the BMS communicates important information to the charge controller, enabling efficient and optimized charging of the battery. Overall, the BMS serves as a vital component in managing and optimizing the performance, safety, and lifespan of batteries in various applications [7], [50].

2.3.3.2.3 AC power transformer

The function of the transformer is to step up the AC voltage from low voltage (LV) to medium voltage (MV) when the BESS is discharging to the grid. It also steps the voltage down when the BESS storage is charging. The actual parameters (voltage and power ratings) may be different for different BESS manufactures and distribution network requirements. The transformer is sized such that it is bigger than the converter rating to ensure that the storage is fully utilised for the benefit of the grid.

2.3.4 Distribution Network Connection for Utility-Scale BESS

Figure 2.5 provides an overview of the distribution network connection topologies for utility-scale BESS system. These systems typically consist of multiple battery packs and inverter units, which collectively contribute to the overall system's energy and power capabilities, [3] The figure illustrates different configurations for integrating power electronics with battery packs, as shown in the Figure 2.5.

- Figure 2.5(a): Battery packs connected in parallel to individual DC/AC converters to a common direct current (DC) bus.
- Figure 2.5 (b) Battery packs connected in parallel to two individual DC/AC converters to a common direct-current (DC) bus.
- Figure 2.5(c): System connection at a low-voltage level.
- Figure 2.5 (d): Connection to higher system levels through a transformer.

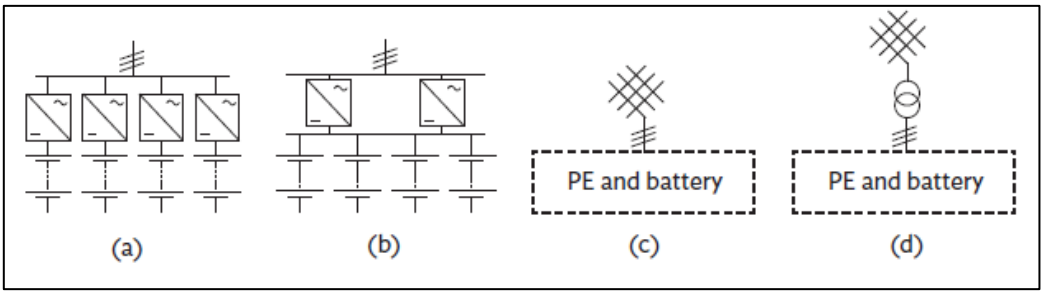

Figure 2.5:Distribution network connections of utility-scale BESSs.

2.3.5 BESS Use Cases & Applications in Distribution Networks

Integrating BESS into distribution networks provides various advantages and support services, benefiting Distribution System Operators (DSOs), DG plant owners, energy retailers, and customers [7]. The rise of disruptive technologies and significant advancements in battery technology have made the combination of RES and BESS particularly effective. This pairing addresses the intermittent nature of RES by storing and dispatching excess power generated from RES [50].

However, the functionality and applicability of BESS have become increasingly diverse, offering a range of set benefits beyond simply supporting the intermittent dispatch nature of disruptive technologies, such as peak-load shaving, demand response, frequency and voltage support, and grid investment deferrals [9], [10], [51], [52]. This advancement has transformed BESS from a technology that solely supports capacity firming into a standalone disruptive technology [3] A single BESS can have multiple use cases, however there can only be one primary use case that the BESS is strictly designed for [7]. The following table 2.1 is a short list of some of the identified use cases for BESS in distribution network [10] and the figure gives a detailed summary of the BESS functions:

Table 2.1:Some of the BESS use cases and application.

USE CASE	DESCRIPTION
Capacity Firming	For small fluctuations in intermittent renewable energy generation
Schedulable Capacity/ Ramping Support (Peak Shaving)	Bulk supply available to meet scheduled demand on the system for a limited time.
Voltage Support	Reactive power absorption or supply to bring voltages within allowable range.
Bottleneck Management / Congestion Relief	Storage and delayed dispatch of locally generated energy to alleviate upstream congestion
Load levelling / Peak shaving for grid upgrade deferral	Reducing limited time peak loads to assist with deterministic planning requirements
Electrification	Off grid systems
Reliability (Islanding)	Micro grid / islanded operation during planned or unplanned system outages.

2.3.6 BESS States and Planning Parameters for BESS Integration

Table 2.2 encompasses a broad range of use cases in the field of distribution network planning. These cases span from basic steady-state application studies to more advanced dynamic level studies, focusing on sizing and placement considerations before integrating BESS into distribution networks. To facilitate the integration process, it is crucial to identify the pertinent network planning parameters that need to be assessed based on the different operational states of a BESS system.

Unlike conventional generators, BESS operates in three active states: charging, discharging, and idle [9]. During the charging state, the BESS functions as a load, whereas during the discharging state, it behaves as a generator [53]. These two operating states have distinct impacts on the network, necessitating specific evaluations. Table 2.2 outlines the distribution planning parameters that require monitoring and evaluation to successfully integrate BESS into the network for various operating states within the DigSilent PowerFactory software.

Table 2.2:Parameters for BESS Integration in Distribution Networks.

Assessment Criteria	Bess Operating State	Limits Applied	Reference
Network Voltage Limits.	Charging & Discharging.	(0.95 – 1.05pu)	Distribution Voltage Regulation and Apportionment Limits Standard (240-70465489).
Network Thermal Limits	Charging & Discharging.	(Rate A – Normal Rating)	Network Planning Guideline for Transformers (240-105735370). Network Planning Guideline for Lines & Cables (240-61227438).

Rapid Voltage Change	Charging & Discharging	(5%)	Rapid Voltage Change Limit for BESS Integration Studies for Planning (240-146900837).
Load & Generation Rejection	Charging & Discharging	(0.90 – 1.1pu)	Voltage Characteristics, Compatibility Levels, Limits and Assessment Methods (NRS 048 - 2, 2007).
Fault Level	-	(Equipment Fault Level Ratings)	Short-Circuit Current Management Policy (46-2460).

2.4 Sizing and placement of Battery Energy Storage Systems in Distribution network integrated with PV System

The optimal placement of BESS in distribution networks with high penetration of PV systems is a critical challenge in modern power system planning. As the integration of PV systems increases, distribution networks face issues such as voltage fluctuations, reverse power flow, and power quality problems, etc. Strategic placement of BESS can effectively mitigate these challenges by providing voltage support, power flow control, and energy time-shifting capabilities.

It is important to note that while this dissertation focuses primarily on the optimal placement of BESS, the sizing of BESS was not within the scope of work. Instead, a reference size for BESS was used, based on considerations such as:

- The deficit during peak demand
- Historical load growth over the past ten years
- The lifespan of the BESS plant
- Additional power required to meet load demand.
- Inverter size
- Assistance in achieving N-1 contingency in case of losing one of the two auto transformers (132/66/11kV) at Witzenberg substation.

However, it is crucial to highlight that the effectiveness of BESS in addressing network issues is highly dependent on both its location and size. While optimal placement ensures that the BESS is positioned where it can have the most significant impact on network performance, proper sizing is equally crucial. An undersized BESS may fail to adequately address the network's needs, particularly during peak PV generation or high demand periods. On the contrary, an oversized BESS represents an inefficient use of resources and increased capital costs.

The simulation results from this dissertation focus specifically on optimal BESS placement, though research indicates that sizing and placement of BESS go hand in hand to achieve optimal benefits. While a dual optimization approach could potentially enhance system performance further, this research deliberately concentrated on placement optimization due to several practical constraints: (1) predetermined BESS sizes are often dictated by utility budget limitations and available installation space, (2)

the computational complexity of simultaneous size-location optimization would have significantly increased solution time, and (3) focusing on placement optimization alone enables more detailed analysis of location-specific impacts on system performance.

BESS sizing and placement in a distribution network with penetration of RES should consider various factors such as the location of the RES, the load profile, and the voltage profile of the distribution network. The energy storage requirements and the system's power rating are critical aspects of BESS sizing. On a PV system coupled distribution network, BESS should be capable of storing excess power generated by the PV system and discharging it when the PV system is underproducing.

BESS placement is crucial in enhancing voltage profile improvement, loss minimization, power quality, reduction of line congestions, and overall distribution network enhancement. The placement should consider the distance between the BESS and the RES, the distribution substation, and the load centers to minimize transmission losses and improve the voltage profile [25], [54].The economic yield and costs associated with implementing the BESS also play an important role in both sizing and placement decisions [55]. Proper deployment of BESS is crucial, as improperly sized or placed systems can lead to negative consequences and further exacerbate voltage variations arising from fluctuations [56].

While this dissertation focused on optimal placement using a reference size, it is evident from the literature and simulation results that the sizing and placement of BESS in a distribution network with heavy RES penetration are interlinked and crucial in ensuring improvement of voltage stability, reduction of active power losses, and improvement of overall system efficiency [9], [25], [57]. Future studies could benefit from incorporating both sizing and placement optimization to achieve the full potential of BESS in distribution networks.

BESS placement is also crucial in enhancing voltage profile improvement, loss minimization, power quality, reduction of line congestions and overall giving guarantees to distribution network enhancement. The placement of BESS should consider the distance between the BESS and the RES, the distribution substation, and the load centres. BESS should be located close to the RES and the load centres to minimize transmission losses and improve the voltage profile of the distribution network grid as shown in figure 2.6.

On a PV-coupled grid, the battery will need to be capable of storing the excess power generated by the PV system and discharging the power when the PV system is underproducing power. The optimal sizing of the battery depends on the PV system, its location, how it is installed, climatic conditions, and cloud cover [55]. The economic yield and the costs associated with implementing the BESS also plays an important role in the BESS sizing.

The use of BESS in a distribution network with heavy RES penetration can enhance the network grid voltage support by providing backup power during periods of low -

RES output thereby reducing the voltage variations. The BESS can also help to mitigate the effects of voltage fluctuations caused by the intermittent nature of the RES [44], [54], [58]. The economic yield and the costs associated with implementing the BESS also play an important role in the BESS sizing.

Additionally, the impact of both placement and size of BESS was evaluated on a photovoltaic-based distributed generation network, with the aim of enhancing voltage stability using grid code technical limit criteria tests. It was found that the proper deployment and sizing of BESS is crucial, as improperly sized or placed systems can lead to negative consequences and further exacerbate voltage variations arising from fluctuations. the use of BESS can help to reduce the loading on distribution network grid lines and transformers. The BESS can store excess energy during periods of low demand and discharge it during periods of high demand, thereby reducing the reverse power flow (RPF) load on transmission lines and transformers [25].

Therefore, the sizing and placement of BESS in a distribution network grid with heavy RES penetration are crucial in ensuring improvement of voltage profile regulation in distribution network. The use of BESS can also help to reduce the loading on distribution network lines and transformers, thereby improving the overall efficiency of the distribution network. Figure 2.6 below shows integration of BESS in a distribution network with a penetration of PV systems.

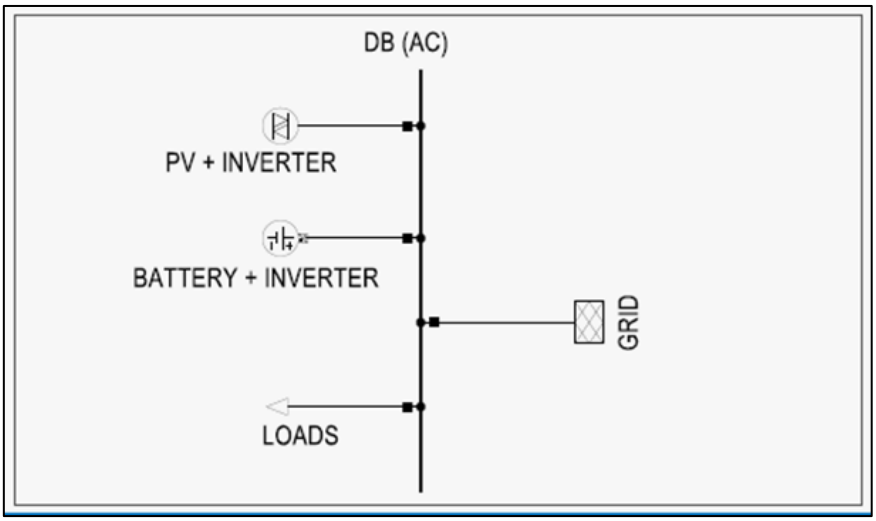

Figure 2.6: Placement of BESS and PV System model in DigSilent PowerFactory.

2.5 Voltage Profile Improvement and Power Loss Reduction

The strategic placement of BESS can notably enhance voltage profiles and decrease power losses within distribution networks [73], [85]. When integrating BESS, several key factors must be considered, including their voltage regulation capabilities, the impact on power flow and network losses, and their interaction with existing voltage control devices. Additionally, compliance with grid codes and standards is crucial [50].

To quantify improvements in voltage stability, metrics such as the Percentage Voltage Deviation Index (PVDI) are employed.

2.6 Optimization Techniques for BESS Placement

The optimal placement of BESS in distribution networks is a complex optimization problem that requires sophisticated techniques to maximize benefits and minimize potential negative impacts. This section introduces two prominent Artificial Intelligence (AI) methods used for this purpose: Genetic Algorithms (GAs) and Particle Swarm Optimization (PSO). These techniques are adaptive heuristic search methods inspired by natural processes, designed to solve complex optimization problems efficiently. Both GAs and PSO have gained significant attention in recent years due to their effectiveness in managing multi-dimensional, non-linear, and multi-modal optimization challenges [59].

GAs is based on evolutionary principles such as natural selection and genetics, utilizing random search strategies to solve optimization problems. They are known for their simplicity, robustness, and quick convergence [60]. In contrast, PSO simulates swarm intelligence by drawing inspiration from the collective behaviour of natural swarms, employing evolutionary computation principles to achieve optimization goals [61], [62].

Optimization techniques are essential for addressing complex problems in various fields, including engineering, finance, and science [63]. Both GA and PSO have garnered significant attention for their effectiveness in managing multi-dimensional, non-linear, and multi-modal optimization challenges.

These nature-inspired metaheuristic algorithms, including GAs and PSO, are essential for addressing complex problems across various fields such as engineering, finance, and science [61]. An overview of these algorithms highlights their fundamental principles, applications, and recent advancements. Both GAs and PSO involve autonomous agents that work collaboratively to achieve specific objectives without human intervention. In the context of BESS placement, these optimization techniques are crucial for maximizing benefits and minimizing negative impacts [61], [64].

2.6.1 Genetic Algorithm (GA)

The GA is a widely used metaheuristic optimization technique inspired by the principles of natural selection and evolution as described by Charles Darwin theory of natural evolution [65]. Introduced by John Holland in 1975, GAs are artificial intelligence methods that simulate evolutionary processes to solve complex optimization problems. The algorithm evolves a population of potential solutions over multiple generations to find the optimal or near-optimal solution [66].

GA operates by starting with an initial population of candidate solutions, known as chromosomes. Each chromosome represents a possible solution to the problem and is evaluated based on a fitness function. The algorithm then generates subsequent generations through processes such as selection, crossover, and mutation. In each generation, the chromosomes are assessed for their fitness, and new offspring are created by combining or modifying existing chromosomes. The process continues iteratively until convergence is achieved, meaning the fitness function value stabilizes or changes minimally. The goal is to converge on the best solution to the problem at hand.

In this dissertation, GA was utilized to optimally determine the placement of BESS within distribution networks with penetration of PV systems. The optimization is performed using MATLAB environment, and the specific GA implementation is detailed in Appendix J.1, which includes the relevant objective functions discussed in Chapter 3. Genetic Algorithms are particularly effective for solving non-linear or non-differentiable optimization problems, making them suitable for the complex integration of electrical units [66]. Figure 2.7 provides a flow chart of the basic GA process, illustrating how the algorithm evolves solutions over generations.

The flow chart of the algorithm is presented in Figure 2.7 below.

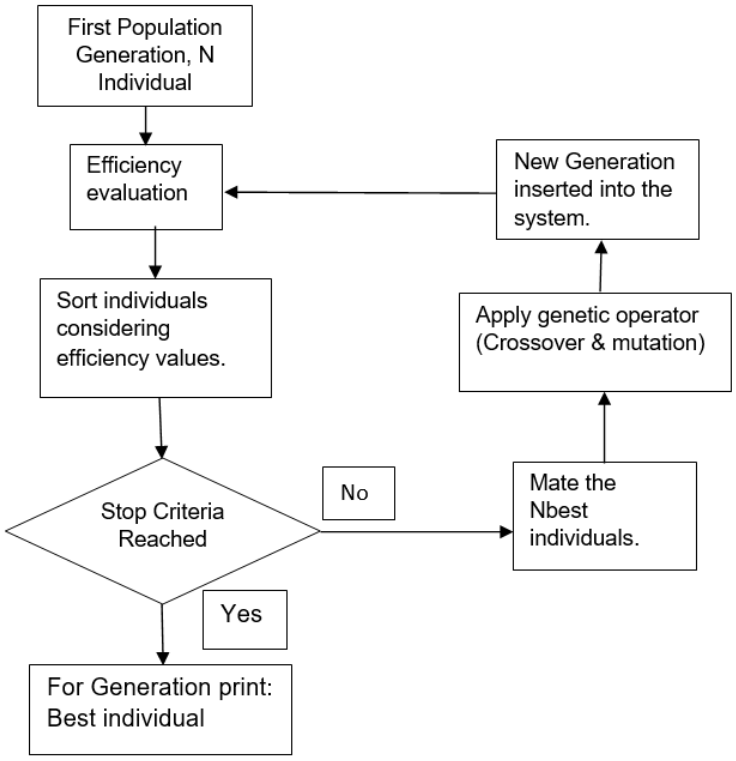

Figure 2.7: Basic Genetic Algorithm flow chart.

2.6.2 Particle Swarm Optimization (PSO)

PSO is an intelligent, swarm-based algorithm classified under metaheuristics. It draws inspiration from the social behaviour observed in flocks of birds and schools of fish, applying these principles to computational optimization problems. Despite its simplicity, PSO is a powerful tool that has been effectively utilized across a range of fields, including machine learning, data mining, operational research, and computer graphics [65].Introduced by James Kennedy and Russell C. Eberhart in 1995, PSO was initially developed to model social behaviour in animals [64].

They recognized the potential to adapt this model for optimization purposes, leading to the creation of PSO. Since then, PSO has become a widely adopted algorithm for solving various optimization challenges due to its straightforward implementation and adaptability. The algorithm simulates interactions among a swarm of particles, each representing a search agent working towards an optimal solution. The effectiveness of PSO is heavily dependent on its parameters, which need to be optimally tuned to enhance performance [67], [68].

PSO has been extensively applied to optimize the placement and sizing of BESS in distribution networks. This includes improving voltage profiles, reducing power losses, and enhancing overall network performance [11], [69], [70]. In this dissertation, PSO is utilized to optimally determine the placement of BESS within distribution networks with high penetration of PV systems. The optimization is performed using MATLAB, and the specific PSO implementation is detailed in Appendix J.2, which includes the relevant objective functions discussed in Chapter 3. Figure 2.8 illustrates the basic block diagram of Particle Swarm Optimization.

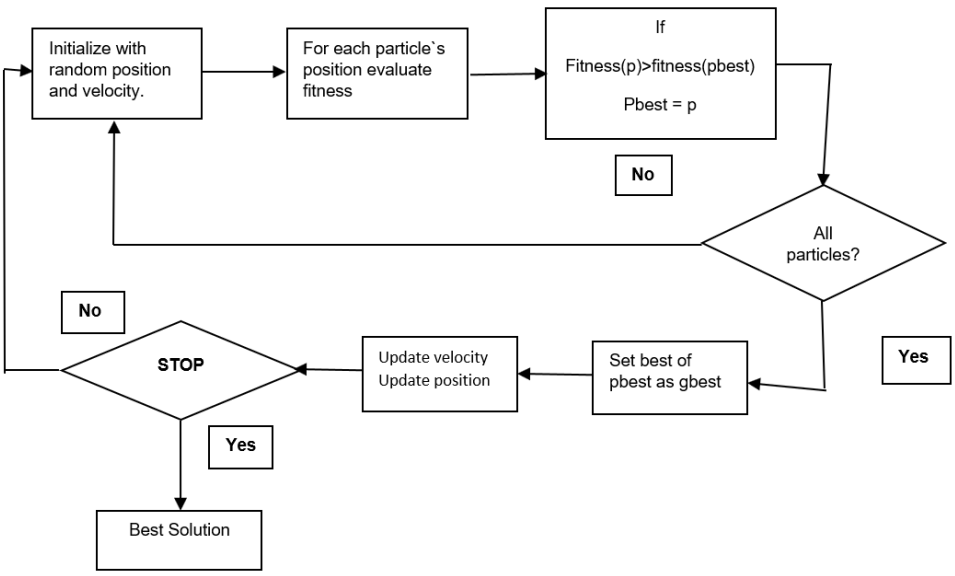

Figure 2.8: Basic block diagram of Particle Swarm Optimization

Although PSO generally converges more effectively than some other optimization methods, it can still suffer from premature convergence. To address this issue, [63] proposed a competitive-based PSO approach to optimize the levelized cost of energy and electricity generation costs while integrating renewable energy sources into distribution networks. This variant update particle positions through a competitive mechanism applied to randomly selected pairs of particles, rather than relying solely on personal and global best positions.

In [67], PSO was applied to the optimal placement of BESS in an IEEE 33-bus system, where the costs of power losses and voltage deviations were incorporated into the optimization model. The results, compared with those obtained using the Fmincon MATLAB solver, helped determine the optimal BESS locations. Similarly, [71] focused on the optimal siting and sizing of BESS in a distribution network with RES. By minimizing costs associated with voltage deviations, power losses, and peak demands, PSO and GA were used to improve network performance. The installation of BESS led to reduced voltage deviations, power losses, and peak demands compared to scenarios without BESS [11].

Overall, PSO has proven effective in optimizing BESS placement in distribution networks, achieving notable improvements such as a 50% reduction in active power losses and enhanced voltage profiles in various simulation studies [60], [72], [73].

Advantages and Limitations

PSO has many advantages which include:

- Fast convergence rate in comparison to most optimization techniques including Genetic Algorithm.
- The search can be carried out by the speed of the particle, since it has no overlapping and mutation calculation like GA.
- Optimist particle can transmit information onto other particle during the development of several generations, and it has a very fast searching speed.

The only major limitations of PSO are:

- They produce less accurate results at regulation speed, this is because they easily suffer from partials optimism.
- Non-coordinate problems such as the solution to the energy field and the moving rules of the particles in the energy field, application of the method may not work out properly.
- May converge prematurely in some cases, performance can be sensitive to parameter settings, may struggle with highly multi-modal problems.

2.6.3 Comparison of PSO and GA for BESS Optimal Placement

Both Particle Swarm Optimization (PSO) and Genetic Algorithm (GA) are effective for determining optimal Battery Energy Storage System (BESS) placement. PSO is suitable for smaller problems where quick convergence and computational efficiency are prioritized, offering good solutions but struggling with complex, high-dimensional systems due to its tendency to get stuck in local optima. On the other hand, GA is slower to converge initially but is better suited for large-scale, complex problems, offering higher solution quality and robustness. Although it is computationally less efficient, GA's ability to explore the solution space and find the global optimum makes it ideal for problems with multiple constraints or non-linearities. Ultimately, the choice between PSO and GA depends on the problem size, complexity, and solution requirements. For dynamic or real-time optimization, PSO is preferred, while GA is more appropriate for large-scale tasks that require robust solutions.

2.7 Summary

This literature review has provided an overview of the key concepts and technologies relevant to the optimal placement of BESS in distribution networks with high PV system penetration. It has highlighted the challenges associated with RES integration, the potential of BESS as a solution, and the optimization techniques used to determine optimal BESS placement. The review sets the foundation for the subsequent chapters, which will detail the mathematical modelling, problem formulation, and analysis of BESS placement in the Witzenberg distribution network.

Chapter 3 : Mathematical Modelling and Problem Formulation

This chapter presents a comprehensive overview of the mathematical modelling and problem formulation for the sampled Witzenberg distribution network. This section focuses on a modified 16-bus distribution network. This model includes various important components of the Witzenberg distribution network which includes power transformers, overhead power lines, PV system, loads, and shunt filter capacitors.

The mathematical model summarizes the electrical characteristics and interactions of the network components. The network model provides a foundation for analysing power flow, voltage profiles, and network power losses. This model serves as the basis for subsequent optimization studies, for strategic location for BESS placement to improve voltage profile deviations regulations and reduction of active power losses in the Witzenberg distribution network.

3.1 Voltage Profiles and Loading Violations

The load flow analysis of the Witzenberg distribution network reveals significant voltage profile variations across its three primary voltage levels: 132 kV, 66 kV, and 11 kV. The 132 kV buses (1, 3, 6, 10, 12, 13, and17) generally operate within acceptable limits, with voltages ranging from 0.94 to 1.04 per unit (p.u.), though bus 13 notably underperforms at 0.94 p.u. In contrast, the 66 kV buses (2, 4, 5, 7, and 14) level presents substantial under-voltage conditions across all buses with voltages spanning from 0.83 to 0.88 p.u., indicating a critical need for voltage profile enhancement and support. Bus 7 presents the most severe case at 0.83 p.u., deviating 17.6% below nominal voltage.

The 11 kV tertiary windings at Witzenberg substation also operate below standard at 0.88 p.u. These results underscore the necessity for targeted voltage profile enhancement measures, particularly at the 66 kV and 11 kV levels. The objective of this research work is to remedy this situation and enhance the voltage profile while reducing active power losses. While traditional solutions like reactive power compensation or transformer tap changer adjustments could address these voltage issues, the increasing penetration of Renewable Energy Sources (RESs) in this network requires more flexible solutions. This dissertation investigates the optimal placement of Battery Energy Storage Systems (BESS) to address both voltage regulation challenges and the intermittency of renewable generation.

3.2 Witzenberg Distribution Network Overview

The Witzenberg network is supplied on a radial 132kV line from Romansrivier substation (bus 10) which is supplied from Bacchus MTS (bus 1) via Boskloof switching station (bus 3). Boskloof switching station (bus 3) also supplies Hex (bus 6) and Klipdrif substations (bus 17) which supply the Worcester and Ashton areas respectively. Boskloof also supplies load towards the interconnected Droerivier MTS via the Quarry traction substation (bus 9). The Touwsrivier IPP which generates 36MW PV is connected to Touwsrivier substation (bus 12) which cuts in and out of the Boskloof-Quarry 132kV line.

Witzenberg substation (bus 13) is installed with 2x80MVA 132/66/11kV transformers which supply Gydo (bus 5) and Leeurivier (bus 7) to the north, Slagboom (bus 11) to the west, and Ceres (bus 4) and Bon Chretien (bus 2) to the south. It also supplies an 11kV load off the tertiaries (2x10MVA) of the transformers. The Witzenberg distribution network diagram model in DigSilent PowerFactory 2023 overview is shown in appendix C.

Table 3.1 below gives an overall summary list of all the components utilized to model the sampled modified Witzenberg distribution network for this dissertation.

Table 3.1: Witzenberg Distribution network overall list of components

Number of Voltage Levels	Number of Buses	Number of lines	Number of 3 winding Transformers	Number of PV Systems	Number of loads	Number of Shunt / Filters
3	16	14	2	1	14	1

Table 3.2 is the list of the external network main feeder summary parameters. Therefore, the transmission network is replaced at Bacchus substation by the external network since the transmission network is not part of the scope of work of this study.

Table 3.2: List of the external network main feeder summary parameters.

Name	Terminal	Active Power (MW)	Reactive Power (Mvar)	Apparent Power (MVA)	Voltage Setpoint (p.u)
Bachus 132kV	Bus 1	61.9	67.1	91.3	1.04

3.2.1 Line Parameters Modelling

The network consists of overhead (OH) power lines operating at 132 kV and 66 kV levels with lengths ranging from 3.6 km to 50.2 km. Since the network is an AC network all the lines modelled are AC lines operating at 50Hz. The only direct current in the

network is for BESS system. Table 3.3 displays information about the modified Witzenberg distribution network HV power lines. The phase and earth conductors were selected based on the rated voltage expected to be applied across the conductors and the rated current expected to flow through the conductors. Line data is unique for each line. Below is Table 3.3 which gives the parameters for each distribution line.

Table 3.3: Distribution Line parameters between distribution network substation buses.

Name	Bus I & J (Sending / Receiving)	Length in km	R_1 Ohms (Ω)	X_1 Ohms (Ω)	R_0 Ohms (Ω)	X_0 Ohms (Ω)
Bacchus – Boskloof 132_1	Bus 1 _ Bus 3	25.59	1.54	8.26	91.11	10.79
Bacchus – Boskloof 132_2	Bus 1 _ Bus 3	25.59	1.54	8.26	91.11	10.79
Bon Chrestien – Ceres 66_1	Bus 2 _ Bus 4	3.66	0.43	1.33	11.48	1.38
Boskloof – Touwsriver 132_1	Bus 3 _ Bus 12	50.20	10.52	21.69	134.21	30.61
Boskloof – Touwsriver 132_1(1)	Bus 3 _ Bus 12	50.20	10.52	21.69	134.21	30.61
Boskloof – Hex 132_1	Bus 3 _ Bus 6	3.55	0.74	1.53	9.49	2.16
Boskloof – Hex 132_1(1)	Bus 3 _ Bus 6	7.10	1.49	3.07	18.98	4.33
Boskloof – Klipdrif 132_1	Bus 3 _ Bus 17	43.70	9.16	18.88	116.83	26.65
Boskloof – Romansrivier 132_1	Bus 3 _ Bus 10	40.37	4.83	17.17	109.48	20.56
Boskloof – Romansrivier 132_2	Bus 3 _ Bus 12	40.37	4.83	17.17	109.48	20.56
Ceres – Witzenberg 66_1	Bus 4 _ Bus 16	17.00	2.02	6.17	53.34	6.41
Gydo – Witzenberg 66_1	Bus 5 _ Bus 14	10.62	1.64	3.91	33.24	3.55
Gydo _ Leeurivier 66_1	Bus 5 _ Bus 7	26.99	8.61	10.84	77.11	14.67
Romansrivier – Witzenberg 132_1	Bus 12 _ Bus 13	40.40	4.83	16.81	112.31	17.41
Slaagboom – Witzenberg 66_1	Bus 11 _ Bus 14	5.92	5.52	2.73	14.86	7.93

where:

- R_1: Positive sequence resistance of the line (Ω/km).
- X_1: Positive sequence reactance of the line (Ω/km).
- R_0: Zero sequence resistance of the line (Ω/km).
- X_0: Zero sequence reactance of the line (Ω/km).
- i: Sending end bus number.
- j: Receiving end bus number.

These parameters are essential for power flow analysis and fault calculations in three-phase distribution systems.

3.2.2 Load Modelling

The load data for the Witzenberg distribution network provides valuable insights into the power consumption patterns and characteristics across various buses. This information is crucial for understanding the network's behaviour and identifying potential areas for voltage profile improvements and active power loss reduction. The network demonstrates a diverse range of loads across the different network voltage levels. The total active power demand is approximately 123.6 MW, with reactive power consumption of about 31.7 Mvar. This results in the distribution network power factor of approximately 0.97, indicating generally good power factor correction practices. At the 132 kV level, loads are present at HEX, Quarry, and Klipdriff substations, with Klipdriff having the largest load (20 MW, 5 Mvar). The 66 kV network hosts most of the loads, with significant demand at Bon Chrestien (two loads totalling 27.8 MW), Gydo (15.9 MW), and Ceres (10 MW). The 11 kV loads at Witzenberg substation, connected through tertiary windings, each demand 6.4 MW. The power factors across the network are high ranging from 0.94 to 0.99, with most loads above 0.96.

The AI algorithms techniques for optimal BESS placement will consider these load characteristics, focusing on areas with high power demand, lower voltage magnitudes, and slightly lower power factors. The dissertation aims to improve voltage profile enhancement especially in the 66 kV network, reduce overall network active power losses, and enhance the network's ability to handle load variations efficiently. Table 3.4 contains a list of all the load parameters.

Table 3.4: Witzenberg Distribution network load data.

Bus Name	Bus	Voltage per Unit (p.u)	Active Power (MW)	Reactive Power (Mvar)	Apparent Power (MVA)	Power Factor (pf)
Bon Chrestien LD1	2	0.85	13.90	3.10	14.30	0.977
Bon Chrestien LD2	2	0.85	13.90	5.10	14.80	0.94
Ceres LD1	4	0.85	10.00	3.60	10.60	0.94
Gydo LD1	5	0.86	15.90	4.20	16.40	0.966
General Load	10	0.99	0.00	0.00	0.00	1
General Load (1)	1	1.04	0.00	0.00	0.00	1
HEX LD1	6	1.02	10.50	2.50	10.80	0.973
Leeurivier LD1	7	0.82	5.80	0.90	5.90	0.99
Leeurivier LD2	7	0.82	5.80	1.60	6.10	0.962
Quarry LD1	9	1.03	10.00	2.50	10.30	0.97
Slaagboom LD1	11	0.87	5.00	1.20	5.10	0.971
Witzenberg 11 KV LD1	15	0.88	6.40	1.00	6.50	0.987

Witzenberg 11 KV LD2	16	0.88	6.40	1.00	6.50	0.987
Klipdriff LD1	17	1.01	20.00	5.00	20.60	0.97
Bon Chrestien LD1	2	0.85	13.90	3.10	14.30	0.977
Bon Chrestien LD2	2	0.85	13.90	5.10	14.80	0.94
Ceres LD1	4	0.85	10.00	3.60	10.60	0.94
			123.6	31.7	127.9	

3.2.3 Transformer Basic Data Modelling

The mathematical modelling of the Witzenberg distribution network focusses on the distribution network optimization problem aimed at enhancing voltage profiles deviation improvement and reducing active power losses. The model is built around two key 132/66/11 kV power auto transformers, each rated at 80/80/10 MVA, with known impedance parameters and loss characteristics as shown in figure 3.1 and appendix E. The two x 3 winding transformers equipped with On-Load Tap Changers (OLTCs), are modelled as sub transmission lines with series impedances and shunt admittances, incorporating discrete tap ratios that can vary between minimum and maximum values.

The optimization problem is formulated with two primary objectives: improvement of voltage profile deviation from nominal values across all buses and minimizing total active power losses. These objectives are subject to constraints including voltage limits ($0.95 \leq Vi \leq 1.05$ p.u.), reduction of active power losses. Table 3.5 below contains a list of all the load parameters. Transformer parameters used in the model are summarised in Table 3.5 below for 2x 3 - winding transformers. Some of the parameters are included in Figure 3.1.

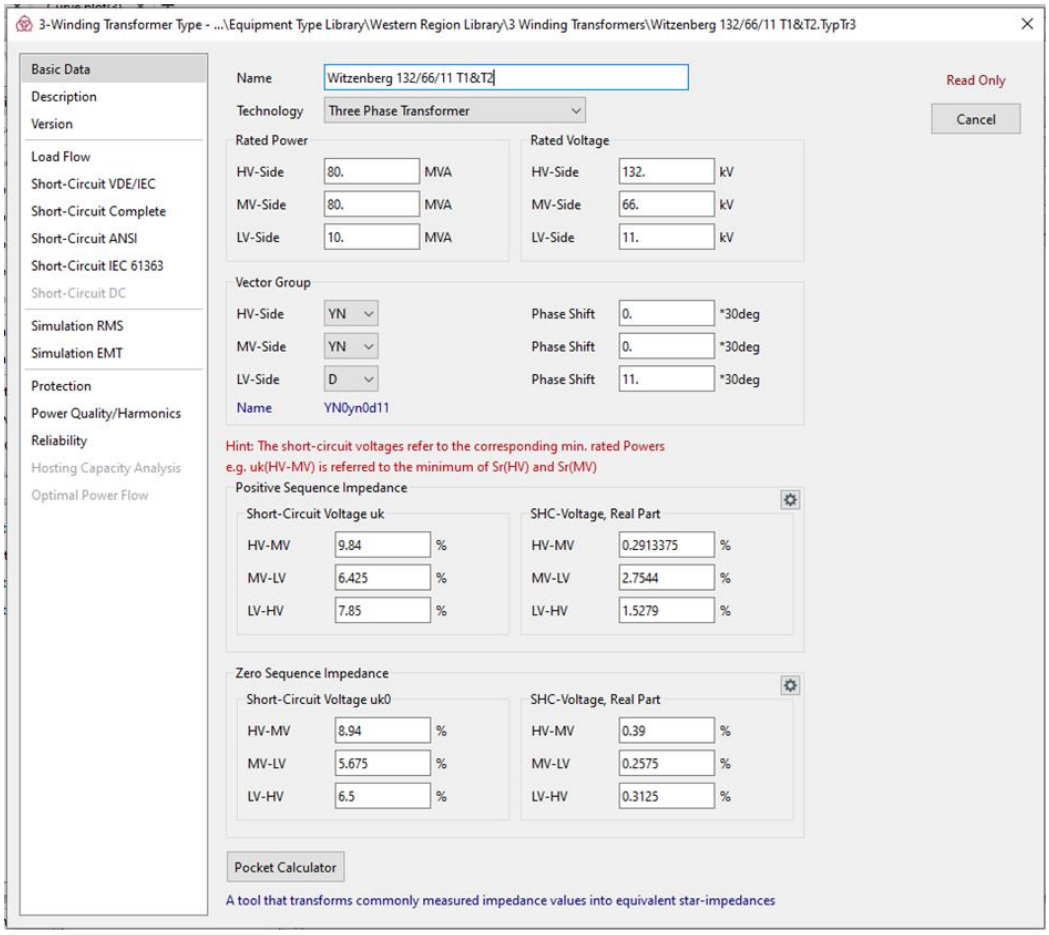

Figure 3.1: Three winding transformers modelling parameters.

The transformer data is important when modelling the network. Transformer data such as impedances, transformer ratio, etc, helps to understand the power flow through the transformer as well as protection settings calculation. Two sets of transformers are used in the modelling of the entire network, namely 2-winding and 3-winding auto transformers.

The main function of transformers in distribution networks is to either step-up or step-down voltages at the various substations, to meet the nominal voltages of the generators (i.e., PV system, and BESS) for different busbar levels. Transformer parameters used in the model are summarised in Table 3.5 below for both two and three winding transformers. The basic data include the name identifier of the apparatus, rated power, vector group, nominal voltages, short circuit data, etc.

Table 3.5: Distribution Network Transformer Parameters

Transformer Name	Transformer Type	Nominal Voltage (kV)	Rating (MVA)	Vector Group	Auto Transformer
Witzenberg 132/66/11 T1	3-winding	132/66/11	80	YN0yn0d11	HV/MV/LV
Witzenberg 132/66/11 T2	3-winding	132/66/11	80	YN0yn0d11	HV/MV/LV
BESS Transformer T1	2-winding	66/0.4	62.5	Dyn11	-
PV Transformer T1	2-winding	22/0.69	40	Dyn1	-
PV Transformer T2	2-winding	66/22	40	YNyn10	-

3.2.4 Photovoltaic (PV) System Modelling

The integration of PV systems into the 16-bus Witzenberg distribution network, introduces both opportunities and challenges for distribution network operators [8], [74]. The mathematical modelling of the PV systems is crucial for understanding their effect on network performance and for developing effective approaches to mitigate potential issues. The PV system is connected to bus 12 and is modelled as a 36 MW power source.

3.2.4.1 Photovoltaic system Components Modelling

The block diagram of the PV system model is represented below in Figure 3.2. The diagram encompasses a PV generator, which harnesses power from sunlight, along with DC cabling, a battery block, and a PV inverter responsible for converting DC to AC and vice versa. Equivalent circuit of the photovoltaic generator model is shown in Figure 3.2 below [34].

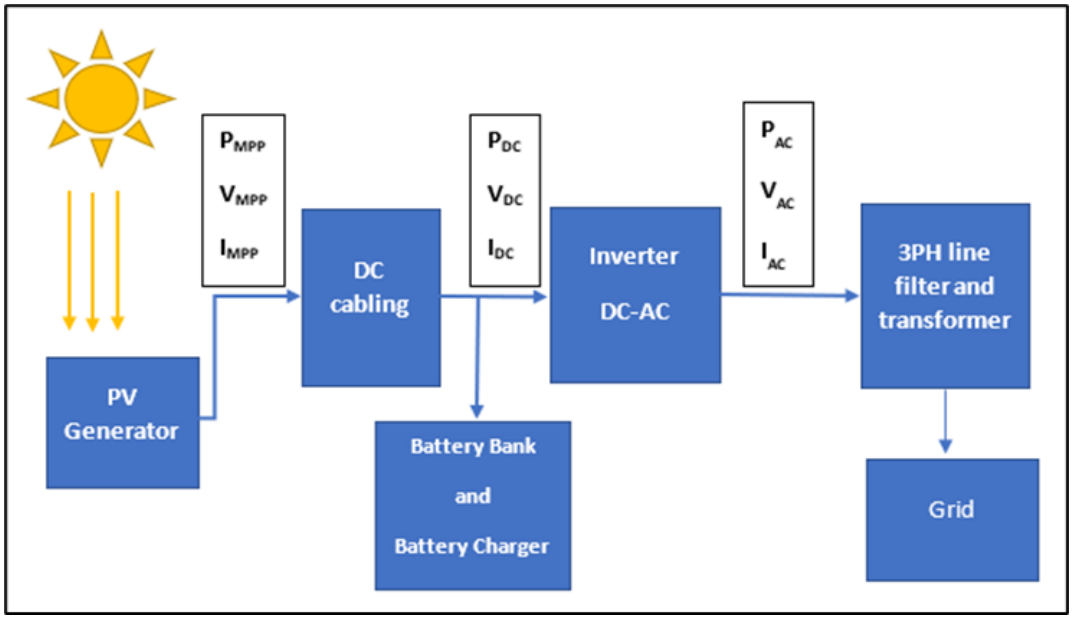

Figure 3.2: Integration of solar energy with the existing grid.

Utilizing a pre-defined PV generator ideality factor, the model utilizes solar radiation and ambient temperature as input parameters to compute the module temperature and Maximum Power Point (MPP) values of the PV voltage, current, and power. The power output of a PV generator is subject to various influencing factors, such as sunlight intensity (irradiance), angle of sunlight incidence, temperature, shading, and the efficiency of the solar cells. The design of the system and appropriate positioning of the PV panels play a critical role in maximizing the energy production of the PV generator.

3.2.4.2 Photovoltaic generator

The photovoltaic generator can best be represented as an ideal solar cell with current source (I_{ph}) parallel to the diode as indicated in Figure 3.3 (a) and can further be described by Kirchhoff's first current law. The output current is described as in (3.1).

$$I = I_{ph} - I_d \quad (3.1)$$

Where:

- I: Output current (A)
- I_{ph}: Photogenerated current (A)
- I_d: Diode current (A)

Shockley's diode current equation, which describes the current-voltage (I-V) characteristics of a PV solar cell, can be derived from the theory of semiconductors. The equation is commonly represented as follows:

$$I_d = I_S \left[\exp\left(\frac{qV_{dc}}{N_S KAT_O}\right) - 1\right] \dots\dots\dots\dots\dots\dots\dots\dots\dots\dots\dots\dots\dots\dots\dots\dots\dots\dots\dots\dots\dots\dots\dots\dots.. (3.2)$$

Where:

- I_S: Diode saturation current (A)
- q: Electronic charge (1.6 × 10^-19 C)
- V_{dc}: Diode voltage (V)
- N_S: Number of cells in series
- K: Boltzmann constant (1.38 × 10^-23 J/K)
- T_o: Operating temperature (K)
- A: Diode ideality factor

By substituting the value of I_d in (3.1) produces the output current I of an ideal solar cell as demonstrated in (3.3).

$$I = I_{ph} - I_s \left[\exp\left(\frac{qV_{dc}}{N_S KAT_O}\right) - 1\right] \dots\dots\dots\dots\dots\dots\dots\dots\dots\dots\dots\dots\dots\dots.\dots\dots\dots\dots\dots\dots\dots.. (3.3)$$

A more realistic circuit model of solar PV cell is a single diode model with series resistance (Rs) and parallel resistance (Rp) represented in figure 3.3 (b) below [31], [34]. The two resistance parameters affect the efficiency of the PV solar cell hence they are important in modelling the PV circuit.

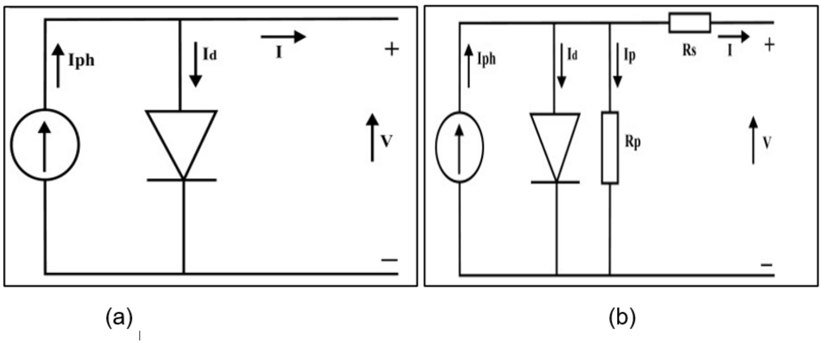

Figure 3.3: (a) A simplified equivalent circuit of a PV panel; (b) equivalent circuit of real model for PV panel.

Considering the PV cells in series-parallel circuit, the output current I is determined as in (3.4).

$$I = N_P \times I_{ph} - I_d \left[\exp\left(\frac{qV_{dc}}{N_S KAT_O}\right) - 1\right] \dots\dots\dots\dots\dots\dots\dots\dots\dots\dots\dots\dots.\dots\dots\dots\dots\dots\dots\dots.. (3.4)$$

3.2.4.3 DC cabling and connections

The current that flows through the conductor between PV generator and PV inverter is active. For this reason, the equivalent scheme of the model consists of one active resistance only. The block represents the losses in DC cabling and connections. The current flow through this resistance results in voltage drop and active losses. The parameters used are the specific resistance of the conductor *ρ*, conductor distance, conductor cross section *s.* The active losses are determined by equation (3.5):

$$\Delta P_{DC.CAB} = R.I^2 \ldots\ldots\ldots\ldots\ldots\ldots\ldots\ldots\ldots\ldots\ldots\ldots\ldots\ldots\ldots\ldots\ldots\ldots\ldots\ldots\ldots\ldots\ldots\ldots (3.5)$$

3.2.4.4 Inverter

In a PV system, inverters play a crucial role in converting the generated DC power into usable AC power as well as connecting the PV system to the distribution network. The inverters are specifically designed to synchronize the voltage and frequency with the distribution network. Their primary function is to ensure that the PV system operates at the optimal operating point, thereby maximizing power output. To achieve this, PV inverters employ a specialized control mechanism known as Maximum Power Point Tracker (MPPT) [31], [32].

Serving as a bridge between the PV power plant and the AC distribution electrical network, the inverter transforms the DC power from the PV generator into AC power, which is then injected into the distribution network [31].

The efficiency of a PV inverter can be mathematically represented as a polynomial function of its output power. This relationship is crucial for understanding the inverter's performance across different power levels. The polynomial equation describing the inverter efficiency is given by [31]:

$$y = a_1 x^n + a_2 x^{n-1} + \cdots \ldots + a_n x + a_{n+1} \ldots\ldots\ldots\ldots\ldots\ldots\ldots\ldots\ldots\ldots\ldots\ldots\ldots\ldots\ldots\ldots (3.6)$$

Where:

- y: Inverter efficiency (%)
- x: Output power (p.u.)
- a_i: Polynomial coefficients
- n: Order of the polynomial

Figure 3.4 illustrates this relationship, showing how inverter efficiency varies with output power for different inverter manufacturers. The curves demonstrate that inverter efficiency typically increases with output power until reaching a plateau at higher power levels.

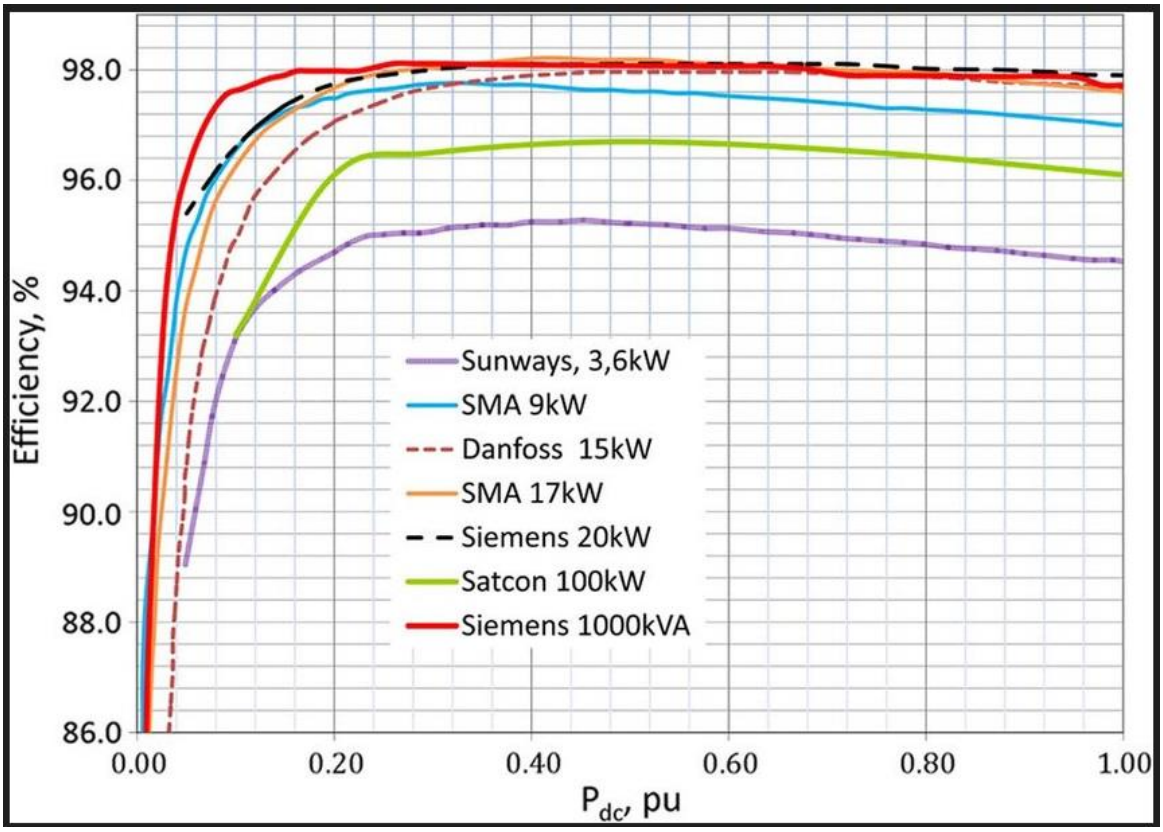

Figure 3.4: Inverter efficiency as a polynomial function of the generated power for different manufacturers.

3.3 Photovoltaic (PV) System Modelling in DigSilent PowerFactory.

DigSilent PowerFactory is a power system analysis software developed by DigSilent GmbH (Digital Simulation and Electrical Network calculation program). It serves as an engineering tool for analysing power systems, ranging from industrial plants to large transmission networks. The software integrates functions for power system modelling, analysis, and optimization in a single environment. Originally developed in 1985, PowerFactory has evolved to become an industry-standard tool used by utilities, power companies, and research institutions worldwide.

For this dissertation, PowerFactory is used to model and analyse the Witzenberg distribution network with its integrated PV systems. The software enables comprehensive steady-state analysis through load flow calculations, allowing assessment of voltage profiles, power flows, and system losses. Its graphical interface facilitates network visualization and data interpretation, while its analytical capabilities support the evaluation of different BESS placement scenarios.

The software supports various types of analyses, including power flow, fault analysis, transient stability, and optimal power flow. It is particularly useful for studying the integration of renewable energy sources, BESS integration, assessing grid stability,

and designing control and protection strategies. PowerFactory provides advanced capabilities for modelling both AC and DC systems, including HVDC lines and FACTS devices, which are critical in modern grids.

The PV system model, shown in Figure 3.5, consists of PV generators, busbars, two two-winding transformers, Point of Connection (POC), and an HV breaker for isolation. The PV plant has 40 parallel units rated at 0.5 MVA at 0.95 power factor with a nominal voltage of 690 volts. The first transformer is a three-phase two-winding type rated at 40 MVA with a nominal frequency of 50 Hz, 22/0.69 kV with DYN1 vector group. The second transformer is a two-winding 66/22 kV type with rated apparent power of 40 MVA, 50 Hz, YNYN vector group.

The first busbar is rated at 690 V to correspond to the PV plant rated nominal voltage and the LV side of the first transformer. The second busbar is rated at 22 kV and connects to both the HV side of transformer one and LV side of transformer two. Figure 3.5 shows the complete PV plant model in PowerFactory.

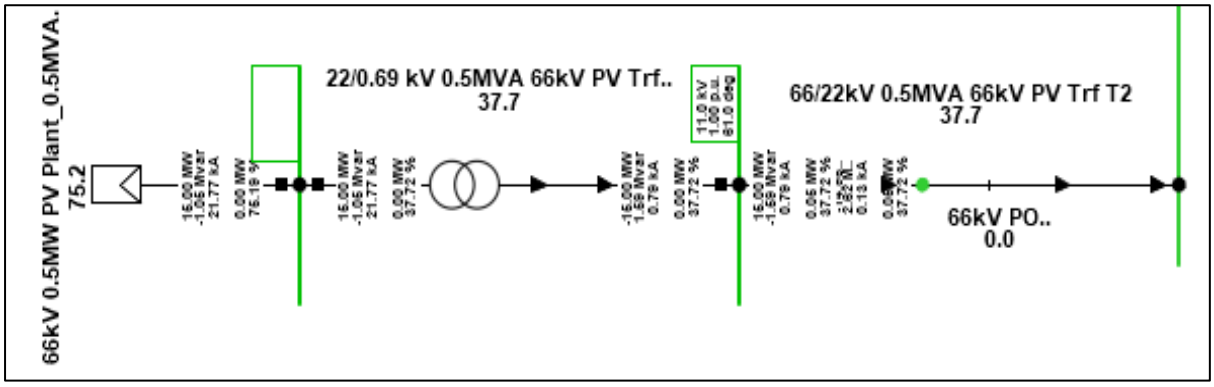

Figure 3.5: Single line PV plant Model in DigSilent PowerFactory.

3.4 The Need for BESS in the Witzenberg Distribution Network

The modified 16-bus Witzenberg distribution network presents several operational challenges that necessitate the implementation of BESS. Currently, the network includes a 36MW PV system at Touwsrivier 132kV bus, which, while contributing to renewable energy goals, introduces power quality and voltage stability challenges due to its intermittent nature. The network experiences significant voltage profile deviations, particularly in the 66kV portion, where several buses operate below the acceptable voltage range specified by South African grid codes. Additionally, the radial nature of the network, combined with long transmission distances, results in substantial active power losses that need to be addressed.

Future planning indicates increased renewable energy source penetration in the network, which will amplify existing challenges related to voltage fluctuations, power quality issues, and system stability concerns. This anticipated growth in renewable integration necessitates robust solutions for maintaining network stability and

reliability. The implementation of BESS presents itself as a comprehensive solution to these current and future challenges.

BESS implementation offers several key benefits that directly address these network challenges. In terms of voltage profile enhancement, BESS provides crucial voltage support through reactive power injection, helps maintain voltage levels within acceptable ranges, and mitigates voltage fluctuations caused by intermittent renewable generation. For power loss reduction, BESS enables energy storage during periods of excess generation and allows for strategic power dispatch during peak demand, thereby reducing the need for long-distance power transmission [75].

Furthermore, BESS implementation serves as a future-proofing strategy for the network. It creates the necessary flexibility to accommodate future renewable energy integration, provides a foundation for grid modernization initiatives, and enhances overall network resilience. The integration of BESS is therefore not just a technical solution but a strategic necessity for the Witzenberg network's current operations and future development.

Understanding these fundamental needs and benefits of BESS implementation is crucial before proceeding with the mathematical modelling. This understanding ensures that the subsequent modelling accurately captures the network's requirements and informs the optimization techniques needed to address both immediate challenges and future needs. The mathematical models must effectively represent these operational requirements while considering the specific characteristics and constraints of the Witzenberg distribution network.

This comprehensive understanding of why BESS is needed provides the foundation for developing appropriate mathematical models and optimization techniques. These models must not only address current voltage profile deviations and power loss issues but also account for future renewable energy integration and network expansion plans. The subsequent sections will detail the mathematical modelling approach used to ensure effective BESS deployment that maximizes these benefits while considering both technical and operational constraints.

3.4.1 Battery Energy Storage System Modelling

Modeling BESS is crucial for evaluating their performance and optimizing integration into distribution networks for voltage profile enhancement and reduction of power losses. BESS models must capture dynamic battery behavior, including charge and discharge characteristics, efficiency, and degradation over time, while also considering various operating conditions such as load profiles, renewable energy generation, and grid disturbances. Accurate BESS modeling enables utilities and researchers to assess the impact of BESS deployment on voltage stability, system

reliability, and energy efficiency, facilitating informed decision-making and effective planning for grid modernization initiatives [3], [7].

Monitoring the State of Charge (SOC) which measures the battery's current capacity in comparison to its full capacity, with reduced daily variation in SOC helping to increase battery life [42] and the State of Health (SOH) of BESS helps determine operational state and performance, with factors like temperature control and Depth of Discharge (DOD) playing crucial roles in improving BESS performance and prolonging battery life [48].

For an example for Li-ion, temperature range is between 15 and 35°C. Maintaining a Depth of Discharge (DOD) of approximately 80% of the battery's rated capacity, along with low charging and discharging rates, can help avoid high temperatures and reduce the risk of decreased battery life [3].

3.4.1.1 BESS Modelling in DigSilent PowerFactory

BESS play a crucial role in modern power systems, offering energy storage and grid support capabilities. Modeling BESS in DigSilent PowerFactory requires careful consideration of its components and characteristics. This section presents a comprehensive approach to BESS modeling, focusing on the mathematical representations and key components. A comprehensive approach to BESS modeling is presented, focusing on the mathematical representations and key components that enable precise simulation of BESS behavior in power system studies.

A typical BESS consists of two main components: a storage component responsible for energy storage and restoration through an electrochemical process, and a rectifier/inverter that converts the DC voltage from the storage part to the required AC voltage for the grid, and vice versa [51], [53] . The modeling process presents unique challenges, primarily due to the diverse battery technologies available, each with its own distinct characteristics. As a result, the focus often shifts to accurately modeling the rectifier/inverter component, which plays a crucial role in grid integration [37], [46].

When modeling BESS, several important factors must be considered. These include internal resistance, rate of charge/discharge, discharge mode (continuous or intermittent), frequency of charge/discharge cycles, State of Charge (SOC), and State of Health (SOH). Furthermore, three modes of discharge are commonly considered: constant load, where the BESS drives the load with a constant resistance; constant current, where the load draws a constant current from the BESS; and constant power, where the BESS delivers constant electrical power to the load [48].

The simplified battery model implemented in DigSilent Power Factory’s Dynamic Simulation Language (DSL) is based on an equivalent circuit representation. The simplified battery model in Dynamic Simulation Language (DSL) is shown in Figure 3.6 below.

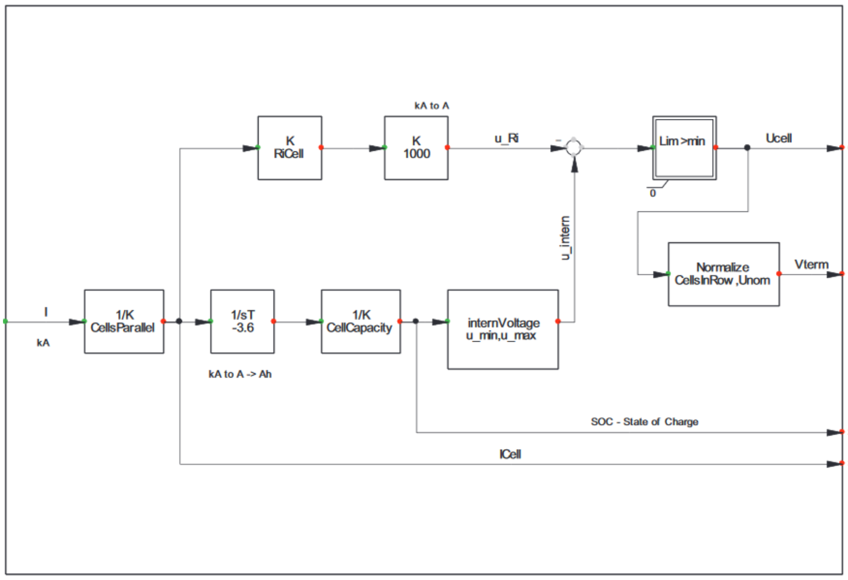

Figure 3.6: Simplified Battery Model in DSL.

This model assumes a constant internal impedance (Z) that depends on the State of Charge (SOC) and a discharge voltage source that also varies with SOC. The battery voltage can be represented by (3.7):

$$U_{DC} = U_{max}.SOC + U_{min}.(1 - SOC) - I.Z_i \dots\dots\dots\dots\dots\dots\dots\dots\dots\dots\dots\dots\dots\dots\dots\dots\dots\dots\dots (3.7)$$

where:

- U_{DC} is the DC voltage of the battery measured in volts (V).
- U_{max} and U_{min} are the cell voltages of a fully loaded and discharged cell respectively measured in volts (V).
- SOC is the State of Charge of the battery and is dimensionless.
- *I*: Battery current [A]
- Z_i: Internal impedance of the battery [Ω]
- (1-SOC): Depth of discharge, representing the complement of SOC.
- $I \cdot Z_i$: Voltage drop across the internal impedance [V]

The equation shows how the battery voltage (U_{DC}) is determined by:

- The weighted sum of maximum voltage ($U_{max} \cdot SOC$) based on charge level.
- The weighted sum of minimum voltage ($U_{min} \cdot (1-SOC)$) based on discharge level.
- The voltage drop ($I \cdot Z_i$) due to internal impedance.

The BESS controller implemented in DigSilent PowerFactory as sown in figure 3.7 consists of several key components, including a frequency control block, an active and reactive power (PQ) control block, a charge control block, and a Pulse Width Modulator (PWM) converter block. This framework allows for the implementation of various control strategies and ensures the BESS can provide the desired functionality

within the distribution network. The BESS model implemented on DSL is shown in Figure 3.7 [48].

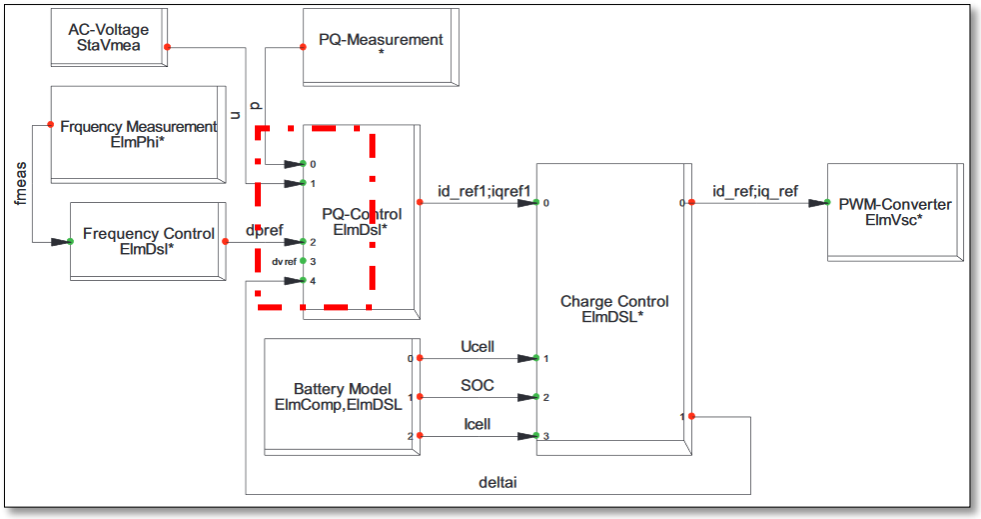

Figure 3.7: Framework of BESS Controller on DigSILENT PowerFactory.

The BESS control system can be mathematically represented using equations for active power control, reactive power control, and State of Charge calculation.

The PQ Control in the BESS model enables the management of reactive power flow to support voltage control and power factor correction in the grid. By injecting or absorbing reactive power, the BESS can help stabilize bus voltages, regulate power factor, and mitigate voltage fluctuations. The BESS control system can be mathematically represented using equations for active power control, reactive power control, and State of Charge calculation. The active power control equation is given by:

$$P_{ref} = P_{set} + K_f * (f_{ref} - f_{meas}) \quad \text{(3.8)}$$

where,

- P_{ref} is the reference active power output.
- P_{set} is the active power setpoint.
- K_f is the frequency droop constant, and f_{ref} and f_{meas} are the reference and measured grid frequencies respectively.

Similarly, the reactive power control is represented by:

$$Q_{ref} = Q_{set} + K_v * (V_{ref} - V_{meas}) \quad \text{(3.9)}$$

where,

- Q_{ref} is the reference reactive power output,
- Q_{set} is the reactive power setpoint.
- K_v is the voltage droop constant.
- and V_{ref} and V_{meas} are the reference and measured grid voltages respectively.

The State of Charge (SOC) calculation is given by:

$$SOC(t) = SOC(t-1) + \frac{(P_{batt} * \Delta t)}{(E_{nom} * \mu)} \quad \text{..... (3.10)}$$

where,

- SOC(t) is the State of Charge at time t.
- P_{batt} is the battery power (positive for charging, negative for discharging).
- Δt is the time step.
- E_{nom} is the nominal battery energy capacity,
- and μ is the battery efficiency (for charging or discharging).

Bus voltage control is an integral part of PQ Control in the BESS model. By monitoring the bus voltage level, the control system can adjust the active and reactive power outputs of the BESS to maintain the desired voltage profile. This ensures that the BESS operates within acceptable voltage limits and helps maintain grid stability and power quality [48].

Figure 3.8 represents a one-line diagram that demonstrates the configuration of the BESS [76]. The BESS is connected to the AC-type BESS Bus, showcasing the interconnection between the BESS and the AC bus. This diagram offers a visual representation of the system layout, providing insights into the arrangement and connection of the BESS components.

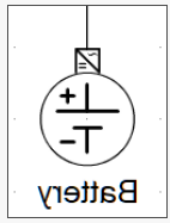

Figure 3.8: Single line diagram of BESS in DigSilent PowerFactory.

3.4.1.2 BESS Connection Requirements

To ensure network voltage profile deviation improvements and reduction in active power losses, BESS placement location connection must adhere to South African BESS Grid connection code. The South African Grid code for BESS specifies the minimum technical and design requirements for connecting BESS to the transmission or distribution network [77] . Table 3.6 illustrates the BESS classification connection into the distribution network for the different power ranges:

Table 3.6: BESS classification connection into the distribution network.

Sub – categories of BESS	Power Rage	Nominal Voltage, Un (kV)	Minimum Voltage Umin (p.u.)	Maximum Voltage Umax (p.u.)	Voltage Limits percentage (%)
A	>0 to <1MW	MW - HV	0.85	1.05	-15 to +10
A1	>0 to <13.8kW	MW - HV	0.85	1.05	-15 to +10
A2	>13.8kW to <100kW	MW - HV	0.85	1.05	-15 to +10
A3	≥100kW to <1MW	MW - HV	0.95	1.05	-15 to +10
B	≥1MW to <20MW	MW - HV	0.95	1.05	±10
B1	≥1MW to <5MW	MW - HV	0.9	1.0985	±10
B2	≥5MW to <20MW	MW - HV	0.9	1.0985	±10
C	≥20MW to <20MW	MW - HV	0.9	1.0985	±10

The baseline load flow analysis of the Witzenberg distribution network revealed significant voltage profile challenges across the 16-bus network. Prior to BESS placement several buses displayed voltage levels deviating from the ideal 1.0 per unit (p.u.) value with some buses showing voltages below 0.95 p.u. indicating potential power quality challenges.

This is particularly concerning when viewed in the context of South African grid requirements. According to the South African Grid Code for Renewable Power Plants (RPPs) which includes provisions for energy storage systems, voltage deviations at the Point of Connection (POC) should typically be maintained within ±5% of nominal voltage under normal operating conditions [77].

However, the baseline results showed that multiple buses especially at the 66kV, were operating outside the ±5% restrictions. The voltage profiles at the buses not only risk non-compliance with grid codes but also pose challenges for the overall network profile stability and efficiency. The 132kV buses are more stable and showed deviations that if aggravated could approach the upper limits of acceptable voltage ranges. These baseline findings underscore the need for voltage support mechanisms within the network.

Highlighting why the strategic placement of BESS is crucial for improving voltage profiles. The high penetration of PV systems in the network further complicates the voltage regulation challenges contributing to the observed voltage profile deviations and emphasizing the potential role of BESS in mitigating the two challenges of voltage profile deviations and reduction of active power losses. This baseline scenario sets the stage for evaluating how different BESS placement strategies might address and improve the voltage profile deviation regulation challenges and active power losses thereby bring the network into better alignment with South African grid requirements.

The next section will focus on the voltage profile analysis scenarios after BESS placement.

3.5 Problem Formulation

The problem formulation for integrating BESS in distribution networks, such as the modified Witzenberg distribution network, involves a comprehensive consideration of various factors and objectives. The network factors encompass the characteristics of the distribution network, which includes line impedances, load profiles, and existing generation sources. These factors form the foundation upon which the integration strategy is built, ensuring that the proposed solution aligns with the specific needs and constraints of the network.

At the heart of the problem formulation lies the definition of objective functions. These functions encapsulate the primary goals of BESS integration, typically focusing on minimizing power losses and improving voltage profiles deviations thereby enhancing system reliability and maximizing renewable energy utilization. By clearly defining these objectives, the formulation provides a measurable framework for assessing the effectiveness of different integration strategies.

3.5.1 Total distribution network power loss

One of the main objectives of the proposed approach is to minimize the total system active power losses through optimal placement of BESS location in the Witzenberg distribution network and the objective function is mathematically formulated in (3.11) as follows:

$$Minimise\ S_{loss} = \sqrt{P_{loss}^2 + Q_{loss}^2} \quad \text{..... (3.11)}$$

Total active power losses in a distribution network are given in (3.12) by:

$$P_{LOSS} = (\sum_{i=1}^{n}(I_i)^2 * R_i) \text{..... (3.12)}$$

Total reactive power loss in a distribution network is given in (3.13) by.

$$Q_{loss} = (\sum_{i=1}^{n}(I_i)^2 * X_i) \text{..... (3.13)}$$

where,

- n represents the number of lines at bus I_i.
- Is the line current in amps.
- R_i is the line resistance in ohms.
- and X_i is the line reactance in ohms respectively.

The total power loss is also formulated exact loss formula (3.11) which includes real and reactive power losses, respectively. The exact real and reactive power loss are

given by equations (3.14) and (3.15), respectively and the detail of their formulation is given in [13], [78].

$$P_{loss} = \sum_{i=1}^{n}\sum_{j=1}^{n}\left[a_{ij}\left(P_iP_j + Q_iQ_j\right) + b_{ij}\left(Q_iP_j + P_iQ_j\right)\right] \quad (3.14)$$

where

$$Q_{loss} = \sum_{i=1}^{n}\sum_{j=1}^{n}\left[c_{ij}\left(P_iP_j + Q_iQ_j\right) + d_{ij}\left(Q_iP_j + P_iQ_j\right)\right] \quad (3.15)$$

where,

$$a_{ij} = \frac{R_{ij}}{V_iV_j} * cos\left(\delta_i - \delta_j\right);\ b_{ij} = \frac{R_{ij}}{V_iV_j} * sin\left(\delta_i - \delta_j\right) \quad (3.16)$$

and

$$c_{ij} = \frac{X_{ij}}{V_iV_j} * cos\left(\delta_i - \delta_j\right);\ d_{ij} = \frac{X_{ij}}{V_iV_j} * sin\left(\delta_i - \delta_j\right) \quad (3.17)$$

n is the bus number. a_{ij}, b_{ij}, c_{ij} and d_{ij} represents functions of loss coefficient between bus $i\ and\ j$. P_i, $P_j$is real power flow at buses $i\ and\ j$ respectively in [p.u.]. Q_i, $Q_j$is reactive power flow at buses $i\ and\ j$ respectively in [p.u.]. R_{ij} is resistance of the line connecting buses i and j in [p.u.] . P_i, P_j is real power flow at buses $i\ and\ j$ in [p.u.]. X_{ij} is Reactance of the line connecting buses $i\ and\ j$ in [p.u.]. V_i and V_j are bus voltage magnitudes at buses $i\ and\ j$ in p.u. ∂_i and ∂_j is bus voltage angles in radians at bus $i\ and\ j$.
The total impedance between the bus $i\ and\ j$ is given by equation (3.18) below:

$$Z_{ij} = R_{ij} + jX_{ij} \quad (3.18)$$

3.5.2 Change in Real Power Flow Analysis

The real power flow in a line k connecting two buses i and j can be expressed as:

$$P_i = V_iV_jY_{ij}\cos\left(\theta_{ij} + \partial_j - \partial_i\right) + V_i^2\,Y_{ii}\cos\theta_{ii} \quad (3.19)$$

were,
$V_i\ and\ V_j$ are the voltage magnitudes at buses i and j, respectively. ∂_j and ∂_i are the voltage angles at buses i and j respectively. Y_{ii} is the magnitude of $_{ith}$ element of the $YBus$ matrix. Y_{ij} is the magnitude of the $ijth$ element of the $YBus$ matrix. θ_{ii} is the angle of the ith element of the $YBus$ matrix. θ_{ij} is the angle of the $_{ijth}$ element of the $YBus$ matrix.

3.5.3 Change in real Power Loss Analysis

From the circuit diagram shown in Figure 3.9, the active power loss of the line lumped model (π-circuit) can be calculated. This analysis helps understand power flow direction and loss characteristics in the distribution network.

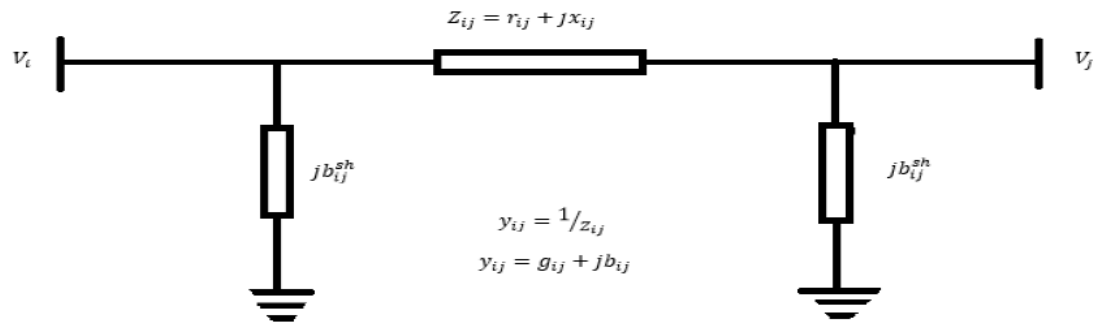

Figure 3.9: Circuit diagram of a lumped distribution line (π-circuit).

The active power loss of the line lumped model shown in the line (π-circuit) circuit is Figure 3.9 is given by:

$$P_{L(ij)} = \sum_{l=1}^{nl}\left[g_{ij}\left(V_i^2 + V_j^2 - 2V_iV_j\cos\delta_{ij}\right)\right] \quad \text{(3.20)}$$

Where:

- N_l - Number of lines in the network.
- g_{ij} - Conductance of the line between buses i and j [p.u.].
- V_i - Node voltage magnitude at bus I [p.u.].
- V_j - Node voltage magnitude at bus j [p.u.].
- δ_{ij} - Voltage angle difference between buses i and j [radians].

The direction of the active power flow at the slack bus of the distribution network can be determined by its sign: positive power flow indicates power flowing into the distribution network, while negative power flow represents power flowing out from the distribution network.

3.6 Objective Function

The objective function in this dissertation is designed to address multiple facets of system performance by strategically determining the optimal location of BESS placement. The main primary goal is to minimize total system costs (C_{system}) incurred in distribution network, which include both voltage regulation costs (C_{VR}) and active power losses costs (C_{PL}) along the lines.

Two key performance indices are included: the Active Power Loss Reduction (APLR) and the Voltage Profile improvement (VPI). The APLR quantifies the reduction in system losses achieved through the integration of BESS, while the VPI measures the improvement in voltage profiles across the network nodes. These indices are combined into a single objective function (F_n).

$$F_n = Min_{(Csystem)} \quad \text{(3.21)}$$

where $Csystem$ represents the total system costs in the distribution network due to total active power losses along the lines and voltage regulation costs and is given by equation (3.22).

$$C_{system} = C_{PL} + C_{VR} \quad (3.22)$$

Where in equation 3.23, C_{PL} represents the total costs of active power losses along the lines over time.

$$C_{PL} = \sum_{t=1}^{T} \sum_{i,j=1}^{m} \left[(V_i)^2 + (V_j)^2 - 2(V_i V_j)\cos\left(\partial_i - \partial_j\right)\right] * \left[\left(G_{ij}\right)(\gamma_{PL})\right] * \Delta t \quad (3.23)$$

where,

- m : Number of branches
- Vi, Vj: Voltage magnitudes at buses i and j [kV]
- ∂i, ∂j: is the phase angle difference between the buses i and j [radians]
- Gij: Conductance of the line between buses i and j [S]
- γ_{PL}: Rate for active power loss cost 0.284$/kWh [70].
- T: is the Total period.
- Δt: time duration per period in hours.

In equation (3.24), CVR quantifies the voltage regulation costs.

$$C_{VR} = \sum_{t=1}^{T} \sum_{i=1}^{N} \left[\left[V_i^2 - V_{ref}^2\right]\right]^{\frac{1}{2}} * (\gamma_{VR}) \quad (3.24)$$

where,

- N : Total number of buses.
- $Vref$: Reference voltage which is equal to 1 p.u.
- γ_{VR} : the rate of voltage regulation cost γ_{VR} is $0.142\$/\text{p.u.}$ [11]

To effectively formulate the APLR and VPI, a load flow analysis is conducted using the Newton-Raphson load flow method. This analysis employs the Jacobian matrix of the load flow to derive factors for both real and reactive power flows. The power loss factor reflects how changes in node injections influence overall system losses, while the voltage factor demonstrates the impact of power injections on node voltages. This load flow analysis provides critical insights into network behavior, facilitating more accurate optimization of BESS placement and operation.

The mathematical formulation of this analysis is based on the relationship between changes in power injections and voltage variations, as represented by the Jacobian matrix. This relationship is essential for understanding how BESS integration affects overall network performance. The APLR is calculated as the ratio of power loss reduction achieved through BESS integration to the original power loss, offering a clear measure of network efficiency improvement. Similarly, the VPI is calculated as the average deviation of node voltages from the reference voltage, providing a quantitative assessment of voltage profile improvement.

This comprehensive formulation establishes a robust framework for optimizing BESS integration in distribution networks, such as the Witzenberg distribution network. By balancing the reduction of power losses with improvements in voltage profiles, the formulation supports enhanced network performance. The use of load flow analysis based on the Newton-Raphson method ensures accurate quantification of BESS impacts, leading to more effective decision-making in the planning and operation of distribution networks with high-RES penetration.

3.7 System Constraints on Voltage and State of Charge (SoC)

To optimize the distribution system, we must consider both the objective function and the associated constraints. According to [70] [79], the objective function is to be minimized while adhering to specific voltage and battery limitations. One crucial constraint is the voltage magnitude, which must be maintained within predetermined bounds as per the South Africa Grid code. The constraint equation given in equation (3.25) is applied to the optimization process and the Voltage at each bus is bound to the range which is ±5% of the reference voltage,[67] This voltage constraint is expressed by the following equation (3.25):

$$V_{min} < |V_i^t| < V_{max} \dots\dots\dots\dots\dots\dots\dots\dots\dots\dots\dots\dots\dots\dots\dots\dots\dots\dots\dots\dots\dots\dots\dots\dots\dots\dots\dots\dots .. (3.25)$$

where V_{min} and V_{max} are the minimum and maximum voltage magnitudes, respectively, and V_i^t is the voltage magnitude at bus i at time t.

The state of charge (SOC) constraint is crucial for maintaining the operational integrity of battery storage systems. This constraint ensures that the battery's charge level remains within safe and efficient operating limits. The bound charge limits are expressed by the following equation 3.26:

$$SOCmin \leq SOC \leq SOC\ max \dots\dots\dots\dots\dots\dots\dots\dots\dots\dots\dots\dots\dots\dots\dots\dots\dots\dots\dots .. (3.26)$$

where $SOCmin$ and $SOC\ max$ represent the minimum and maximum allowable charge levels, respectively, this constraint prevents overcharging and deep discharging. They are set as 20% and 80% for $SOCmin$ and $SOC\ max$, respectively. This allowed for extending battery life and ensuring system reliability.

3.8 Sizing and placement of Battery Energy Storage System

While optimal BESS placement was the primary focus of this dissertation, literature emphasizes that sizing and placement are inherently interconnected aspects of BESS integration. In the unique context of the Witzenberg distribution system, the BESS sizing approach deviated from conventional optimization methods, instead adopting a

reference size based on N-1 contingency requirements. With both transformers operating at 70% loading capacity, the failure of one transformer would create a critical vulnerability in the 66kV distribution network.

Therefore, the BESS size was strategically determined to provide sufficient capacity to manage downstream loads during a transformer failure, ensuring network stability through N-1 contingency compliance. This practical approach to BESS sizing, coupled with optimal placement analysis, creates a robust solution that addresses both immediate network efficiency needs and critical infrastructure resilience requirements.

Table 3.7: BESS size parameters.

Parameter	Value	Unit
Active Power	80	MW
Reactive Power	1000	kvar
Apparent Power	80	MVA
Power Losses	0	MW
Power factor	1	-
Loading	80	%

3.9 System Performance Evaluation

In this dissertation, the efficiency of the Witzenberg distribution network is analyzed following the strategic placement of BESS. This evaluation focuses on several key performance indicators, including the reduction of active power losses, improvements in voltage profile deviations, and enhancements in Voltage Profile Deviation Index (VPDI). Specifically, we will assess how BESS placement impacts voltage profile deviations and reduces active power losses. The results of this analysis, along with their implications, will be discussed in detail in Chapter 4.

3.9.1 Voltage Profile Deviation Index (VPDI).

The calculation of the percentage of voltage profile deviation (VPDI) is performed to evaluate the improvement of the voltage profile regulation. The lower the percentage of VPDI, the better the voltage profile deviation is improved. The VPDI was applied to represent the voltage deviation of each bus case. Th VPDI compared the voltage level of each bus in ($V_{bi} in\ p.u.$) with the reference voltage ($V_{ref} = 1\ p.u.$) The calculation of the percentage of VPDI is expressed by the equations (3.27) and (3.28) as follows:

$$\%VPDI_i = max_i^T \left(\frac{|V_{ref} - V_i|}{V_{ref}} \right) x\ 100 \quad \text{(3.27)}$$

$$\%VPDI = \sum_{i=1}^{N_{bus}} \%VPDI, \quad \text{(3.28)}$$

Where the maximum value of VPDI of bus i during the time interval *T* is represented as $\%VPDI_i$, the reference voltage is set at 1 per unit (p.u.) and referred to as V_{ref}, the

voltage of bus i is represented as V_i, the overall percentage of VPDI for the entire distribution network is denoted as %VPDI, and N_{bus} represents the total number of buses in the distribution network. The baseline case results of voltage profile deviation index and the results after BESS placement is discussed in chapter 4.

3.9.2 Active Power Losses

Active power losses of the distribution network are compared in the bus cases with BESS and without BESS and results are discussed in chapter 4. The active power losses are computed as follows.

$$P_L = \sum_{i=1}^{T} \sum_{l=1}^{m} P_L^l \quad (3.29)$$

Where P_L, is the active power losses, l is the number of branches. T is the total period. m is the total number of branches.

The next chapter will use these models to analyze the impact of optimal BESS placement on the network performance.

3.10 Summary

Chapter 3 presents a comprehensive overview of the mathematical modeling and problem formulation for the modified 16-bus Witzenberg distribution network. The chapter details the modeling of various network components, including power transformers, overhead power lines, PV systems, loads, and shunt filter capacitors. The chapter explains the necessity of BESS implementation for voltage regulation and renewable energy integration. This mathematical framework serves as the foundation for optimization studies to determine strategic BESS placement for improved voltage regulation and reduced power losses. It introduces the mathematical models for the 36 MW PV system at Touwsrivier and the BESS integration, focusing on their impact on voltage profiles and power losses. The problem formulation addresses the network's key challenges: significant voltage profile variations across different voltage levels (132 kV, and 66 kV) and the need for power loss reduction. Detailed equations are provided for calculating total power losses, power flow, voltage profile deviation index (VPDI), and system constraints.

Chapter 4 : Simulation Results, and Discussions

This chapter presents and analyzes the results obtained from both load flow studies from DigSilent PowerFactory and MATLAB optimization for the modified 16-bus Witzenberg distribution network. The analysis focuses on two primary aspects: voltage profile improvement and reduction in active power losses. By examining these key parameters, the aim is to assess the impact of optimal BESS placement on the distribution networks for improved power quality of electric power delivered.

4.1 Parameter Settings and Convergence Analysis of PSO and GA

Both PSO and GA demonstrated effectiveness in determining optimal BESS placement locations, consistently converging on the same solutions across all buses. However, some differences in convergence characteristics were observed. PSO demonstrated rapid convergence, often reaching the optimal solution within the first few iterations and GA showed a more gradual convergence pattern and displayed more scattered points, indicating a wider exploration of the solution space.

4.1.1 Parameter Settings for PSO and GA

Both PSO and GA were implemented in MATLAB to determine the optimal BESS placement location, with parameter selection playing a crucial role in ensuring effective convergence and solution quality. Drawing from preliminary testing, PSO parameters were configured with a population size of 100 particles, an inertia weight of 0.45 to balance global exploration and local exploitation and learning coefficients (c1 = c2 = 1.0) to ensure equal influence between personal and social learning components.

Similarly, GA parameters were selected based on optimization literature and previous successful implementations, utilizing a matching population size of 100 for comparative analysis, a higher crossover probability of 0.8 to promote effective solution space exploration, and a low mutation probability of 0.02 to maintain population diversity while preventing excessive random perturbation. Both algorithms were set to run for 100 iterations, determined through convergence testing to ensure solution stability.

As shown in Table 4.1, both algorithms targeted the same objective function of minimizing total system costs, including active power losses and voltage deviations, while operating in different search spaces - continuous for PSO and discrete for GA.

The convergence criteria for both methods were based on either reaching maximum iterations or achieving a specified fitness threshold.

Table 4.1: Optimization techniques setting parameters.

Parameters	PSO	GA
Population size	100	100
Maximum Iterations	100	100
Algorithms specific Parameters	Inertia weight: 0.7	Crossover probability: 0.8
Algorithms specific Parameters	Learning coefficients (C1 = C2 = 1)	Mutation probability: 0.02
Search Space	Continuous	Discrete
Convergence Criteria	Maximum iterations or tolerance threshold	Maximum iterations or tolerance threshold

The flowchart in figure 4.1, summarizes the key optimization steps for determining the best location to place a BESS within the 16 bus Witzenberg distribution network. The proposed approach involves the following steps:

1. Input the 16 bus Witzenberg network data. (BESS size was predetermined).
2. Select one candidate bus placement location for BESS.
3. Perform load flow analysis in DigSilent PowerFactory for any selected BESS placement location.
4. Determine the value of the objective function and update once completed.
5. Once the last bus is chosen, proceed to step 6, if not proceed step 2.
6. Find the best location for BESS placement installation, which is the candidate bus providing the minimum value of the objective function (MATLAB Environment).

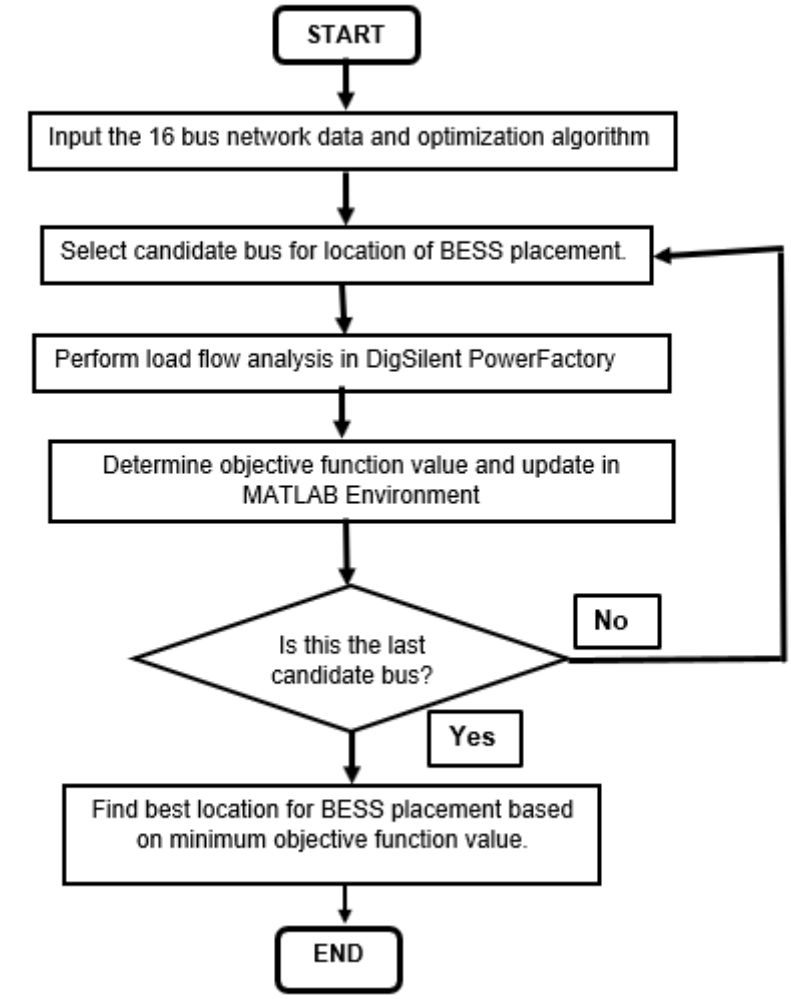

Figure 4.1: Represents the flowchart for the key optimization steps for identifying the best location for BESS placement in the Witzenberg distribution system.

4.1.2 Convergence Plots of PSO and GA

Figures 4.2 to 4.12 present the convergence plot values before and after BESS placement, with Figure 4.2 specifically showing the PSO convergence values prior to BESS installation. The consistent convergence results obtained from both optimization methods (PSO and GA) enhance the reliability of these findings, providing a robust foundation for decision-making. Figure 4.2: Represents the convergence value plot before BESS placement using PSO.

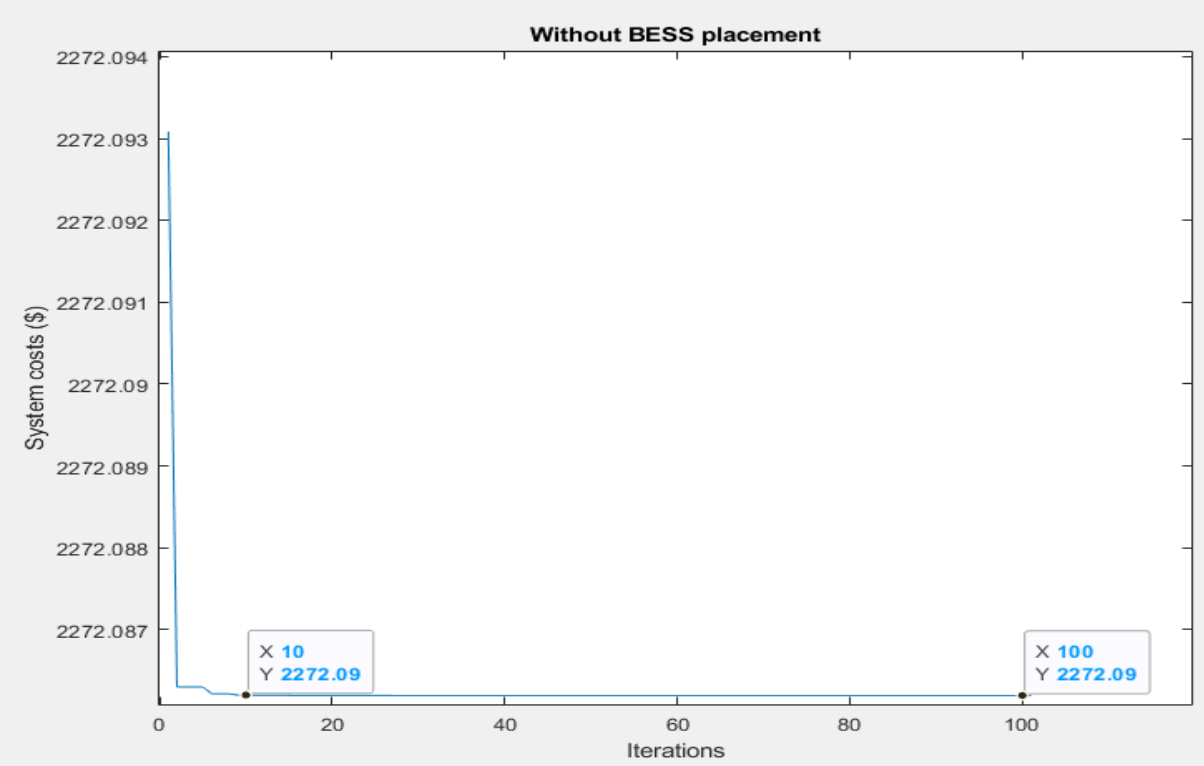

Figure 4.2: Convergence plot using PSO (100 iterations) before BESS placement.

Figures 4.3 to 4.12 are the convergence plots in both PSO and GA respectively. Figures 4.3 and 4.4 are the convergence plots for both PSO and GA, respectively, with BESS location optimally placed, respectively. Figures 4.11 and 4.12 are the convergence plots for both PSO and GA, respectively, with BESS not optimally placed. Hence the observation of the high system costs when BESS is in both busses. The analysis revealed that bus 13 emerged as the most suitable location for BESS placement, with minimum system costs of $937.29 based on the minimization of the active power losses (3.3 MW) and voltage deviations (voltage profiles listed in table H-2). This result was consistently obtained by both PSO and GA, underscoring the robustness of the optimization techniques employed though PSO proved to be quicker to convergence.

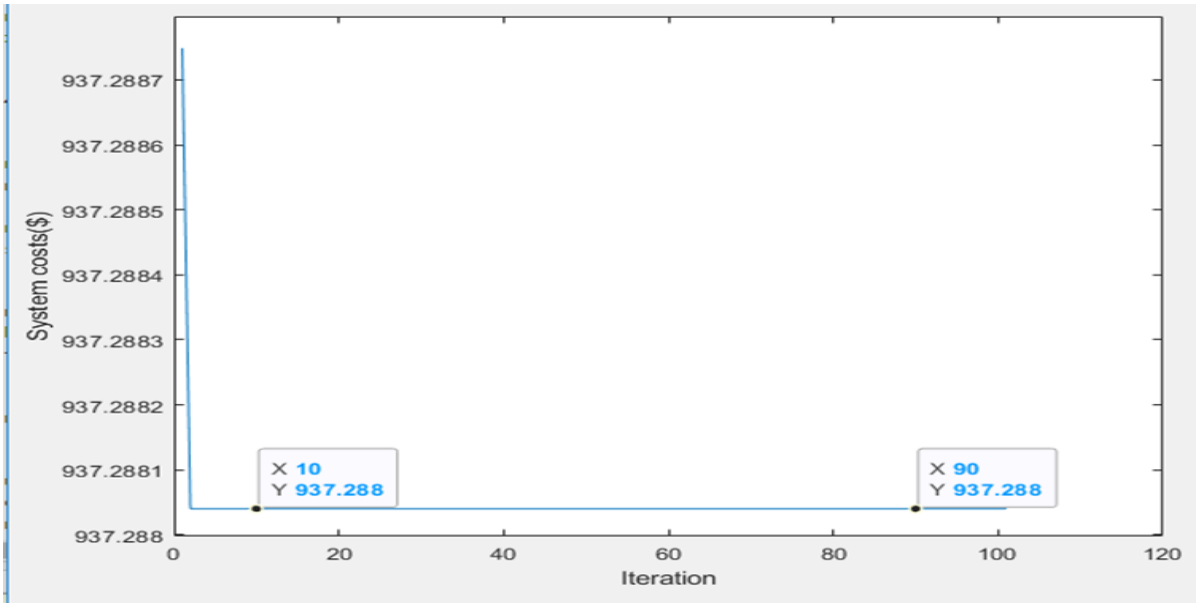

Figure 4.3: Convergence plot using PSO (100 iterations) with BESS optimally placed at bus 13.

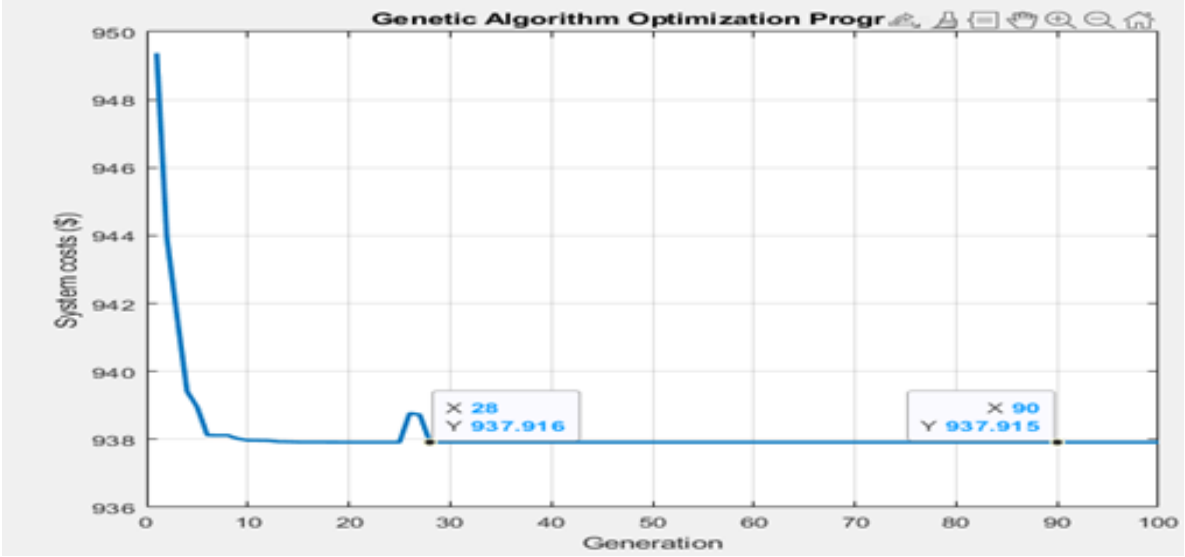

Figure 4.4: Convergence plot (100 iterations) using GA for BESS optimally placed at bus 13.

The second most favourable location for BESS placement was identified as bus 14 with system costs of $1050.88 based on the minimization of active power losses (3.7 MW) and voltage deviations (voltage profiles are listed in table H-3). Figures 4.5 and 4.6 illustrate the convergence plots for BESS at bus 14.

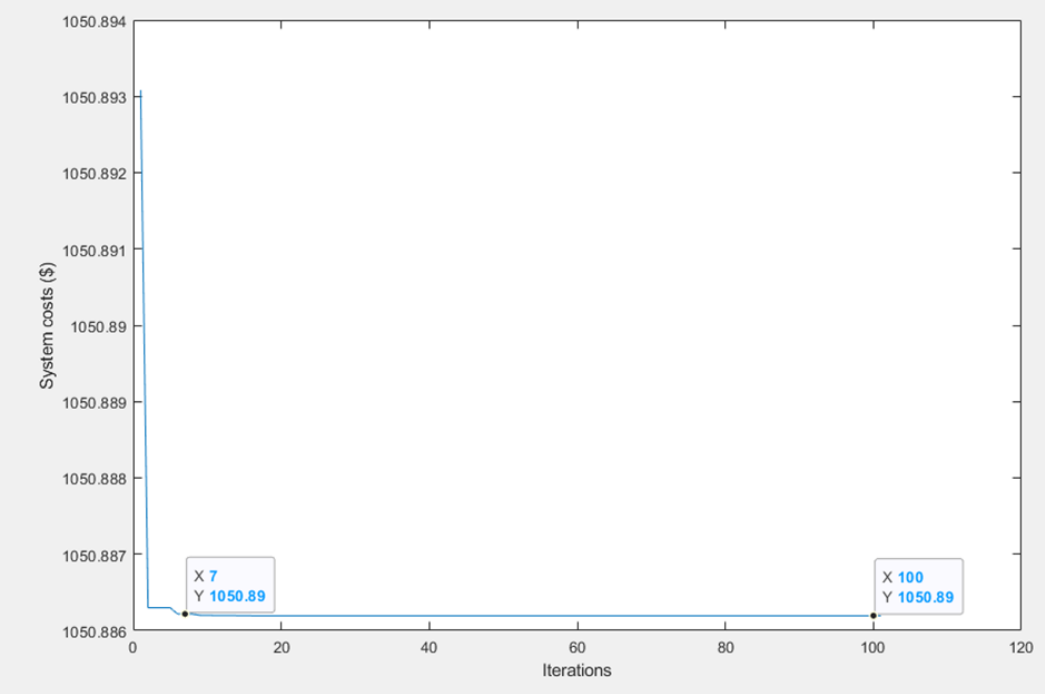

Figure 4.5: Convergence plot using PSO (100 iterations) for BESS placed at bus 14.

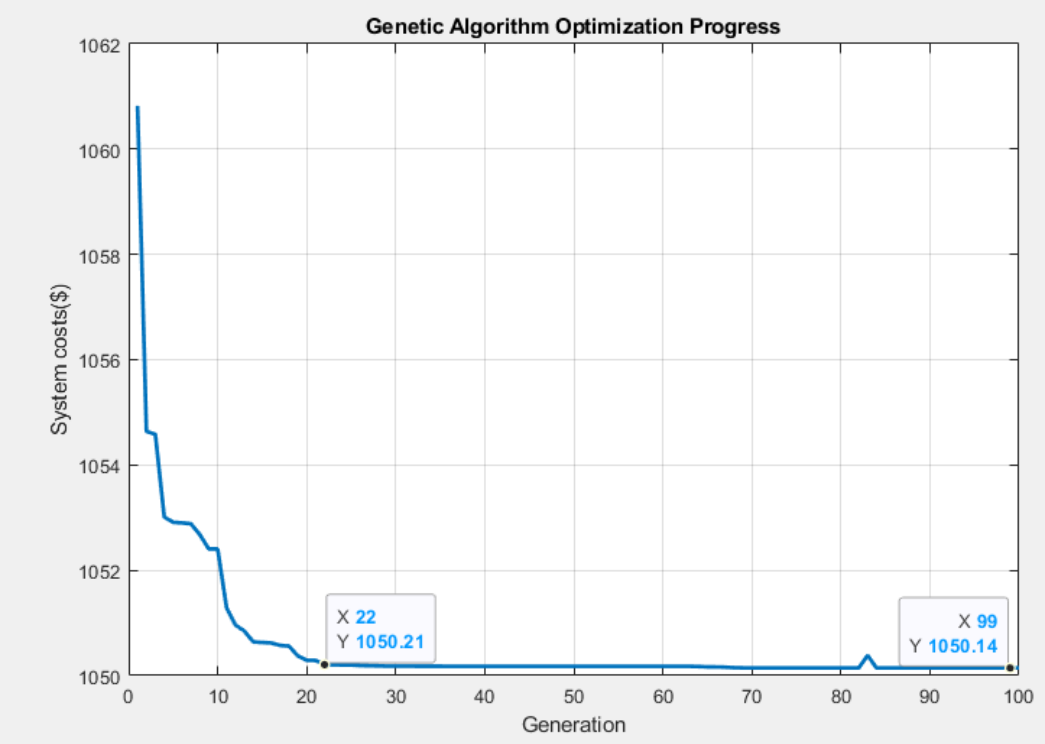

Figure 4.6: Convergence plot using GA (100 iterations) for BESS placed at bus 14.

A notable observation from the analysis is the similarity in active power losses and system costs among bus 1, bus 3, and bus 4. This similarity points to the potential area of the network with comparable characteristics which might benefit from a

coordinated approach to power management and BESS integration. Figures 4.7 and 4.8 show the convergence plots when BESS is placed at buses 1,3 and 4.

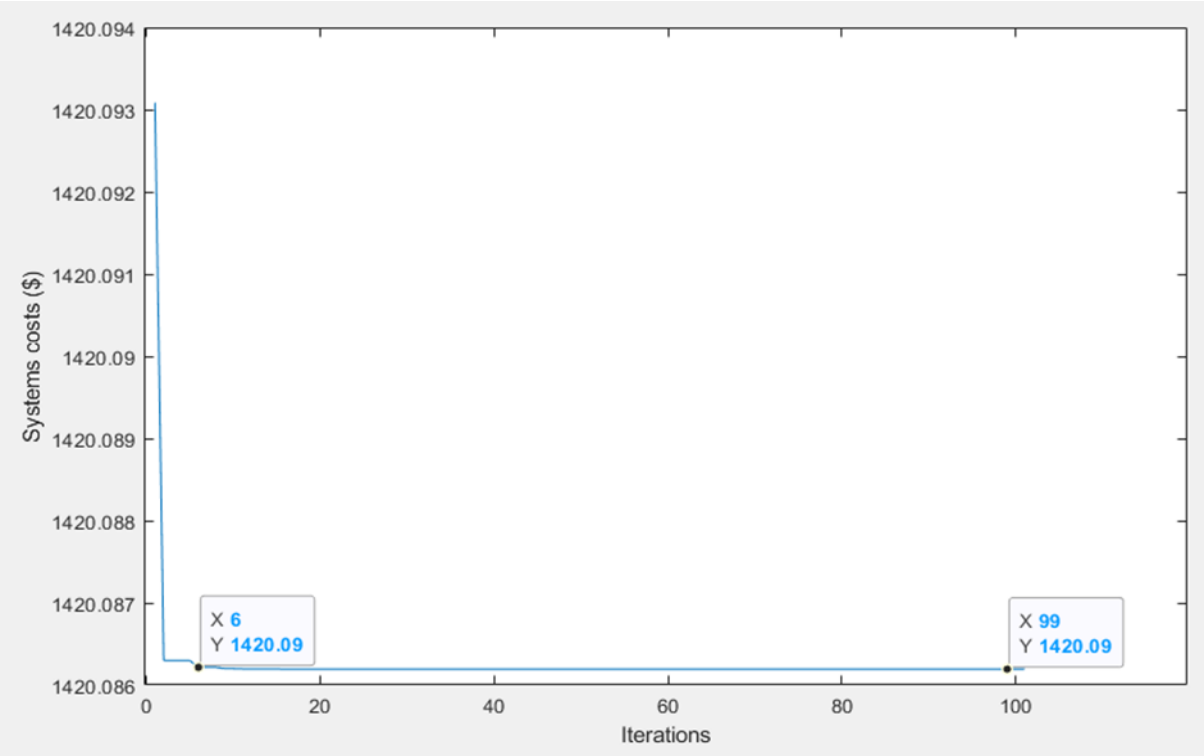

Figure 4.7: Convergence plot using PSO (100 Iterations) for BESS placed at buses 1,3 and 4.

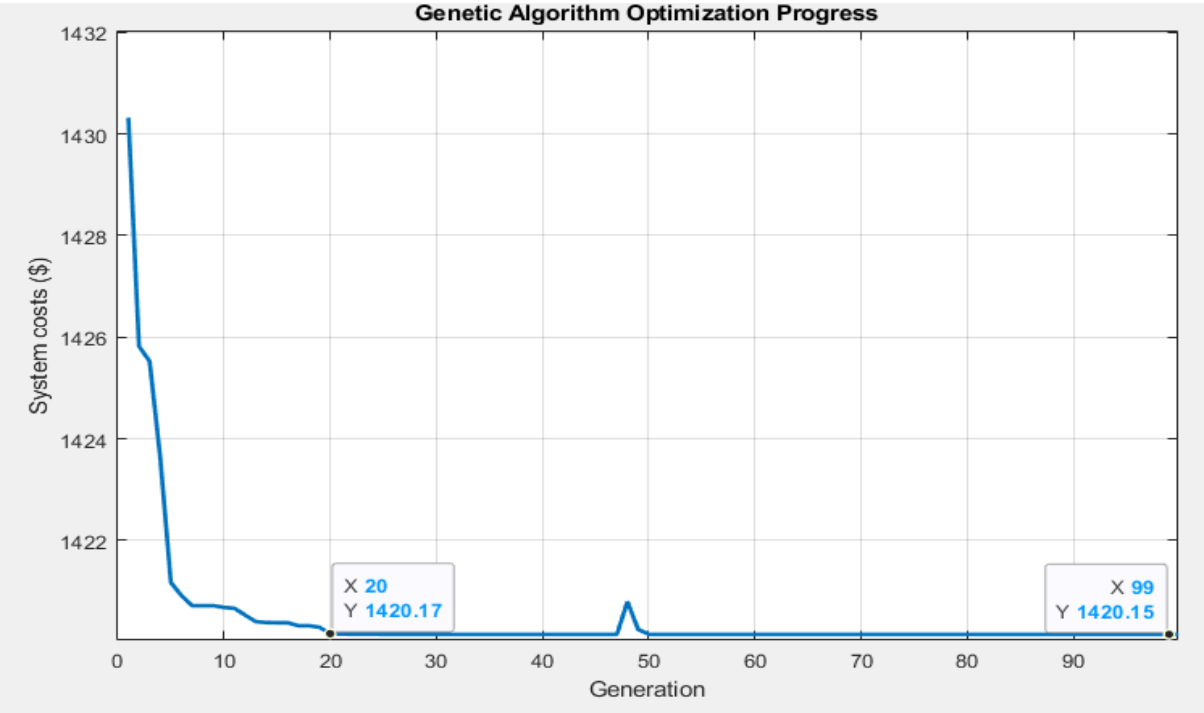

Figure 4.8: Convergence plot using GA (100 iterations) for BESS placed at Buses 1,3 and 4.

The analysis also highlighted significant challenges at certain buses, particularly bus 9 and bus 12 with existing PV systems. Bus 9 and bus 12 emerged as the least favourable locations for BESS placement as they displayed the worst results for active power losses and voltage deviations. The results underscore the complexities involved in integrating RES such as PV systems and the critical need for strategic BESS placement to mitigate associated issues. Figures 4.9 through 4.12 illustrate the convergence characteristics for these buses.

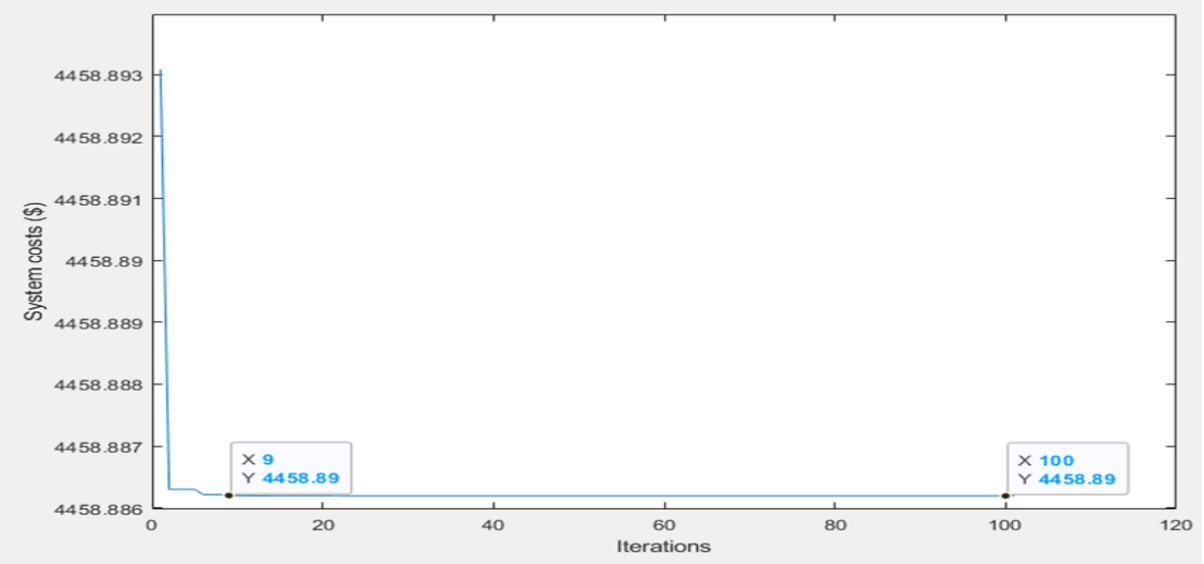

Figure 4.9: Convergence plot using PSO (100 iterations) for BESS placed at bus 9.

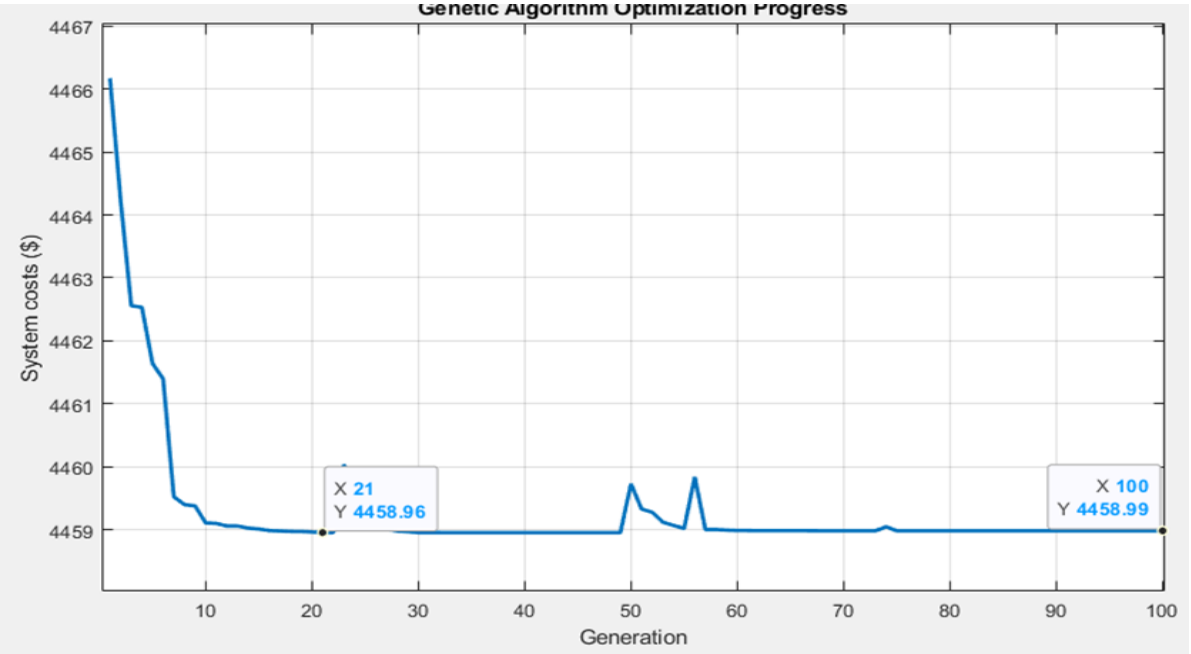

Figure 4.10: Convergence plot using GA (100 iterations) for BESS placed at bus 9.

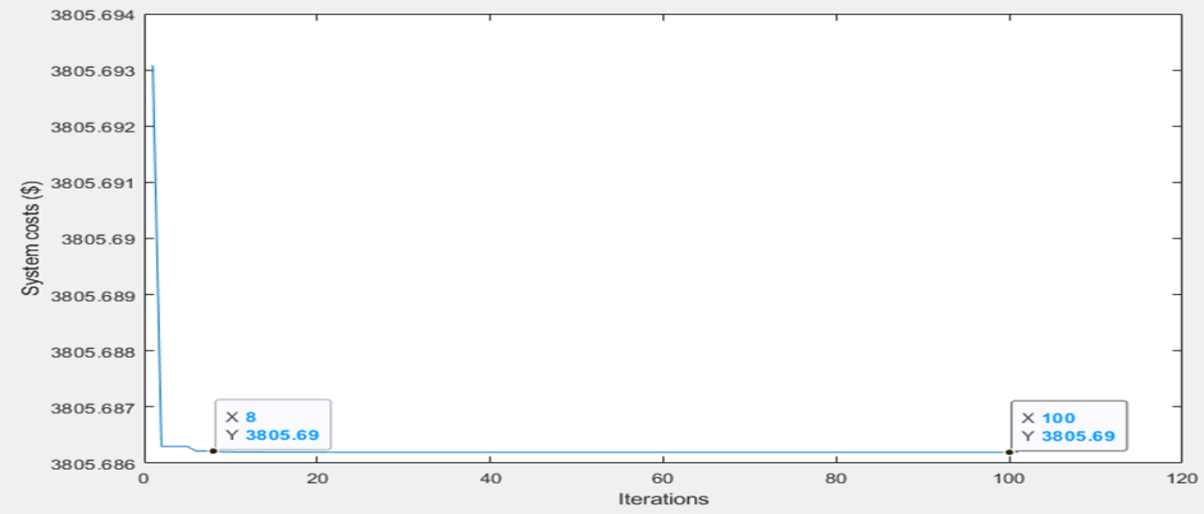

Figure 4.11: Convergence plot using PSO 100 iterations) for BESS placed at bus 12.

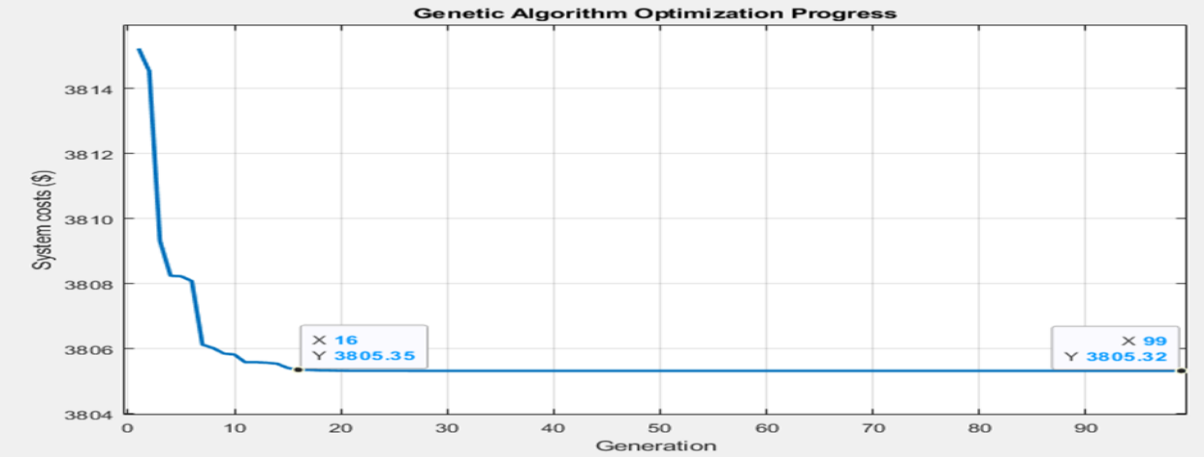

Figure 4.12: Convergence plot using GA (100 iterations) for BESS placed at bus 12.

The analysis reveals a substantial variation in system costs across different bus locations, highlighting the critical impact of BESS placement on overall network efficiency. Table 4.2 give a complete list of the priority analysis for Witzenberg distribution system. Bus 13 proved to be the most cost-effective, other locations such as bus 14 and bus 10 also showed promise as secondary options. Conversely, bus 9 and bus 12 were identified as the least favorable locations with significantly higher system costs.

Proper consideration of the overall priority analysis results strongly suggested that the placement of BESS at bus 13 can maximize system costs benefits and improve the efficiency of the studied distribution network. However, it is crucial to note that while cost optimization is a primary factor, final placement decisions should also consider other operational and strategic factors such as land availability, proximity to existing infrastructure, environmental impact, future network expansion plans, maintenance accessibility, and interconnection requirements.

The role of certain buses in the network, such as bus 1 serving as a slack bus, may influence placement options beyond pure cost considerations. This balanced approach ensures that BESS deployment not only minimizes system costs but also aligns with the broader operational goals and constraints of the network, ultimately leading to a more robust and efficient distribution network.

4.2. Priority Analysis for BESS Placement

As discussed previously, the priority analysis for optimal BESS placement was conducted using both Particle Swarm Optimization (PSO) and Genetic Algorithm (GA) in MATLAB. The objective function focused on minimizing both active power losses and voltage deviation costs. The analysis results, summarized in Table 4.2, present the system costs calculated for BESS placement at each system network bus. Using the optimization algorithms as detailed in [11], [70] the bus location yielding the lowest total system costs was identified as the optimal placement for the BESS in the 16 bus Witzenberg distribution network.

Table 4.2: The Priority Analysis results for optimal BESS placement

Location	System Costs ($)	Priority	Percentage Cost Reduction (%)
Without BESS placement			
2272.254			
With BESS placement			
Bus 13	937.29	1	58.75
Bus 14	1050.88	2	53.75
Bus 10	1249.79	3	45.00
Bus 5	1391.68	4	38.75
Bus 1	1420.13	5	37.50
Bus 3	1420.13	6	37.50
Bus 4	1448.53	7	37.50
Bus 6	1420.24	8	36.25
Bus 2	1533.69	9	32.50
Bus 17	1846.14	10	18.75
Bus 7	2811.7	11	-23.74
Bus 11	2840.1	12	-24.99
Bus 12	3805.75	13	-67.49
Bus 9	4458.95	14	-96.23

Note: negative sign means an increase

The priority analysis of BESS placement in the Witzenberg distribution network has yielded significant insights for the system optimization. Both PSO and GA techniques consistently identified bus 13 as the optimal location for BESS placement, demonstrating the lowest system cost of $937.29 and reducing the original system costs (without BESS optimal placement) by 58.75%, while effectively improving

voltage profiles and reducing active power losses. In contrast, bus 9 emerged as the least optimal location with system costs of $4,458.95, representing a substantial 96.23% increase in costs, along with notably higher power losses. This strategic selection of bus 13 balances cost considerations with the bus's critical role in the network, maximizing operational benefits while ensuring system reliability. The convergence of the results from both optimization methods provides robust validation of bus 13's selection as the most cost-effective BESS placement location and confirms the unsuitability of bus 9 for BESS installation.

The priority analysis and optimization convergence results strongly favour placing BESS at 132kV voltage buses, particularly at bus 13. The clear order of preferable locations provided by the priority list results can guide a phased implementation of BESS in the network, potentially optimizing investment and operational efficiency.

Further investigation is needed for buses with existing PV systems particularly bus 12 and bus 9, to manage the higher losses and costs associated with BESS placement at these locations. This result highlights the need for integrated planning when combining BESS with existing RESs such as PV systems.

4.3 Active Power Losses Analysis

The active power losses analysis in the Witzenberg distribution network reveals significant variations across different BESS placement scenarios. Table 4.3: presents a detailed summary of the total Witzenberg network active power losses. This comparative analysis provides critical insights into the effectiveness of strategic BESS deployment and emphasizes the importance of strategic placement.

Table 4.3: Summary analysis of the total network active power losses.

Location	Scenario	Power Loss (MW)	Percentage Reduction (%)
Without BESS placement			
		8	-
With BESS placement			
Bus 13 (Optimal)	With BESS Optimally Placement	3.30	58.75
Bus 14	With BESS	3.70	53.75
Bus 10	With BESS	4.40	45.00
Bus 5	With BESS	4.90	38.75
Bus 1	With BESS	5.00	37.50
Bus 3	With BESS	5.00	37.50
Bus 4	With BESS	5.00	37.50

Bus 6	With BESS	5.10	36.25
Bus 2	With BESS	5.40	32.50
Bus 17	With BESS	6.50	18.75
Bus 7	With BESS	9.90	-23.75
Bus 11	With BESS	10.00	-25.00
Bus 12	With BESS	13.40	-67.50
Bus 9 (not optimal)	Least optimal placement	15.70	-96.25

Note: negative sign means an increase

A comprehensive analysis of active power losses in the Witzenberg distribution network revealed significant variations across different BESS placement scenarios. The baseline network without BESS installation experienced total power losses of 8 MW, serving as the reference point for comparative analysis. The results identified bus 13 as the optimal location, achieving a reduction in power losses to 3.3 MW, representing a 58.75% improvement from the baseline. Similar positive outcomes were observed at bus 14 and bus 10, which achieved losses of 3.7 MW (53.75% reduction) and 4.4 MW (45% reduction), respectively. A moderate group of locations, including buses 1, 3, and 4, each demonstrated consistent performance with losses of 5.0 MW (37.5% reduction), while bus 6 showed slightly higher losses at 5.1 MW (36.25% reduction).

However, the analysis also revealed locations were BESS placement significantly degraded network performance. The least effective placements were at bus 9 with 15.7 MW losses (96.25% increase) and bus 12 with 13.4 MW losses (67.5% increase). Other poor performing locations included bus 7 (9.9 MW, 23.75% increase) and bus 11 (10.0 MW, 25% increase). These results demonstrate the negative impact of non-optimal BESS placement in the distribution network, where active power losses increased by more than 60% from the initial baseline.

The results validate the importance of using advanced optimization techniques such as PSO and GA to determine the most effective BESS placement locations. The stark contrast between optimal and non-optimal placements emphasizes the necessity of comprehensive network analysis and simulation studies prior to BESS deployment to ensure maximum system benefits and avoid unintended negative consequences in network operation. This analysis has highlighted that while strategic BESS placement can significantly improve network efficiency and reduce operational costs, improper location selection can substantially worsen system performance in terms of both active power losses and voltage profiles.

4.4 Voltage profiles Analysis

The voltage profile analysis of the Witzenberg distribution network integrated with PV system provides crucial insights into the network's performance before and after the integration of BESS. This analysis is essential for understanding the impact of BESS on voltage profile and active power losses across the 16-bus network integrated with PV system. Before discussing the effects of BESS integration, it's important to establish the baseline voltage profile. Table 4.4 shows the network nominal bus voltages vs. baseline voltage values.

Table 4.4: Network nominal bus voltages vs. baseline voltage values.

Bus No.	Nominal Voltage (k.V)	Nominal Voltage (p.u.)	Baseline Voltage (p.u.)
Bus 1	132	1.000	1.040
Bus 2	66	1.000	0.907
Bus 3	132	1.000	1.027
Bus 4	66	1.000	0.911
Bus 5	66	1.000	0.907
Bus 6	132	1.000	1.027
Bus 7	66	1.000	1.027
Bus 8	10	1.000	0
Bus 9	132	1.000	1.031
Bus 10	132	1.000	1.009
Bus 11	66	1.000	0.915
Bus 12	132	1.000	1.039
Bus 13	132	1.000	0.975
Bus 14	66	1.000	0.922
Bus 15	11	1.000	0.916
Bus 16	11	1.000	0.916
Bus 17	132	1.000	1.011

4.4.1. Voltage Profile Analysis Before BESS Installation

The voltage profile analysis for the Witzenberg distribution network compares two key voltage measurements: nominal voltages and baseline voltages. The nominal voltage, represented by blue bars in Figure 4.13, indicates the standard operating voltage of 1.0 per unit (p.u.) for each bus in the network. This reference value remains constant at 1.0 p.u. regardless of the actual kilovolt (kV) level of the bus. In contrast, the baseline voltage, shown by orange bars in the figure, represents the actual operating conditions of the network before BESS installation. These baseline measurements reveal the existing voltage conditions and highlight deviations from the nominal values across the network. The network comprises three distinct voltage level categories:

132kV buses (including buses 1, 3, 6, 9, 10, 12, 13, and 17), 66kV buses (encompassing buses 2, 4, 5, 7, 11, and 14), and low voltage buses (8, 15, and 16) operating at 10/11kV. Figure 4.13 provides a comprehensive baseline load flow summary, illustrating the voltage profile results before the installation of BESS. This visualization clearly displays both the nominal reference voltages for the 66 kV and 132 kV buses and their corresponding per unit voltage values, offering a clear comparison between ideal operating conditions and actual network performance.

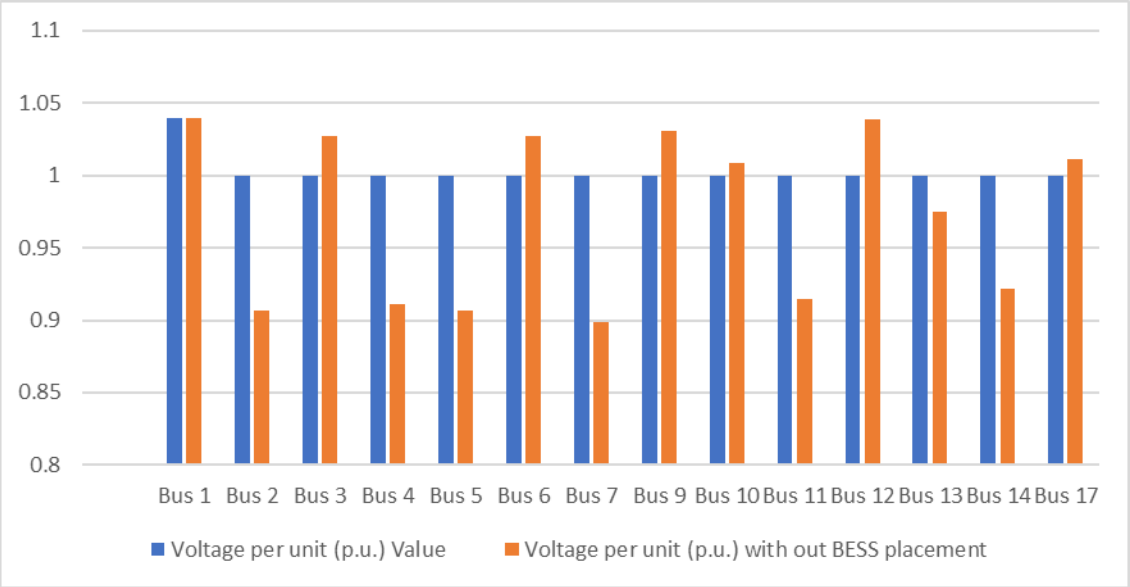

Figure 4.13: Summary of Baseline voltage profile (orange) results before BESS placement

The load flow analysis conducted in DigSilent PowerFactory revealed significant voltage profile challenges in the 16-bus network. This analysis provided a clear understanding of the baseline network conditions, showing the difference between nominal (ideal) voltages and the actual voltages before BESS implementation. The comparison highlights voltage regulation challenges, particularly in the 66kV network section (i.e., buses 2, 4, 5, 7, 11 and 14).

The analysis of the Witzenberg distribution network's baseline voltage profiles reveal significant variations across different voltage levels, highlighting several areas of concern before the BESS implementation. The network consists of buses operating at three main voltage levels: 132kV, 66kV, and low voltage (10/11kV) buses.

At the 132kV level, the network maintains relatively stable voltage profiles (i.e., buses 3, 6, 9, 12, 13, 17). The slack bus (bus 1) is purposely set to 1.040 p.u. to provide voltage support and compensate for system voltage drops. Other 132kV buses (3, 6, 9, 10, 12, 13, 17) demonstrated generally acceptable performance, with voltages ranging from 0.975 p.u. to 1.039 p.u., mostly operating within the South African Grid Code's acceptable range of ±5% (0.95-1.05 p.u.).

However, the 66 kV buses (2, 4, 5, 7, 11, and 14) portion of the network presents significant concerns. These buses consistently operate below the minimum acceptable threshold of 0.95 p.u., indicating substantial undervoltage issues. Bus 7

exhibits the most critical condition with a voltage of 0.899 p.u., followed by buses 2 and 5 at 0.907 p.u., bus 4 at 0.911 p.u., bus 11 at 0.913 p.u., and bus 14 at 0.910 p.u. These low voltage levels, ranging from 0.899 to 0.913 p.u., show widespread power quality issues and the need for voltage support in this section of the network.

The low voltage (10/11 kV) buses (8, 15, 16) also show concerning voltage profiles, with buses 15 and 16 operating at 0.916 p.u., below the acceptable minimum threshold. Bus 8 presents a disconnected BESS system busbar status 0.0 p.u.

When comparing these operating voltages to their nominal values (all standardized at 1.0 p.u.), the deviations clearly highlight the network's voltage regulation challenges, particularly in the 66kV network section. These baseline conditions emphasize the need for voltage support solutions to bring bus voltages within acceptable operating ranges as specified by the South African Grid Code.

4.4.2 Impact of PV system integration on voltage Profiles

The integration of the 36MW PV system at bus 12 demonstrated significant improvements in the network's voltage profile compared to baseline conditions. The complete voltage profile results are shown in table 4.5 below.

Table 4.5: Voltage Profiles Analysis with PV system integration at Bus 12.

Bus No.	Baseline Voltage (p.u.)	Voltage With PV System (p.u.)	Improvement (%)
Bus 1	1.04	1.040	0.000
Bus 2	0.848	0.939	10.73
Bus 3	1.023	1.033	1.000
Bus 4	0.854	0.945	10.66
Bus 5	0.863	0.945	9.500
Bus 6	1.023	1.032	0.880
Bus 7	0.846	0.929	9.810
Bus 8	0.883	0.962	8.950
Bus 9	1.006	1.015	0.895
Bus 10	0.994	1.027	3.320
Bus 11	0.875	0.955	9.143
Bus 12	1.015	1.016	0.098
Bus 13	0.941	0.973	3.400
Bus 14	0.883	0.962	8.950
Bus 15	0.91	0.923	1.430
Bus 16	0.91	0.923	1.430
Bus 17	1.009	1.017	0.793

Prior to PV integration, the network exhibited concerning voltage violations, with multiple buses operating well below the acceptable range of 0.95-1.05 p.u. The baseline measurements revealed critical voltage issues particularly at buses 2, 4, 5, and 7, which recorded voltages of 0.848, 0.854, 0.863, and 0.846 p.u. respectively.

Following the PV system integration at bus 12, these voltage profiles showed marked improvement, with buses 2, 4, and 5 approaching the acceptable range at 0.939 p.u, 0.945 p.u, and 0.945 p.u. respectively. Bus 13 improved from 0.941 p.u to 0.973 p.u., showing significant enhancement though still below the acceptable threshold. However, despite these substantial improvements, some buses, particularly buses 15 and 16, remained at 0.923 p.u., still below the acceptable threshold. This suggests that while PV integration significantly enhanced the overall network voltage profile, full voltage compliance across all buses may require additional support mechanisms. The results underscore both the effectiveness and limitations of PV integration as a standalone solution for voltage profile improvement in the distribution network.

4.4.3 Voltage Profiles Analysis after BESS Placement

Based on the optimization results, the optimal BESS placement location was identified, with non-optimal bus locations showing negative network impacts. Voltage profile analysis was conducted across various placement scenarios: optimal location (bus 13), near-optimal location (bus 14), and non-optimal locations (bus 12 and bus 9). Each scenario produced distinct effects on the network's voltage profiles, with complete results documented in Appendix I, tabulated in Tables H2 through to H5 of Appendix H.

4.4.3.1 Voltage Profiles Analysis after BESS Placement at Bus 13

The installation of BESS at bus 13 led to significant improvements in voltage profiles across the network. Figure 4.14 summarizes the voltage profile results after BESS placement:

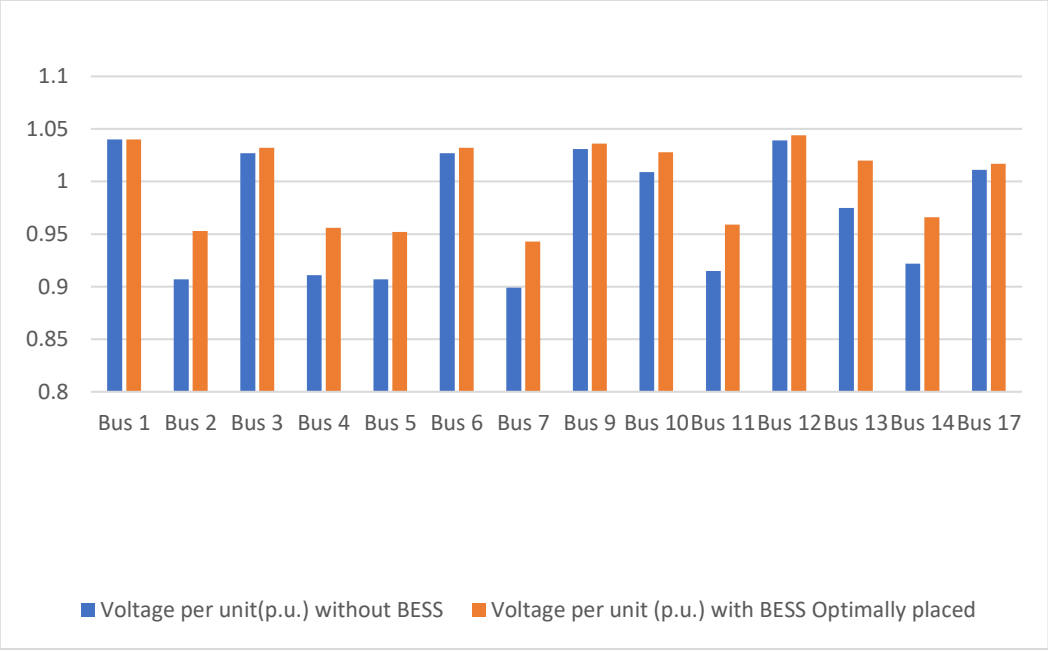

Figure 4.14: summary of voltage profile results after BESS placement at Bus 13.

The installation of BESS at bus 13 demonstrated significant and widespread improvements in voltage profiles across the Witzenberg distribution network, with complete results documented in Appendix H2. Analysis of the 17 buses revealed that bus 15 experienced increased voltage levels, while bus 2 maintained their previous levels, indicating a predominantly positive network-wide impact. The most notable enhancement occurred at the BESS location (bus 13), which achieved a substantial 4.62% improvement from 0.975 p.u. to 1.02 p.u. This improvement extended to nearby buses, particularly in the 66kV network, where bus 2 experienced a 5.1% increase, bus 7 saw a 4.9% increase, and Bus 14 improved by 4.8%.

The impact of BESS placement varied across voltage levels, revealing distinct improvement patterns. While 132kV buses showed modest improvements ranging from 0.5% to 4.5%, the 66kV buses (2, 4, 5, 7, 11, and 14) experienced more substantial improvements, mostly in the 4-5% range. This differential impact proved particularly beneficial as the 66kV buses had previously experienced more severe undervoltage issues.

Importantly, the placement of BESS significantly increased the number of buses operating within the typical voltage South African Grid Code range of ±5%, enhancing overall compliance with voltage standards across the network. This improvement in voltage profile deviations is crucial for maintaining power quality and system stability.

A key result of this analysis is the absence of any negative impacts on bus voltages following BESS installation. This uniformly beneficial or neutral effect across all points in the network underscores the strategic value of the chosen placement location. The Witzenberg buses, directly connected to the BESS placement location, experienced the most substantial improvements in voltage levels, suggesting that bus 13 is an optimally effective location for addressing voltage issues in this part of the network. The overall result is a narrower range of voltage levels throughout the network, indicating a more balanced and stable voltage profile.

Beyond voltage profile improvements, the placement of BESS at bus 13 offers strategic benefits to the Witzenberg distribution network. the BESS placement helps reduce strain on the critical radial line from bus 13 (receiving) to bus 10 (sending) that links to the transmission network. This reduction in strain can lead to improved line efficiency and potentially extend the lifespan of the infrastructure.

The strategic location of the BESS also improved overall network stability by providing voltage support and power flow control. This is especially beneficial during periods of high renewable generation or low load, situations that can often lead to voltage fluctuations and stability issues. By mitigating the voltage profile deviation and active power losses challenges, the BESS contributes to a more resilient and flexible distribution network, capable of accommodating the increasing integration of RESs.

Overall, the placement of BESS at Witzenberg bus 13 has demonstrated clear and multifaceted benefits to the distribution network. It effectively addresses undervoltage issues, particularly in the more vulnerable 66kV network, while enhancing overall voltage profile regulation. The combination of localized voltage improvements, increased compliance with grid standards, prevention of reverse power flow, and reduced strain on critical infrastructure underscores the strategic value of this BESS placement decision. The simulation results suggest that this location is optimally effective for improving voltage stability, enhancing network resilience, and supporting the integration of RESs in the Witzenberg distribution network.

4.4.3.2 Voltage profiles Analysis after BESS Placement at Bus 14

Figure 4.15 is the summary of voltage profile results after BESS placement at bus 14.

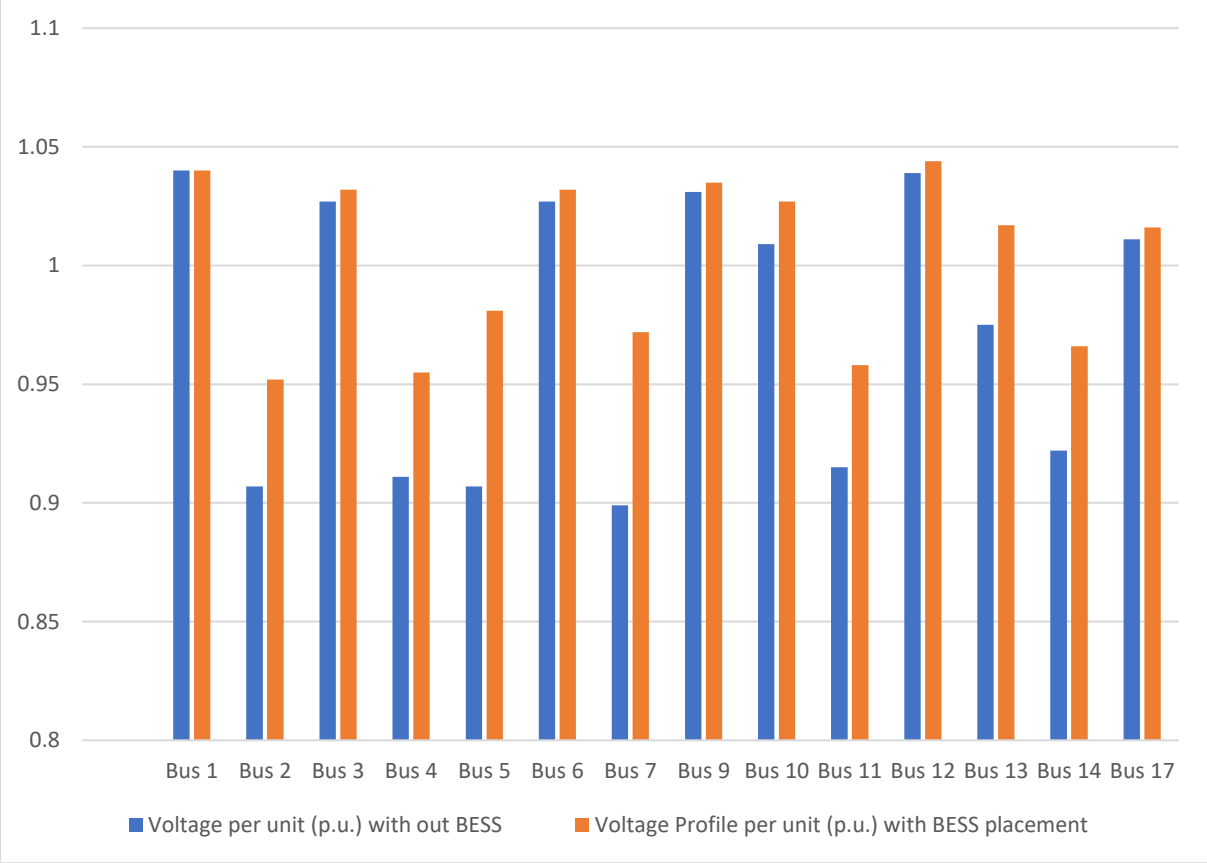

Figure 4.15: summary of voltage profile results after BESS placement at Bus 14.

Note: Bus 8 is not shown as it represents the LV bus of BESS (deactivated). Buses 15 and 16 represent 11 kV tertiary windings.

The placement of BESS at bus 14 resulted in significant voltage profile improvements across the network, as shown in Figure 4.15. The figure provides a comprehensive summary of voltage profiles after BESS placement, with complete results documented in Appendix I2. Analysis of the measured buses showed widespread voltage level improvements, with bus 1 (Bacchus 132 kV) remaining constant at 1.04 p.u. as it

serves as the slack bus. This widespread positive impact demonstrates the effectiveness of BESS placement in enhancing overall network voltage stability.

The most substantial improvements, clearly visible in Figure 4.15 and tabulated in appendix H3, were observed in the 66kV buses (2, 4, 5, 7, 11, and 14), which previously experienced the lowest voltage levels. Improvements in this voltage class ranged from 4.70% to 8.16%, with bus 7 and bus 5 experiencing the largest increases of 8.12% and 8.16%, respectively. The figure effectively emphasizes the significant improvements in the 66kV network, addressing voltage issues where they were most prevalent.

In contrast, as depicted in Figure 4.15, the 132kV buses (3, 6, 9, 10, 12,13 and 17) showed more modest improvements. Bus 13 saw the largest increase in this class at 4.31%, while other 132kV buses had improvements ranging from 0.39% to 1.78%. This differential impact across voltage levels clearly illustrated in the figure, demonstrates the BESS's ability to provide targeted support where it is most needed in the network.

The BESS placement has significantly improved voltage profile adjustment across the network, a trend that is visually evident in Figure 4.15. Prior to BESS implementation, voltage profile levels ranged from 0.899 p.u. to 1.039 p.u. After installation, the voltage range tightened to between 0.932 p.u. and 1.044 p.u., demonstrating improved voltage stability and uniformity. The figure clearly shows how this improvement has brought more buses into compliance with the South African Grid Code acceptable voltage range of 0.95 -1.05 p.u.

Notably, as can be observed in Figure 4.15, before BESS installation, five 66kV buses (2, 4, 5, 7, 11 and 14) were below 0.95 p.u., but after installation, none were below the grid code 5% tolerance band. This improvement in compliance visually represented in the figure, is crucial for maintaining power quality and network stability.

The analysis, which complements the data presented in Figure 4.15, further supports these improvements. The mean voltage across the network increased from 0.962 p.u. to 0.993 p.u., indicating an overall elevation of voltage levels. Furthermore, the standard deviation decreased from 0.0561 p.u to 0.0391 p.u, signifying a reduction in voltage variability across the network. These changes quantify the BESS's impact in both raising and stabilizing voltage levels throughout the distribution network, a trend that is visually apparent in the figure.

In conclusion, Figure 4.15 provides a clear and comprehensive representation of the significant benefits of integrating BESS at bus 14. The figure effectively illustrates how this strategic placement has addressed undervoltage issues particularly in the 66kV network buses (2, 4, 5, 7, 11 and 14) and improved overall voltage profiles. This visual evidence combined with the statistical analysis, underscores the potential of BESS deployment.

The comprehensive improvements observed, including increased compliance with grid code standards, reduced voltage profile variability, and targeted support for lower voltage levels, underscore the potential of BESS as a versatile tool for modern distribution network management. The simulation results provide compelling evidence

for the value of strategically optimally placing BESS as an effective tool for voltage profile improvement in distribution networks.

4.4.3.3 Voltage profiles Analysis after BESS Placement at Bus 12

For BESS placement at bus 12, Figure 4.16 is the summary of voltage profile results after BESS placement.

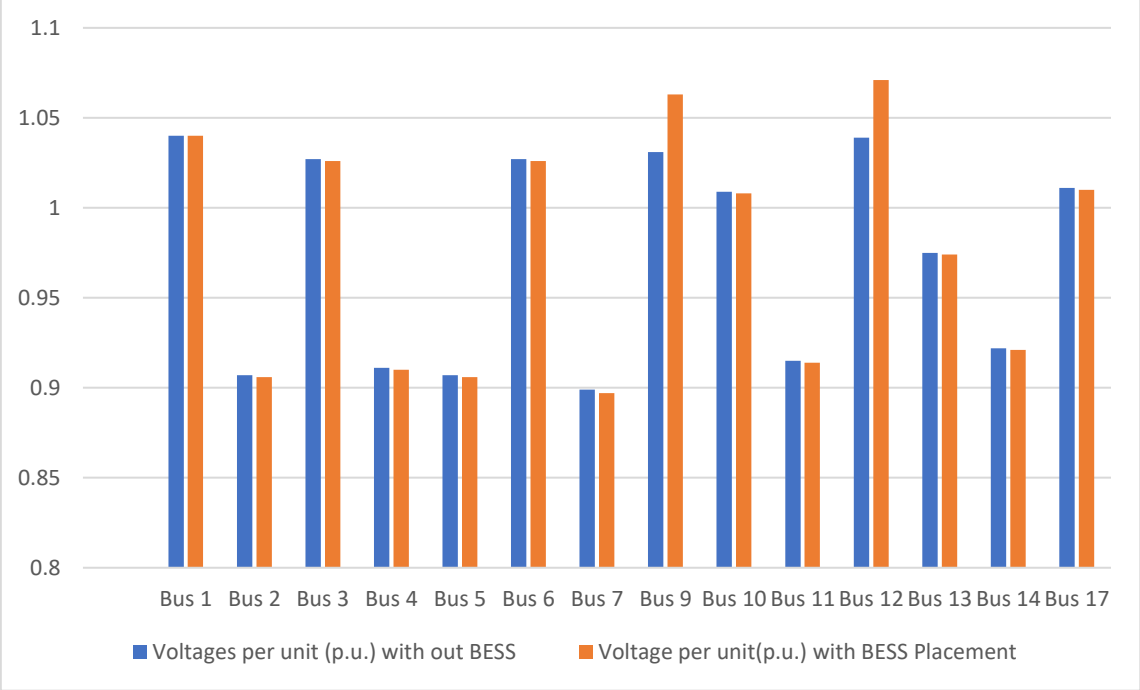

Figure 4.16: summary of voltage profile results after BESS placement at bus 12.

Note: Bus 8 is not shown as it represents the LV bus of BESS (deactivated). Buses 15 and 16 represent 11 kV tertiary windings.

The placement of BESS at bus 12 in the Witzenberg distribution network has resulted in a complex set of voltage profile changes across the network, as illustrated in Figure 4.16, with complete results documented in Appendix H4. This figure provides a comprehensive overview of the voltage levels at each bus following BESS placement revealing a mix of impacts that vary significantly across various parts of the network. As evident from Figure 4.16, the most significant impact was observed at the BESS placement location at bus 12. Bus 12 experienced a substantial increase from 1.039 p.u. to 1.071 p.u., representing a 3.08% rise.

The figure clearly shows that the significant voltage increases at three buses (8, 9 and 12) have pushed them above the typical upper limit of 1.05 p.u., introducing overvoltage concerns. Equally, Figure 4.16 reveals that most of the network (10 out of 17 buses) experienced slight decreases in voltage profile levels, with 4 buses seeing an increase and 3 remaining unchanged. The 132kV buses, as shown in the Figure 4.16, generally maintained their voltage levels or experienced very small changes. For

instance, Bus 1 remained constant at 1.04 p.u., while others like bus 3 and bus 6 saw negligible decreases of 0.001 p.u.

The impact of BESS placement varied across different voltage levels in the network, a trend clearly visible in Figure 4.16. While the 132kV buses showed mixed results, all 66kV buses experienced slight decreases in voltage. This is particularly concerning as these buses were already operating below the preferred 0.95 p.u. threshold. For example, the figure shows that bus 2 and bus 5 both decreased from 0.907 p.u. to 0.906 p.u., while bus 7 decreased from 0.899 p.u. to 0.897 p.u. These changes although small, further intensify the existing undervoltage issues in the 66kV level of the network.

Figure 4.16 highlights the distribution of voltage changes, suggesting that the BESS placement had its most significant impacts at and near its location, with more distant buses experiencing minimal changes or slight decreases.

These results as illustrated in Figure 4.16, underscore the complex nature of BESS placement location in distribution networks. While the placement at bus 12 has increased voltages in its vicinity. BESS placement has also introduced potential overvoltage issues at three buses and has not addressed, and in some cases slightly worsened the undervoltage problems in the 66kV portion of the network.

Overall, Figure 4.16 provides clear visual evidence that BESS placement location is not optimal for overall network voltage profile improvement. The varied impacts across different voltage levels and bus locations as shown in the figure 4.16, underscore the need for careful consideration of placement strategies to balance voltage support across all voltage levels in the network.

This analysis, supported by the comprehensive data visualization in Figure 4.16, emphasizes the importance of strategic BESS placement to achieve desired voltage profile improvements without introducing new power quality concerns. Therefore, the results show that BESS placement location was not optimal for overall network voltage profile improvement and underscores the need for careful consideration of placement strategies.

4.4.3.4. Voltage profiles Analysis after BESS Placement at Bus 9

For BESS placement at bus 9, Figure 4.17 is the summary of voltage profile results after BESS placement.

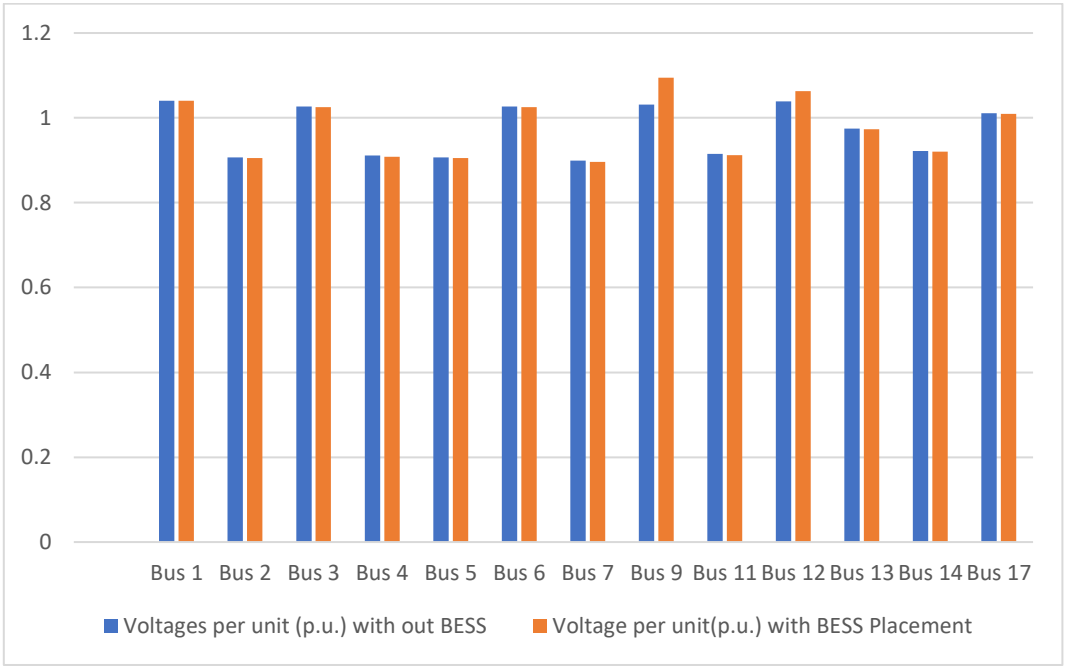

Figure 4.17: summary of voltage profile results after BESS placement at bus 9.

Note: Bus 8 is not shown as it represents the LV bus of BESS (deactivated). Buses 15 and 16 represent 11 kV tertiary windings.

The implementation of a BESS at bus 9 in the Witzenberg distribution network has produced a complex set of outcomes across various voltage levels, as clearly illustrated in Figure 4.17. This placement has emerged as one of the least optimal locations for BESS placement, with the results highlighting significant challenges and limited benefits to overall network voltage steadiness.

As evident from Figure 4.17, with complete results documented in Appendix H5, the impact of BESS placement at bus 9 varies considerably across different voltage levels. At the 132kV level, the impacts are mixed and challenging. While some buses, such as bus 1, maintained their voltage at 1.04 p.u., others experienced minor decreases of 0.001 to 0.002 p.u. However, two notable exceptions emerged, presenting significant concerns. Bus 9 saw a substantial increase from 1.031 p.u. to 1.095 p.u., and bus 12 rose from 1.039 p.u. to 1.063 p.u. These considerable increases, clearly visible in Figure 4.17, push both buses well above the typical upper limit of 1.05 p.u. as per the grid code, introducing new challenges related to overvoltage.

The situation at the 66kV level, as shown in Figure 4.17, presents an even more concerning picture, underscoring why this location is non-optimal for the BESS placement. All 66kV buses (2, 4, 5, 7,11, and 14) which were already operating below

the preferred 0.95 p.u. threshold before BESS placement, experienced further slight decreases. For instance, the figure shows that bus 2 and bus 5 declined from 0.907 p.u. to 0.905 p.u., while bus 7 already the lowest, further decreased from 0.899 p.u. to 0.896 p.u. This aggravation of existing undervoltage issues in the 66kV portion of the network may negatively impact the quality of power delivery to connected customers.

Figure 4.17 clearly illustrates the divergent outcomes at different voltage levels, suggesting that the BESS's influence is not uniformly beneficial across the network. The localized nature of the BESS impact when placed at bus 9 is evident. While it has significantly increased voltages at its location and one other specific point, its effect on the rest of the network is minimal or even slightly detrimental, particularly for the already undervolted 66kV buses.

The results, as demonstrated in Figure 4.17, stresses the reason bus 9 is considered one of the least optimal BESS placement locations. The placement has not effectively addressed the undervoltage issues in the 66kV portion of the network, as these buses remain below the 0.95 p.u. threshold. Moreover, it has introduced potential overvoltage issues at two 132kV buses, complicating the voltage profile regulation of the network.

In conclusion, the results presented in Figure 4.17 provide clear evidence that BESS placement at bus 9 is not optimal for improving voltage profile issues across the entire Witzenberg distribution network. While there are some localized voltage increases, these come at the cost of potential overvoltage issues and a failure to address. Some cases a slight worsening of undervoltage problems in the 66kV voltage level. This analysis underscores the critical importance of careful consideration in BESS placement strategies. It demonstrates that improper placement can not only fail to solve existing voltage problems but can also introduce new challenges, emphasizing the need for a more balanced approach to achieve effective voltage support across all voltage levels in the distribution network.

4.5 Percentage Voltage Deviation Index Analysis.

The PVDI analysis for the Witzenberg distribution network showed marked improvement following BESS placement at bus 13. The baseline PVDI of 11.98% before BESS installation indicates significant voltage deviations across the network. Complete results of voltage deviation improvements are documented in Appendix I, Table I, demonstrating the varied impact of BESS placement across different network buses.

The results indicate that 13 out of 14 BESS placement locations demonstrated positive improvements in voltage deviation, with improvements ranging from 22.0% to an impressive 71.0%. The most effective BESS placements were observed at bus 13, which showed a remarkable 71.0% improvement, followed by bus 14 with a 67.9% improvement, and bus 5 with a 67.6% improvement. These substantial improvements underscore the potential of strategically placed BESS in significantly improving voltage profiles.

A notable trend occurs when comparing the performance of different voltage levels. The 66kV buses generally outperformed the 132kV buses in improving voltage profiles. Five out of six 66kV buses (2,4, 5, 7 and 11) showed improvements greater than 60%, demonstrating their high responsiveness to BESS integration. In contrast, the 132kV buses demonstrated more moderate but consistent improvements, mostly in the 40-50% range. This consistency at the 132kV buses (3, 6, 9, 10, 12, 13, 17) suggests a reliable benefit from BESS placement, while the more varied results at the 66kV level indicate a higher sensitivity to specific network characteristics.

4.6 Summary

The results demonstrate that strategic BESS placement can significantly improve voltage profiles and reduce active power losses in the Witzenberg distribution network (see Appendix J). The optimization techniques (PSO and GA) proved effective in identifying optimal placement location. However, the analysis also highlighted the potential negative impacts of non-optimal BESS placement, emphasizing the importance of careful planning and analysis.

The analysis also highlighted important considerations for BESS placement strategies. While 11 out of 14 bus placement locations showed improvements greater than 40%, the bus 4 stood out as an anomaly. It was the only location where BESS placement worsened the voltage deviation, resulting in a 9.8% increase in PVDI. This unexpected result underscores the necessity of comprehensive network analysis and simulation before BESS deployment, as non-optimal placement can lead to unintended negative consequences.

The varied results, especially among 66kV buses, suggest that network topology plays a crucial role in the effectiveness of BESS placement. Factors such as proximity to loads, interaction with existing voltage regulation equipment, and the overall network structure likely influence the outcomes. These findings demonstrate the significant potential of strategically placed BESS in improving voltage profiles in distribution networks with high PV penetration.

In conclusion, the PVDI analysis reveals that BESS placement has largely been successful in improving voltage profile deviations across the Witzenberg distribution network. The overall Percentage Voltage Deviation Index for the 16-bus system was calculated at 5.24%, indicating the average deviation of bus voltages from the nominal 1.0 p.u. value after BESS placement. This metric reflects the effectiveness of the BESS in stabilizing voltage levels across the network. However, the varied results also underscore the importance of optimal placement specific bus analysis in maximizing the benefits of BESS deployment and avoiding potential negative impacts.

Chapter 5 : Conclusion and Recommendations for future work

This chapter presents the conclusions and recommendations for future work of this dissertation.

5.1 Conclusions

The focus of this dissertation was analysing optimal BESS deployment as an enabler for RES in the Witzenberg distribution network. This dissertation addressed the integration of RESs in the distribution system through strategic deployment of BESS. The 16-bus distribution network, integrating PV system, required energy storage solutions to manage intermittent RES generation effectively. The research methodology employed both PSO and GA methods, with MATLAB handling the optimization processes and DIgSILENT performing load flow analyses for network parameter determination. Through this dual-platform approach, the study achieved comprehensive technical validation of the proposed solutions.

The optimization analysis, utilizing both GA and PSO methodologies, converged on bus 13 as the optimal BESS placement location, providing healthy validation for this strategic decision. Optimal BESS placement demonstrated remarkable improvements in network performance, with active power losses reducing significantly from 8 MW to 3.3 MW, representing a 58.75% improvement in network efficiency. Furthermore, critical voltage profiles at buses (2, 4, 5, 7, 11, 14, 15, and 16) were successfully brought within the grid code's acceptable ±5% range. The PVDI showed substantial improvement, decreasing from 11.98% to 5.24%, demonstrating a 56.26% enhancement in overall voltage stability across the network.

The optimization process effectively balanced multiple objectives, including total costs associated with voltage profile deviations and power losses within the distribution system. Both GA and PSO implementations confirmed the viability of BESS installation for improving distribution network efficiency. PSO demonstrated superior performance compared to GA in several key aspects: it achieved faster convergence (reaching optimal solution), showed more consistent results across multiple runs with lower standard deviation in final solutions and required less computational time for this specific optimization challenge. The methodology successfully integrated considerations for cost minimization, voltage profile improvement, and loss reduction, providing a comprehensive solution for modern distribution network challenges.

The simulation results demonstrated that strategic BESS placement significantly improves distribution network performance through reduced total network power losses and improved network buses voltage profiles. Furthermore, the successful integration of RES validated the effectiveness of this approach for Witzenberg distribution network optimization. The dissertation findings highlight the significant potential of optimally placing BESS in supporting renewable energy integration while

maintaining network stability, marking an important contribution to the field of distribution system improvement.

5.2 Recommendations for future work

Based on the findings of this dissertation, the following recommendations are proposed for future work:

- Develop dynamic models of the Witzenberg network to analyze BESS performance under various load and generation scenarios, including extreme conditions and fault situations.
- Implement multi-objective optimization algorithms to balance multiple performance metrics simultaneously (e.g., voltage stability, power loss reduction, and cost) when determining BESS placement and sizing.
- Examine the potential for multiple smaller BESS units distributed across the network versus one larger unit, assessing the trade-offs in terms of performance, cost, and reliability.
- Analyze the impact of increasing penetration of RESs particularly solar PV, on optimal BESS placement and sizing strategies.

These recommendations aim to explore new avenues for enhancing BESS integration in distribution networks ultimately leading to more stable, reliable, and sustainable distribution network.

References

[1] Eskom, “https://www.eskom.co.za/as-komati-coal-fired-power-station-reaches-end-of-life-renewable-energy-project-takes-shape/.” Accessed: Oct. 26, 2024. [Online]. Available: https://www.eskom.co.za/as-komati-coal-fired-power-station-reaches-end-of-life-renewable-energy-project-takes-shape/

[2] Minerals and Resources and Energy Department Minister E.S.G Mantashe, “Integrated Resource plan (IRP) - October 2019,” no. October 2019 ... 2019. No. 42778 11., pp. 1–100, Oct. 2019, Accessed: Jul. 26, 2024. [Online]. Available: https://www.gov.za/sites/default/files/gcis_document/201910/42778gon1359.pdf

[3] Yongping Zhai, Dae Kyeong Kim, “Handbook on Battery Energy Storage System,” Sustainable Development and Climate Change Department, Manila, Philippines, Dec. 2018. doi: 10.22617/TCS189791-2.

[4] D. Maradin, “Advantages and disadvantages of renewable energy sources utilization,” *International Journal of Energy Economics and Policy*, vol. 11, no. 3, pp. 176–183, 2021, doi: 10.32479/ijeep.11027.

[5] B. Muruganantham, R. Gnanadass, and N. P. Padhy, “Challenges with renewable energy sources and storage in practical distribution systems,” *Renewable and Sustainable Energy Reviews*, vol. 73, pp. 125–134, 2017, doi: https://doi.org/10.1016/j.rser.2017.01.089.

[6] N. Phuangpornpitak and S. Tia, “Opportunities and Challenges of Integrating Renewable Energy in Smart Grid System,” *Energy Procedia*, vol. 34, pp. 282–290, 2013, doi: https://doi.org/10.1016/j.egypro.2013.06.756.

[7] M. Stecca, L. R. Elizondo, T. B. Soeiro, P. Bauer, and P. Palensky, “A comprehensive review of the integration of battery energy storage systems into distribution networks,” 2020, *Institute of Electrical and Electronics Engineers Inc.* doi: 10.1109/OJIES.2020.2981832.

[8] P. Trehan, T. Puri, B. Banda Singh Bahadur Engineering College, and F. Shahib, “PERFORMANCE ANALYSIS OF PV AND BESS BASED HYBRID SYSTEM FOR RESIDENTIAL LOAD,” 2020.

[9] E. Rivas Trujillo, J. M. López Lezama, and T. E. Gutiérrez Castro, “Literature review of BESS implementation in DER,” *Revista vínculos*, vol. 16, no. 2, pp. 321–326, Nov. 2019, doi: 10.14483/2322939x.16662.

[10] P. Moyo, “Eskom`s Flagship Battery Energy Storage Systems (BESS) Project,” South Africa, Johannesbburg, Jun. 2000. [Online]. Available: www.energystorageexchange.org

[11] C. E. Okafor and K. A. Folly, “Optimal Placement of a Battery Energy Storage System (BESS) in a Distribution Network,” in *2023 31st Southern African Universities Power Engineering Conference (SAUPEC)*, 2023, pp. 1–6. doi: 10.1109/SAUPEC57889.2023.10057659.

[12] S. Khunkitti, P. Boonluk, and A. Siritaratiwat, “Optimal Location and Sizing of BESS for Performance Improvement of Distribution Systems with High DG Penetration,” *International Transactions on Electrical Energy Systems*, vol. 2022, no. 1, p. 6361243, 2022, doi: https://doi.org/10.1155/2022/6361243.

[13] DR HESHAM HAMDAM HAMDAN & BERGEN VITTAL, “POWER SYSTEM ANALYSIS BY BERG VITTAL M3nd,” 2000. Accessed: Mar. 07, 2023. [Online]. Available: https://www.mendeley.com/reference-manager/reader/88fdd8a5-015d-35b3-8c96-12bc770701b7/231592cf-7e58-793d-5da2-0317890df041

[14] S. P. Burger, J. D. Jenkins, S. C. Huntington, and I. J. Pérez-Arriaga, “Why Distributed?: A Critical Review of the Tradeoffs Between Centralized and Decentralized Resources; Why Distributed?: A Critical Review of the Tradeoffs Between Centralized and Decentralized Resources,” 2019, doi: 10.1109/MPE.2018.2885203.

[15] United Nations Framework Convention on Climate Change (UNFCCC), “ADOPTION OF THE PARIS AGREEMENT - The Paris Agreement text English,” Dec. 2015. Accessed: Nov. 26, 2024. [Online]. Available: https://unfccc.int/sites/default/files/resource/parisagreement_publication.pdf

[16] A. De, “Optimal sizing and positioning of grid integrated distributed generator: a review,” *International Journal of Engineering & Technology*, vol. 9, p. 299, Nov. 2020, doi: 10.14419/ijet.v9i2.30177.

[17] P. Pokharel and L. Poudel, “Impact of Distributed Generation in Distribution Network Losses and Voltage Profile,” *International Journal of Engineering and Applied Sciences (IJEAS)*, vol. 6, Nov. 2019, doi: 10.31873/IJEAS.6.10.06.

[18] V. Vita, T. Alimardan, and L. Ekonomou, “The Impact of Distributed Generation in the Distribution Networks’ Voltage Profile and Energy Losses,” in *2015 IEEE European Modelling Symposium (EMS)*, 2015, pp. 260–265. doi: 10.1109/EMS.2015.46.

[19] India Smart Grid Knowledge Portal, “https://indiasmartgrid.org/Distributed-Generation.php.” Accessed: Dec. 13, 2022. [Online]. Available: https://indiasmartgrid.org/Distributed-Generation.php

[20] A. De, “Optimal sizing and positioning of grid integrated distributed generator: a review,” *International Journal of Engineering & Technology*, vol. 9, p. 299, Nov. 2020, doi: 10.14419/ijet.v9i2.30177.

[21] Mr T Mchunu, “The South African Grid Code” vol. 10, pp. 1–65, Aug. 2019, doi: 10.0.

[22] M. S. of E. Hadi Saadat, “Power-System-Analysis-by-Hadi-Saadat-Electrical-Engineering-libre,” vol. 012235–5, pp. 1–720, Feb. 1999, Accessed: Nov. 29, 2024. [Online]. Available: http://www.mhhe.com

[23] B. Muruganantham, R. Gnanadass, and N. P. Padhy, “Challenges with renewable energy sources and storage in practical distribution systems,” *Renewable and Sustainable Energy Reviews*, vol. 73, pp. 125–134, 2017, doi: https://doi.org/10.1016/j.rser.2017.01.089.

[24] R. R. Rao, M. Mani, and P. C. Ramamurthy, “An updated review on factors and their inter-linked influences on photovoltaic system performance,” *Heliyon*, vol. 4, no. 9, p. e00815, 2018, doi: https://doi.org/10.1016/j.heliyon.2018.e00815.

[25] P. Unahalekhaka and P. Sripakarach, “Reduction of Reverse Power Flow Using the Appropriate Size and Installation Position of a BESS for a PV Power Plant,” *IEEE Access*, vol. 8, pp. 102897–102906, 2020, doi: 10.1109/ACCESS.2020.2997821.

[26] V. Salehi, S. Afsharnia, and S. Kahrobaee, “Improvement of voltage stability in wind farm connection to distribution network using FACTS devices,” in *IECON Proceedings (Industrial Electronics Conference)*, 2006, pp. 4242–4247. doi: 10.1109/IECON.2006.347720.

[27] H.-J. Wagner, “Introduction to wind energy systems,” *EPJ Web Conf*, vol. 189, p. 5, Nov. 2018, doi: 10.1051/epjconf/201818900005.

[28] Z. Leonowicz, Institute of Electrical and Electronics Engineers, IEEE Electromagnetic Compatibility Society, IEEE Power & Energy Society, IEEE Industry Applications Society, and IEEE Industrial and Commercial Power Systems Europe 4. 2020 Online, *Conference proceedings 2020 IEEE International Conference on Environment and Electrical Engineering and 2020 IEEE Industrial and Commercial Power Systems Europe (EEEIC/I & CPS Europe) 9-12 June, 2020, Madrid, Spain : the 2020 edition will be held on scheduled days from 09th to 12th June 2020 in web streaming*.

[29] A. Bellini, S. Bifaretti, V. Iacovone, and C. Cornaro, “Simplified model of a photovoltaic module,” in *2009 Applied Electronics*, 2009, pp. 47–51.

[30] X. Wang, J. Gao, W. Hu, Z. shi, and B. Tang, “Research of effect on distribution network with penetration of photovoltaic system,” *Proceedings of the Universities Power Engineering Conference*, Nov. 2010.

[31] R. Stanev and T. Tanev, “Mathematical model of photovoltaic power plant,” in *2018 20th International Symposium on Electrical Apparatus and Technologies, SIELA 2018 - Proceedings*, Institute of Electrical and Electronics Engineers Inc., Aug. 2018. doi: 10.1109/SIELA.2018.8447173.

[32] R. Venkateswari and S. Sreejith, “Factors influencing the efficiency of photovoltaic system,” *Renewable and Sustainable Energy Reviews*, vol. 101, pp. 376–394, Mar. 2019, doi: 10.1016/J.RSER.2018.11.012.

[33] S. Pukhrem, “Investigation into Photovoltaic Distributed Generation Penetration Investigation into Photovoltaic Distributed Generation Penetration in the Low Voltage Distribution Network in the Low Voltage Distribution Network”, doi: 10.21427/yhta-1g97.

[34] A. Bellini, S. Bifaretti, V. Iacovone, and C. Cornaro, “Simplified model of a photovoltaic module; Simplified model of a photovoltaic module,” 2009.

[35] H. S. Mohammed, C. K. Gan, and M. R. A. Ghani, “Technical impacts of solar photovoltaic systems integration into malaysian medium voltage reference networks,” *International Journal of Nonlinear Analysis and Applications*, vol. 11, no. Special Issue, pp. 265–276, 2020, doi: 10.22075/IJNAA.2020.4601.

[36] N. Phuangpornpitak and S. Tia, “Opportunities and challenges of integrating renewable energy in smart grid system,” *Energy Procedia*, vol. 34, pp. 282–290, 2013, doi: 10.1016/j.egypro.2013.06.756.

[37] B. Muruganantham, R. Gnanadass, and N. P. Padhy, “Challenges with renewable energy sources and storage in practical distribution systems,” 2017, *Elsevier Ltd*. doi: 10.1016/j.rser.2017.01.089.

[38] M. S. Whittingham, “History, evolution, and future status of energy storage,” in *Proceedings of the IEEE*, Institute of Electrical and Electronics Engineers Inc., May 2012, pp. 1518–1534. doi: 10.1109/JPROC.2012.2190170.

[39] M. D. Anderson and D. S. Carr, “Battery energy storage technologies,” *Proceedings of the IEEE*, vol. 81, no. 3, pp. 475–479, 1993, doi: 10.1109/5.241482.

[40] J. Gustavsson, “Energy Storage Technology Comparison-A knowledge guide to simplify selection of energy storage technology.” [Online]. Available: http://www.greenenergystorage.eu

[41] K. Mongird *et al.*, “Energy Storage Technology and Cost Characterization Report,” 2019.

[42] D. Connolly, “Aalborg Universitet A Review of Energy Storage Technologies For the integration of fluctuating renewable energy,” Denmark, Dec. 2010. Accessed: Jul. 26, 2024. [Online]. Available: https://vbn.aau.dk/ws/portalfiles/portal/100570335/Energy_Storage_Techniques_v4.1.pdf

[43] M. Stecca, L. R. Elizondo, T. B. Soeiro, P. Bauer, and P. Palensky, “A Comprehensive Review of the Integration of Battery Energy Storage Systems Into Distribution Networks,” *IEEE Open Journal of the Industrial Electronics Society*, vol. 1, pp. 46–65, 2020, doi: 10.1109/OJIES.2020.2981832.

[44] C. K. Das, O. Bass, G. Kothapalli, T. S. Mahmoud, and D. Habibi, “Overview of energy storage systems in distribution networks: Placement, sizing, operation, and power quality,” Aug. 01, 2018, *Elsevier Ltd*. doi: 10.1016/j.rser.2018.03.068.

[45] S. X. Chen, K. J. Tseng, and S. S. Choi, “Modeling of lithium-ion battery for energy storage system simulation,” in *Asia-Pacific Power and Energy Engineering Conference, APPEEC*, 2009. doi: 10.1109/APPEEC.2009.4918501.

[46] H. C. Hesse, M. Schimpe, D. Kucevic, and A. Jossen, “Lithium-ion battery storage for the grid - A review of stationary battery storage system design tailored for applications in modern power grids,” Dec. 01, 2017, *MDPI AG*. doi: 10.3390/en10122107.

[47] L. I. M. Asri, W. N. S. F. W. Ariffin, A. S. M. Zain, J. Nordin, and N. S. Saad, “Comparative Study of Energy Storage Systems (ESSs),” in *Journal of Physics: Conference Series*, IOP Publishing Ltd, Jul. 2021. doi: 10.1088/1742-6596/1962/1/012035.

[48] BUYISA DigSILENT, “DIgSILENT PowerFactory Application Example Battery Energy Storing Systems,” Germany, Feb. 2010. Accessed: Jun. 26, 2024. [Online]. Available: https://www.digsilent.de/en/faq-reader-powerfactory/do-you-have-an-application-example-for-a-battery-energy-storage-system-bess.html

[49] M. D. Anderson and D. S. Carr, “Battery Energy Storage Technologies,” *Proceedings of the IEEE*, vol. 81, no. 3, pp. 475–479, 1993, doi: 10.1109/5.241482.

[50] M. T. Lawder *et al.*, “Battery energy storage system (BESS) and battery management system (BMS) for grid-scale applications,” *Proceedings of the IEEE*, vol. 102, no. 6, pp. 1014–1030, 2014, doi: 10.1109/JPROC.2014.2317451.

[51] J. Horne, “GIZ SAGEN Programme BESS model workshop.” [Online]. Available: www.moellerpoeller.co.uk

[52] “Large-Scale Battery Storage Opportunity in South Africa ESKOM Flagship Battery Energy Storage Systems (BESS) Project,” 2019.

[53] Q. Li, Y. Tao, Z. Li, Y. Zhang, and Z. Zhang, “Simulation and modeling for active distribution network BESS system in DIgSILENT,” *Energy Reports*, vol. 8, pp. 97–102, Jul. 2022, doi: 10.1016/j.egyr.2022.01.113.

[54] L. A. Wong, V. K. Ramachandaramurthy, S. L. Walker, and J. B. Ekanayake, “Optimal placement and sizing of battery energy storage system considering the duck curve phenomenon,” *IEEE Access*, vol. 8, pp. 197236–197248, 2020, doi: 10.1109/ACCESS.2020.3034349.

[55] E. Mahad Buḥūth al-Iliktrūnīyāt (Cairo, Institute of Electrical and Electronics Engineers. Egypt Section, Institute of Electrical and Electronics Engineers, and E. International Conference on New Paradigms in Electronics & Information Technology (5th : 2019 : Ghardaqah, *ACCS/PEIT 2019 : 2019 6th International Conference on Advanced Control Circuits and Systems (ACCS) & 2019 5th International*

Conference on New Paradigms in Electronics & information Technology (PEIT) : Hurghada, Egypt 17-20 November 2019.

[56] C. K. Das, O. Bass, G. Kothapalli, T. S. Mahmoud, and D. Habibi, "Overview of energy storage systems in distribution networks: Placement, sizing, operation, and power quality," *Renewable and Sustainable Energy Reviews*, vol. 91, pp. 1205–1230, 2018, doi: https://doi.org/10.1016/j.rser.2018.03.068.

[57] S. Khunkitti, P. Boonluk, and A. Siritaratiwat, "Optimal Location and Sizing of BESS for Performance Improvement of Distribution Systems with High DG Penetration," *International Transactions on Electrical Energy Systems*, vol. 2022, 2022, doi: 10.1155/2022/6361243.

[58] P. Pokharel and L. Poudel, "Impact of Distributed Generation in Distribution Network Losses and Voltage Profile", [Online]. Available: www.ijeas.org

[59] K. E. Adetunji, I. W. Hofsajer, A. M. Abu-Mahfouz, and L. Cheng, "A Review of Metaheuristic Techniques for Optimal Integration of Electrical Units in Distribution Networks," *IEEE Access*, vol. 9, pp. 5046–5068, 2021, doi: 10.1109/ACCESS.2020.3048438.

[60] A. Alzahrani, H. Alharthi, and M. Khalid, "Minimization of power losses through optimal battery placement in a distributed network with high penetration of photovoltaics," *Energies (Basel)*, vol. 13, no. 1, Dec. 2019, doi: 10.3390/en13010140.

[61] K. Y. and M. A. E.-S. Lee, "Chapter 5 Fundamentals of Particle Swarm Optimization Techniques," 2002. Accessed: Aug. 16, 2024. [Online]. Available: http://web.ecs.baylor.edu/faculty/lee/ELC5364/Lecture%20note/Lecture%20Note26-PSO-tuto.pdf

[62] D. W. Boeringer and D. H. Werner, "Particle swarm optimization versus genetic algorithms for phased array synthesis," *IEEE Trans Antennas Propag*, vol. 52, no. 3, pp. 771–779, Mar. 2004, doi: 10.1109/TAP.2004.825102.

[63] K. E. Adetunji, I. W. Hofsajer, A. M. Abu-Mahfouz, and L. Cheng, "A Review of Metaheuristic Techniques for Optimal Integration of Electrical Units in Distribution Networks," *IEEE Access*, vol. 9, pp. 5046–5068, 2021, doi: 10.1109/ACCESS.2020.3048438.

[64] G. Pereira, "Particle Swarm Optimization," 2014. [Online]. Available: https://www.researchgate.net/publication/228518470

[65] M. Mitchell, "Genetic algorithms: An overview," *Complexity*, vol. 1, no. 1, pp. 31–39, Sep. 1995, doi: 10.1002/cplx.6130010108.

[66] M. Power and E. Conference, "Genetic Algorithm Based Optimal on Load Transformer Tap Setting for Loss Minimisation in Power Transmission System," 2004.

[67] P. Boonluk, A. Siritaratiwat, P. Fuangfoo, and S. Khunkitti, "Optimal siting and sizing of battery energy storage systems for distribution network of distribution system operators," *Batteries*, vol. 6, no. 4, pp. 1–16, Dec. 2020, doi: 10.3390/batteries6040056.

[68] S. Salee and P. Wirasanti, "Optimal siting and sizing of battery energy storage systems for grid-supporting in electrical distribution network," in *1st International ECTI Northern Section Conference on Electrical, Electronics, Computer and Telecommunications Engineering, ECTI-NCON 2018*, Institute of Electrical and Electronics Engineers Inc., Jun. 2018, pp. 100–105. doi: 10.1109/ECTI-NCON.2018.8378290.

[69] P. Pon Ragothama Priya, S. Baskar, S. Tamil Selvi, and C. K. Babulal, “Optimal Allocation of Hybrid Renewable Distributed Generation with Battery Energy Storage System Using MOEA/D-DRA Algorithm,” *International Transactions on Electrical Energy Systems*, vol. 2023, 2023, doi: 10.1155/2023/7316834.

[70] S. Khunkitti, P. Boonluk, and A. Siritaratiwat, “Optimal Location and Sizing of BESS for Performance Improvement of Distribution Systems with High DG Penetration,” *International Transactions on Electrical Energy Systems*, vol. 2022, 2022, doi: 10.1155/2022/6361243.

[71] J. Kennedy, R. Eberhart, and bls gov, “Particle Swarm Optimization.”

[72] A. Selim, S. Kamel, A. S. Alghamdi, and F. Jurado, “Optimal Placement of DGs in Distribution System Using an Improved Harris Hawks Optimizer Based on Single- And Multi-Objective Approaches,” *IEEE Access*, vol. 8, pp. 52815–52829, 2020, doi: 10.1109/ACCESS.2020.2980245.

[73] D. B. Prakash and C. Lakshminarayana, “Multiple DG Placements in Distribution System for Power Loss Reduction Using PSO Algorithm,” *Procedia Technology*, vol. 25, pp. 785–792, 2016, doi: 10.1016/j.protcy.2016.08.173.

[74] R. AbdelHady, “Modeling and simulation of a micro grid-connected solar PV system,” *Water Science*, vol. 31, no. 1, pp. 1–10, 2017, doi: 10.1016/j.wsj.2017.04.001.

[75] Q. Li, Y. Tao, Z. Li, Y. Zhang, and Z. Zhang, “Simulation and modeling for active distribution network BESS system in DIgSILENT,” *Energy Reports*, vol. 8, pp. 97–102, 2022, doi: https://doi.org/10.1016/j.egyr.2022.01.113.

[76] “DIgSILENT PowerFactory 2018 Battery Energy Storing System Template Battery With Frequency Control 10kV 30MVA,” 2017. [Online]. Available: http://www.digsilent.de

[77] T. S. G. C. S. system O. T. D. Mr T Mchunu, “Grid Connection Code For Battery Energy Storage Facilities (BESF) Connected To The Electricity Transmission System (TS) Or The Distribution System (DS) IN South Africa,” Gauteng, May 2020. Accessed: Jun. 06, 2024. [Online]. Available: https://www.nersa.org.za/wp-content/uploads/2021/08/Annexure-A_BESF-Code-Version-5.2.pdf

[78] F. M. Gonzalez-Longatt, J. Luis, and R. Editors, “Power Systems PowerFactory Applications for Power System Analysis.” [Online]. Available: http://www.springer.com/series/4622

[79] L. Lu, X. Han, J. Li, J. Hua, and M. Ouyang, “A review on the key issues for lithium-ion battery management in electric vehicles,” Mar. 15, 2013. doi: 10.1016/j.jpowsour.2012.10.060.

Appendices

Appendix A: Key characteristics of Secondary Battery Types.

Battery Type	Characteristics	Strengths	Weaknesses	Applications
Lead Acid (PbA) [37,40]	Low cost	- Widespread availability - Suitable for starter batteries and backup power sources	- Relatively short lifespan - Hazardous to dispose of due to lead and acid components - Low cycling lifespan (up to 2500 cycles) - Low energy density (20 – 30 Wh/kg),[37].	Automotive (starter batteries), backup power,[40].
Sodium Sulphur (NaS) [40]	High operating temperatures	High energy density long cycling life Reasonable efficiency Suitable for large scale BESS applications,[40].	- Limitations on large-scale application due to high, [40]. -temperature conditions - Need to maintain sulfur in molten form. - Minor threat to environment and operators - Reactivity of pure sodium.	Grid-scale energy storage, renewable integration.
Vanadium Redox Flow [35, 38, 39]	Separation of power and energy ratings	- Not constrained by depth of discharge or life cycle - Potential alternative for grid-scale storage due to economic performance, [35, 38, 39].	- Relatively expensive - Require specialized infrastructure - Low energy density (15–30 Wh/kg) - Efficiency up to 75%. ,[35, 38, 39].	Grid-scale energy storage
Lithium-ion (Li-ion) [40,41,42].	High energy density	- Long life up to 10,000 cycles -Low environmental impact due to recyclability, [40] - High efficiency levels of over 90% - Millisecond-level response time - Ability to provide required power	- Sensitive to high temperatures - Expensive to produce, [40,41,42].	Portable electronics, electric vehicles, grid storage
Redox Flow (RFB) [[40,41,42].	Utilizes two electrolyte reservoirs	- Energy density determined by tank size and number of electrolytes - Power density depends on electrode reaction rates	- Complexity of system - Lower energy density compared to other battery types	Grid-scale energy storage

Appendix B: Distributed Generation (DG) sources Technology options for Decentralised Generation

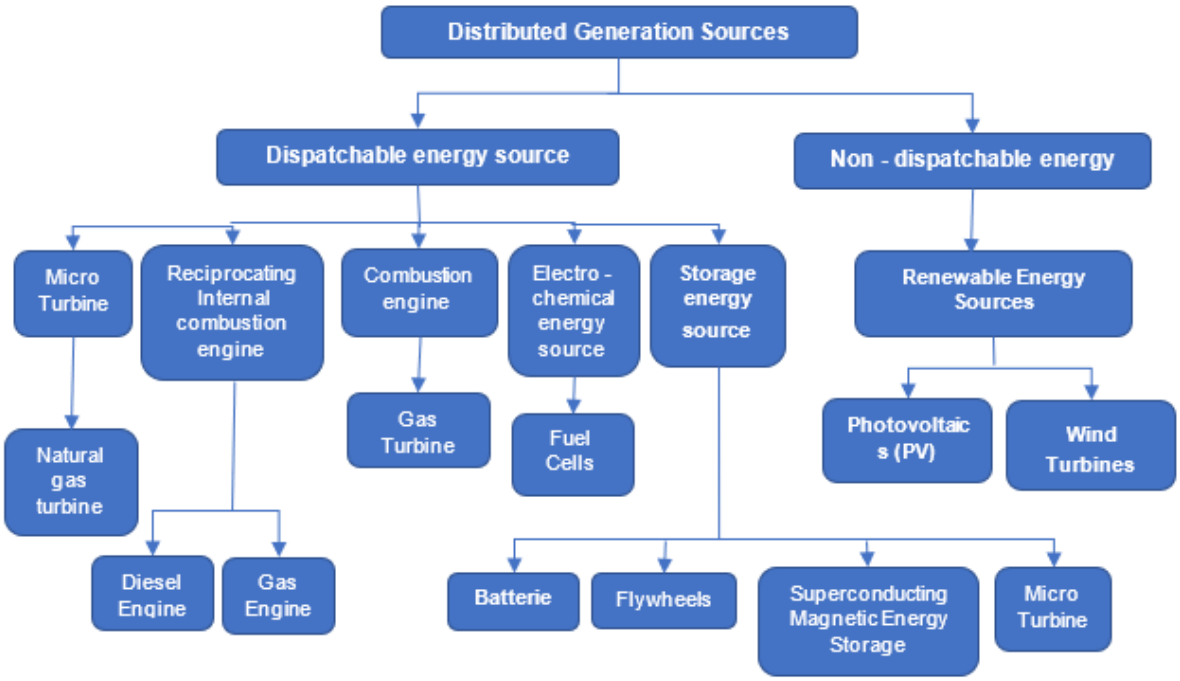

Appendix C: Modified Witzenberg 16-bus Distribution Network Overview.

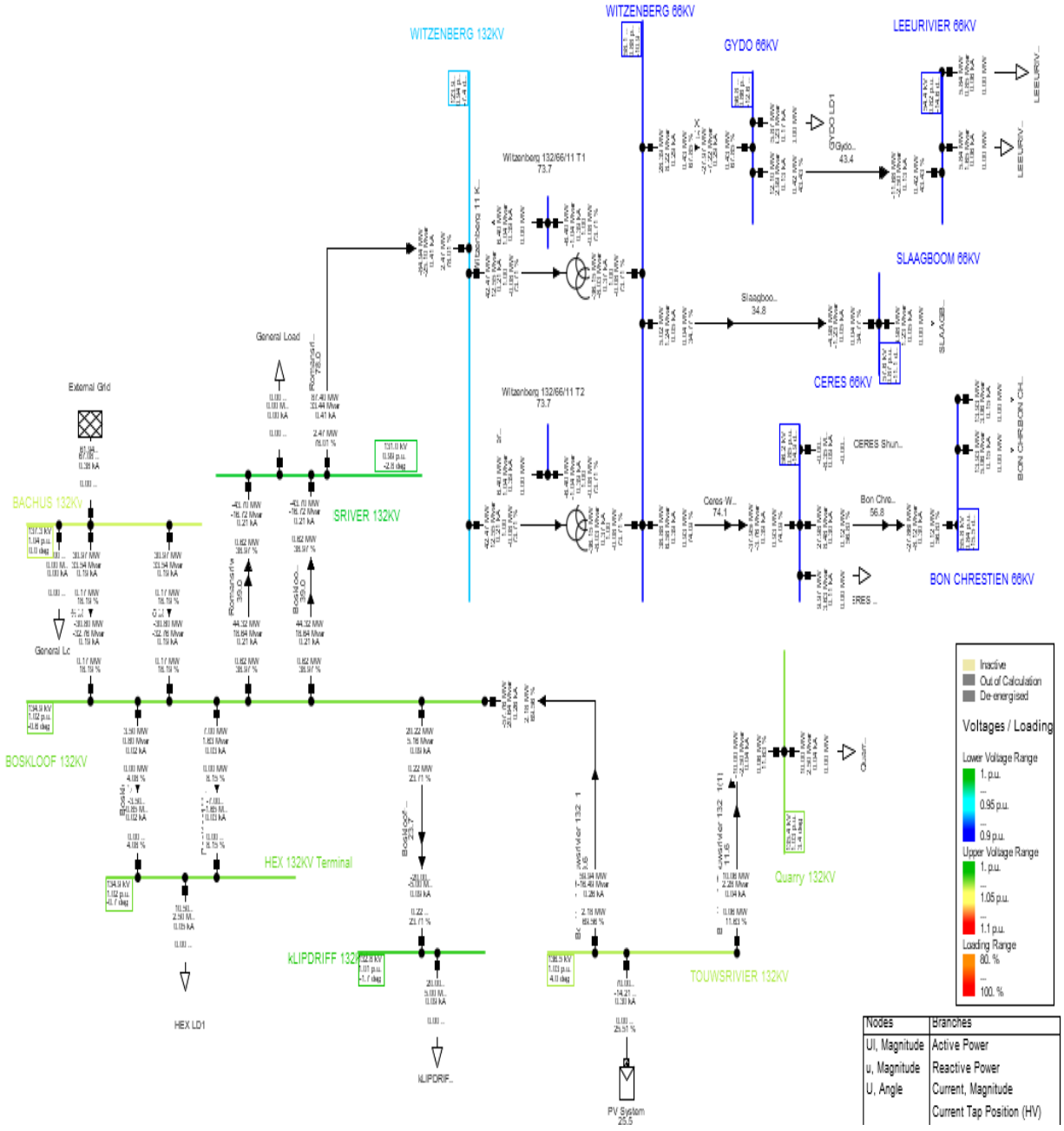

Appendix D: The two Witzenberg substation 3 winding transformer nameplate data.

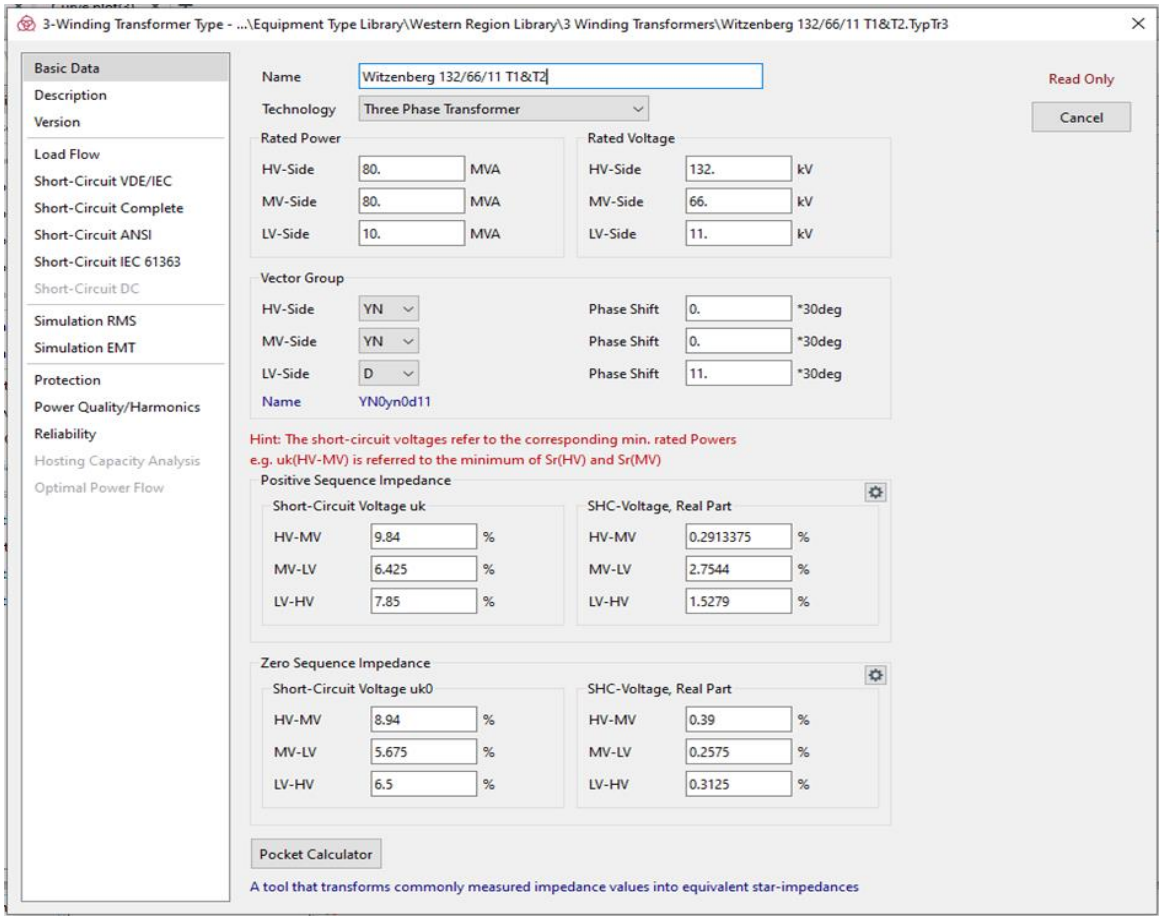

Appendix E: Ceres Shunt/Filter Cap Bank.

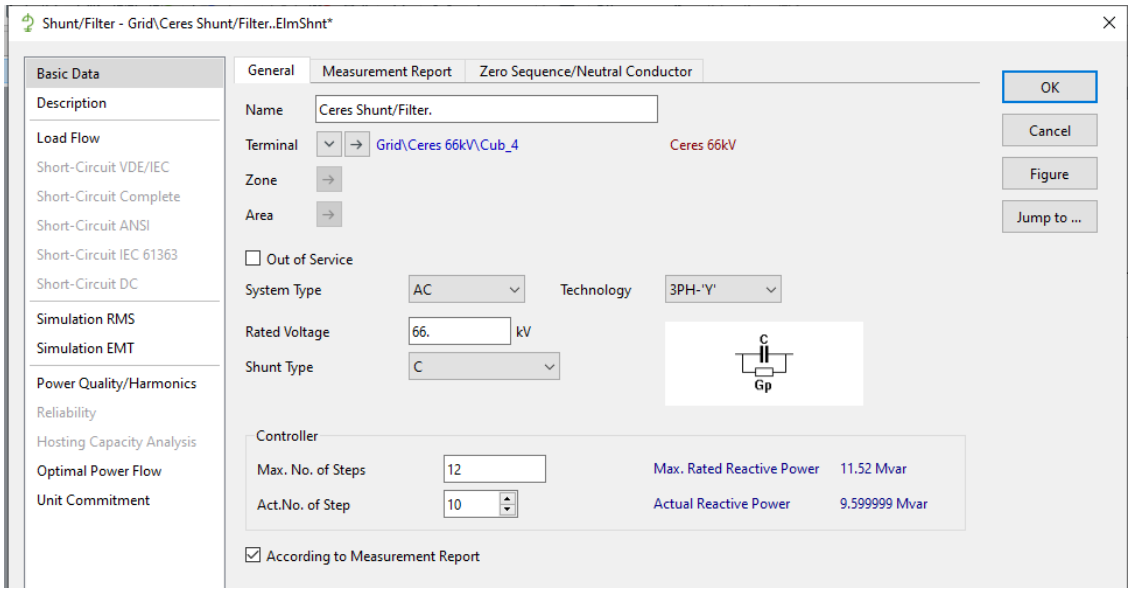

Appendix F: Transformer 1 & 2 load flow results

Parameter	Witzenberg 132/66/11 Transformer 1	Witzenberg 132/66/11 Transformer 2
HV-Side Busbar	Witzenberg 132kV	Witzenberg 132kV
MV-Side Busbar	Witzenberg 66kV	Witzenberg 66kV
LV-Side Busbar	Witzenberg Tertiary winding 11kV T1	Witzenberg Tertiary winding 11kV T2
HV-Side Voltage (p.u.)	0.94	0.94
MV-Side Voltage (p.u.)	0.881	0.881
LV-Side Voltage (p.u.)	0.88	0.88
Maximum Loading (%)	73.6	73.6
Total Active Losses (MW)	-0.1	-0.1
Total Reactive Losses (Mvar)	3.5	3.5
HV-Side Loading (%)	58.9	58.9
MV-Side Loading (%)	52.5	52.5
Iron Losses (kW)	13.7	13.7
Magnetizing Losses (kvar)	261.2	261.2

Appendix G: Summary analysis of network total active power losses.

Location	Scenario	Power Loss (MW)	Percentage Change (%)
Without BESS placement			
		8	-
With BESS placement			
Bus 13 (Optimal)	With BESS Optimally Placement	3.3	58.75
Bus 14	With BESS	3.7	53.75
Bus 10	With BESS	4.4	55
Bus 5	With BESS	4.9	62.5
Bus 1	With BESS	5	62.5
Bus 3	With BESS	5	62.5
Bus 4	With BESS	5	62.5
Bus 6	With BESS	5.1	63.75
Bus 2	With BESS	5.4	67.5
Bus 17	With BESS	6.5	67.5
Bus 7	With BESS	9.9	123.75
Bus 11	With BESS	10	125
Bus 12	With BESS	13.4	167.5
Bus 9 (not optimal)	Least optimal placement	15.7	196.25

Appendix H: Baseline load flow summary of voltage profile results placement.

Table H-1: Baseline voltage profile analysis - Network Bus Voltages - Nominal vs. Baseline Values

Bus No.	Nominal Voltage (k.V)	Nominal Voltage (p.u.)	Baseline Voltage (p.u.)
Bus 1	132	1	1.04
Bus 2	66	1	0.907
Bus 3	132	1	1.027
Bus 4	66	1	0.911
Bus 5	66	1	0.907
Bus 6	132	1	1.027
Bus 7	66	1	1.027
Bus 8	10	1	0
Bus 9	132	1	1.031
Bus 10	132	1	1.009
Bus 11	66	1	0.915
Bus 12	132	1	1.039
Bus 13	132	1	0.975
Bus 14	66	1	0.922
Bus 15	11	1	0.916
Bus 16	11	1	0.916
Bus 17	132	1	1.011

Table H-2: Voltage Profiles Analysis after BESS Placement at Bus 13.

Bus No.	Without BESS (p.u.)	With Optimal BESS (p.u.)	Improvement (%)
Bus 1	1.04	1.04	0.0
Bus 2	0.907	0.953	5.1
Bus 3	1.027	1.032	0.5
Bus 4	0.911	0.956	4.9
Bus 5	0.907	0.952	5
Bus 6	1.027	1.032	0.5
Bus 7	0.899	0.943	4.9
Bus 8	0.00	1.02	N/A
Bus 9	1.031	1.036	0.5
Bus 10	1.009	1.028	1.9
Bus 11	0.915	0.959	4.8
Bus 12	1.039	1.044	0.5
Bus 13	0.975	1.02	4.6
Bus 14	0.922	0.966	4.8
Bus 15	0.916	0.96	4.8
Bus 16	0.916	0.96	4.8
Bus 17	1.011	1.017	0.6

Table H-3: Voltage Profiles Analysis after BESS Placement at Bus 14.

Bus No.	Without BESS (p.u.)	With Optimal BESS (p.u.)	Improvement (%)
Bus 1	1.04	1.04	0.0
Bus 2	0.907	0.952	5.0
Bus 3	1.027	1.032	0.5
Bus 4	0.911	0.955	4.8
Bus 5	0.907	0.981	8.2
Bus 6	1.027	1.032	0.5
Bus 7	0.899	0.972	8.1
Bus 8	0.00	0.980	N/A
Bus 9	1.031	1.035	0.4
Bus 10	1.009	1.027	1.8
Bus 11	0.915	0.958	4.7
Bus 12	1.039	1.044	0.5
Bus 13	0.975	1.017	4.3
Bus 14	0.922	0.966	4.8
Bus 15	0.916	0.932	1.7
Bus 16	0.916	0.32	1.7
Bus 17	1.011	1.016	0.5

Table H-4: Voltage Profiles Analysis after BESS Placement at Bus 12.

Bus No.	Without BESS (p.u.)	With Optimal BESS (p.u.)	Improvement (%)
Bus 1	1.04	1.04	0.0
Bus 2	0.907	0.906	0.1
Bus 3	1.027	1.026	0.1
Bus 4	0.911	0.910	0.1
Bus 5	0.907	0.906	0.1
Bus 6	1.027	1.026	0.1
Bus 7	0.899	0.897	0.2
Bus 8	1.04	1.071	3
Bus 9	1.031	1.063	3.1
Bus 10	1.009	1.008	0.1
Bus 11	0.915	0.914	0.1
Bus 12	1.039	1.071	3.2
Bus 13	0.975	0.974	0.1
Bus 14	0.922	0.921	0.1
Bus 15	0.916	0.915	0.1
Bus 16	0.916	0.915	0.1
Bus 17	1.011	1.010	0.1

Table H-5: Voltage Profiles Analysis after BESS Placement at Bus 9.

Bus No.	Without BESS (p.u.)	With Optimal BESS (p.u.)	Improvement (%)
Bus 1	1.04	1.04	0.0
Bus 2	0.904	0.905	0.1
Bus 3	0.975	1.025	5.1
Bus 4	0.907	0.908	0.1
Bus 5	0.904	0.905	0.1
Bus 6	1.024	1.025	0.1
Bus 7	0.895	0.896	0.1
Bus 8	1.1	1.095	0.5
Bus 9	1.095	1.095	0
Bus 10	1	1.007	0.7
Bus 11	0.912	0.912	0
Bus 12	1.063	1.063	0
Bus 13	0.973	0.973	0
Bus 14	0.92	0.92	0
Bus 15	0.91	0.913	0.3
Bus 16	0.91	0.913	0.3
Bus 17	1.009	1.009	0.6

Appendix I: The Percentage Voltage Deviation Index Results table.

Location Scenario	Percentage Voltage Deviation Index (PVDI)
Without BESS placement	
	11.98
With BESS placement	
Bus 13 (Optimal)	3.47
Bus 14	3.84
Bus 5	3.88
Bus 10	9.34
Bus 1	5.98
Bus 3	5.84
Bus 4	13.16
Bus 6	5.86
Bus 2	3.86
Bus 17	6.22
Bus 7	4.36
Bus 11	4.49
Bus 12	6.61
Bus 9 (not optimal)	6.96

Appendix J: MATLAB Algorithms Codes for Optimization Techniques for optimal BESS placement

Appendix J.1: Genetic Algorithm (GA) Algorithm code for optimal BESS placement

```
% Objective function
objective = @(x)(3300*.284)+(abs(1.04-x)+abs(0.953-x)+abs(1.032-x)+abs(0.956-
x)+abs(0.952-x)+abs(1.032-x)+abs(0.943-x)+abs(1.02-x)+abs(1.036-x)+abs(1.028-
x)+abs(0.959-x)+abs(1.044-x)+abs(1.02-x)+abs(0.966-x)+abs(0.96-x)+abs(0.96-
x)+abs(1.017-x))*0.142;

% Number of variables
nvars = 1;

% Lower and upper bounds
lb = 0.1; % lower bound
ub = 1; % upper bound

% Options for the genetic algorithm
options = optimoptions('ga', ...
    'PlotFcn', @gaplotbestf, ... % Plot the best function value
    'Display', 'iter' ... % Display output at each iteration
);

% Run the genetic algorithm
[x, fval] = ga(objective, nvars, [], [], [], [], lb, ub, [], options);

% Display results
fprintf('Optimal x: %f\n', x);
fprintf('Minimum value: %f\n', fval);

% Plot the objective function and the solution
x_plot = linspace(lb, ub, 50);
y_plot = objective(x_plot);

figure;
plot(x_plot, y_plot, 'b-', 'LineWidth', 2);
hold on;
plot(x, fval, 'ro', 'MarkerSize', 10, 'LineWidth', 2);
title('Objective Function and GA Solution');
xlabel('x');
ylabel('f(x)');
legend('Objective Function', 'GA Solution');
grid on;
hold off;
```

Appendix J.2: Particle Swarm Optimization (PSO) Algorithm code for optimal BESS placement

```
%% PARTICLE SWARM OPTIMIZATION (PSO)

function [bestfitIter,best_Particle, bestParticle_Position] =
PSO(ObjFun,LB,UB,nVar,nPop,MaxIt)
%% Problem Parameters
prob = ObjFun;                  % fitness function
Var = nVar;                     % number of variables
lb = LB;                        % Variable Lower Bound
ub = UB;                        % Variable Upper Bound
cPop = nPop;                    % class population size
Maxiter = MaxIt;                % max no of iteration

%% PSO Parameters
w=0.45;                          % Inertia Weight
c1=1;                           % Personal Learning Coefficient
c2=1;                           % Global Learning Coefficient

%% Starting the Particle Swarm Optimization
f = NaN(cPop,1);                    % vector for fitness fun value of the
population
D = Var;                            % length of decision variables

bestfitIter = NaN(Maxiter+1,1);     % vetcor to store best fitness fun value per
iteration

P = repmat(lb,cPop,1) + repmat((ub-lb),cPop,1).*rand(cPop,D);   % generation of
initial positon of the particles in the population
V = repmat(lb,cPop,1) + repmat((ub-lb),cPop,1).*rand(cPop,D);   % generation of
initial velocity of each particle

for q = 1:cPop
    f(q) = prob(P(q,:));        % evaluating the fitness fun value of initial
population
end

bestfitIter(1) = min(f);            % vector to store best fitness value of the
0th iteration

pbest = P;                      % initalize the personal best solution
f_pbest = f;                    % initalize the fitness of the personal best
solution

[f_gbest,ind] = min(f_pbest);   % initalize the best objective function value
gbest = P(ind,:);               % dtermine the best solution

%% Iteration Loop (Main Loop) (3686.25)*(5520.32+63*x).^-1;

for t = 1:Maxiter
    for q = 1:cPop
        V(q,:) = w*V(q,:) + c1*rand(1,D).*(pbest(q,:)-P(q,:)) +
c2*rand(1,D).*(gbest - P(q,:));     % Determine the new velocity

        P(q,:) = P(q,:) + V(q,:);   % update the position

        P(q,:) = max(P(q,:),LB);    % bounding the violating to their lower bound
```

```
        P(q,:) = min(P(q,:),UB);    % bounding the violating to their upper bound

        f(q) = prob(P(q,:));        % determine the fitness of the new solution

        if f(q) < f_pbest(q)
           f_pbest(q) = f(q);       % update the fitness function value of the
personal best soultion
           pbest(q,:) = P(q,:);     % update the personal best soultion

           if f_pbest(q) < f_gbest
           f_gbest = f_pbest(q);        % update the fitness function value of the
global best soultion
           gbest = pbest(q,:);          % update the global best soultion
           end
        end
    end
    bestfitIter(t+1) = f_gbest;
end

% Results
best_Particle = f_gbest;
bestParticle_Position = gbest;
```

PSO TEST

```
clear All; clc; close All
% This main script is to test PSO algorithms
rng(0,'twister') % your result are consistent

%%%%%%%%% Define your Parameters here %%%%%%%%%%%%%%%%%%%%%%%

%%%%%%%% PSO Tuning Parameters %%%%%%%%%%%%%%%%
Dim=30; Particles = 500; MaxItr = 50 ; run = 100; nVar=1; LB=0.1; UB=1.0;

% Bound
LB = LB.*ones(1,nVar);          % Lower Bounds
UB = UB.*ones(1,nVar);          % Upper Bounds

%%%%%%%%% Objective function % Constraint %%%%%%%%%%

 ObjFun = @(x)(5400*.284)+(abs(1.04-x)+abs(0.989-x)+abs(1.032-x)+abs(0.984-
x)+abs(0.947-x)+abs(1.031-x)+abs(0.939-x)+abs(0.989-x)+abs(1.035-x)+abs(1.026-
x)+abs(0.954-x)+abs(1.044-x)+abs(1.014-x)+abs(0.962-x)+abs(0.928-x)+abs(0.928-
x)+abs(1.016-x))*0.142;

%%%%%%%% Main Loop %%%%%%%%%%%%%
for i = 1:run
[Iteration,Best,Position] = PSO1_test_main(ObjFun,LB,UB,nVar,Particles,MaxItr);
Best_run(i) = Best; %#ok<*SAGROW>
Position_run(i,:) = Position;
end
%%%%%%%%% Plot Result section %%%%%%%%%%
plot(Iteration)
% print solution
disp('Solution')
```